Efficient preparation of PET tracers for visualization of age-related disorders using emerging methods of radiofluorination

Inaugural-Dissertation

zur

Erlangung des Doktorgrades

der Mathematisch-Naturwissenschaftlichen Fakultät

der Universität zu Köln

vorgelegt von

Fadi Zarrad

aus Damaskus, Syrien

2017

Berichterstatter:	Prof. Dr. Bernd Neumaier
	Prof. Dr. Hans-Günther Schmalz
Tag der mündlichen Prüfung:	24.05.2017

Zusammenfassung

Im Jahr 2013 wurde über eine neue Substanzklasse für die Behandlung von Morbus Parkinson berichtet, die auf die Auflösung von α-Synuclein-Oligomer-Aggregaten abzielt.[1] Untersuchungen verschiedener Kandidaten zeigen, dass die Behandlung mit 5-(3-Bromphenyl)-3-(piperonyl)pyrazol (**1a**) zu einer deutlichen Reduktion der Proteinaggregat-Belastung führte. Da der Wirkmechanismus der Proben durch die Bindung an α-Synuclein-Oligomere erklärt wurde, sollten sich ^{18}F-markierte Analoga von **1a** potentiell als Tracer nutzen lassen, um α-Synuclein-Oligomere, die als Vorstufen der Proteinablagerungen gelten, diagnostisch zu erfassen. Das erste ^{18}F-markierte 5-(3-Bromphenyl)-3-(6-[^{18}F]fluorpiperonyl)pyrazol ([^{18}F]**1b**) wurde durch 1,3-dipolare Cycloaddition zwischen 3'-Bromphenylacetylen (**2a**) und [^{18}F]Fluorphenyldiazomethan hergestellt, welches *in situ* aus Tosylhydrazon ([^{18}F]**3b**) erzeugt wurde. Die 1,3-dipolare Cycloaddition zwischen dem aus Tosylhydrazon ([^{18}F]**3a**) hergestellten 4-[^{18}F]Fluorphenyldiazomethan und 4'-Fluorphenylacetylen (**2b**) wurde als Modellreaktion untersucht, um optimierte Reaktionsbedingungen zu erhalten. Dabei konnte die Modellverbindung 3,5-Bis(4-fluorphenyl)-1*H*-pyrazol ([^{18}F]**1d**) mit einer radiochemischen Ausbeute (RCA) von 67% und [^{18}F]**1b** mit einer RCA von 27-34% erhalten werden. Mit einer weiteren Synthesestrategie wurde eine andere α-Synuclein adressierende Verbindung 5-(3-[^{18}F]Fluorphenyl)-3-(piperonyl)pyrazol ([^{18}F]**1c**) synthetisiert. Dazu wurden für die kürzlich beschriebene Kupfer-vermittelte Radiofluorierung Stannylvorläufer als Substrate eingesetzt.[2,3] Trialkylaryl-Zinn-Verbindungen werden bereits seit einigen Jahrzehnten für elektrophile Radiofluorierungen verwendet. Daher sind viele verschiedene Vorläufer für Radiotracer zum Teil kommerziell erhältlich. In dieser Arbeit wurde Trimethyl(phenyl)zinn als Modellverbindung verwendet, um ein Protokoll für die Cu-vermittelte ^{18}F-Fluorodestannylierung zu etablieren. Nach Optimierung der [^{18}F]Fluorid-Aktivierung und der Destannylierungsbedingungen wurden verschiedene Arylstannylverbindungen mit unterschiedlichen elektronischen Effekten in RCA von 16-88% markiert. Der Einsatz der optimierten Bedingungen ermöglichte die Radiosynthese von [^{18}F]**1c** in RCA von 62%. Weiterhin wurde dieses Verfahren ausgehend von kommerziell verfügbaren Vorstufen, zur Synthese von ^{18}F-markierten Arylaminosäuren, verwendet. Dieses manuelle Syntheseverfahren wurde dann auf ein vollautomatisiertes Synthesemodul übertragen. Dadurch wurden schließlich 3-*O*-Methyl-6-[^{18}F]fluor-L-DOPA (6-

[^{18}F]OMFD), 6-[^{18}F]Fluor-L-*m*-tyrosin (6-[^{18}F]FMT), 2-[^{18}F]Fluor-L-tyrosin (2-[^{18}F]F-Tyr) und 6-[^{18}F]Fluor-L-3,4-dihydroxyphenylalanin (6-[^{18}F]FDOPA) in hohen isolierten RCA von 32-57% hergestellt. Bemerkenswerterweise lieferte die automatisierte Radiosynthese von 6-[^{18}F]FDOPA eine RCA von 57%. Die höchste in der Literatur beschriebene RCA für 6-[^{18}F]FDOPA betrug bisher 40%.[4] Ausgehend von 9,2 GBq [^{18}F]Fluorid wurden innerhalb von 65 min 3,5 GBq 6-[^{18}F]FDOPA erhalten, Dies ermöglicht die robuste Herstellung von 6-[^{18}F]FDOPA in Aktivitätsmengen, die weit über den bisher erreichbaren Aktivitätsdosen liegen. Damit sollte diese Methode den Zugang zu aromatischen Aminosäuren deutlich vereinfachen, so dass zu erwarten ist, dass diese zukünftig eine höheren Stellenwert in der PET Diagnostik einnehmen werden.

Abstract

In 2013 novel compounds targeting α-synuclein oligomer aggregates in Parkinson's disease were reported.[1] Especially 5-(3-bromophenyl)-3-(piperonyl)pyrazole (**1a**) showed dramatic therapeutic effects since it was able to eliminate pathological α-synuclein aggregates.[1] Therefore, it was assumed that ^{18}F-labeled analogs of **1a** are potentially useful for the detection of α-synuclein oligomers. The first ^{18}F-labeled compound 5-(3-bromphenyl)-3-(6-[^{18}F]fluorpiperonyl)pyrazol ([^{18}F]**1b**) was prepared by 1,3 dipolar cycloaddition between 3'-bromophenyl acetylene (**2a**) and [^{18}F]fluorophenyldiazomethane generated *in situ* from tosylhydrazone ([^{18}F]**3b**). In order to establish optimized reaction conditions, the 1,3-dipolar cycloaddition between 4-[^{18}F]fluorophenyldiazomethane and 4'-fluorophenyl acetylene (**2b**) was studied as a model reaction. Optimized reaction conditions enabled to obtain 3,5-bis(4-fluorophenyl)-1*H*-pyrazole ([^{18}F]**1d**) in radiochemical yield (RCY) of 67%. The same reaction conditions delivered [^{18}F]**1b** in RCYs of 27–34%. The second approach applied in this work to obtain the α-synuclein targeting compound 5-(3-[^{18}F]fluorphenyl)-3-(piperonyl)pyrazol ([^{18}F]**1c**) was based on copper mediated ^{18}F-fluorodestannylation. The latter method was recently reported by Scott *et. al*.[2,3] This method highly benefits from the fact that trialkylaryl tin compounds are routinely used as precursors for electrophilic radiofluorinations. Therefore, a method using stannyl precursors and "nucleophilic [^{18}F]Fluoride" should be of high interest for the production of radiopharmaceuticals. Initially, trimethyl(phenyl)tin was used as a model substrate to establish the ^{18}F-fluorodestannylation approach. After reaction optimization, this approach was used to label several electron-neutral, -rich and -poor stannyl substrates in RCYs of 16-88%. Additionally, ^{18}F-destannylation was used to produce [^{18}F]**1c** in RCY of 62%. Furthermore, this method was applied in the synthesis of ^{18}F-labeled amino acids starting from commercially available precursors. Finally, a scalable automated synthesis of 3-*O*-methyl-6-[^{18}F]fluoro-L-DOPA (6-[^{18}F]OMFD), 6-[^{18}F]Fluoro-L-*m*-tyrosine (6-[^{18}F]FMT), 2-[^{18}F]fluoro-L-tyrosine (2-[^{18}F]F-Tyr) und 6-[^{18}F]fluoro-L-3,4-dihydroxyphenylalanin (6-[^{18}F]FDOPA) was established affording these compounds in high isolated RCY of 32-57%. Remarkably, the automated radiosynthesis of 6-[^{18}F]FDOPA via Cu-mediated radiofluorination of an appropriate stannane precursor afforded RCYs of 57%. Starting from 9.2 GBq [^{18}F]fluoride 3.5 GBq of 6-[^{18}F]FDOPA was obtained within 65 min suitable for clinical applications.

Acknowledgements

I highly appreciate all who have contributed to the success of this thesis and have supported me on this long journey.

I am grateful to Prof. Dr. Bernd Neumaier for his generous trust in me and the opportunity to carry out this work at the institute of radiochemistry and experimental molecular imaging (IREMB) in the university clinic of Cologne, and later at the institute of neuroscience and medicine, nuclear chemistry (INM-5) in Forschungszentrum Jülich as well as for his great support and encouragement.

I sincerely thank Dr. Boris D. Zlatopolskiy for his valuable advices and all scientists at the institute of radiochemistry and experimental molecular imaging.

My thanks also go to Prof. Johannes Ermert, Dr. Marcus Holschbach, Dr. Dirk Bier and all co-workers of INM-5 for many stimulating discussions and great cooperativeness.

Besides Prof. Dr. Bernd Neumaier, I would like to thank the rest of my thesis committee: Prof. Dr. Hans-Günther Schmalz, Prof. Dr. Axel Klein and Prof. Dr. Johannes Ermert, for their insightful comments and encouragement, and for the questions which incented me to widen my knowledge from various perspectives.

Finally, I find myself speechless to thank my family who was always there for me despite of their absence...

Table of contents

Abbreviations

[^{11}C]PiB	2-(4'-[^{11}C]Methylaminophenyl)-6-hydroxybenzothiazole
[^{18}F]FBEM	*N*-[2-(4-[^{18}F]-Fluorobenzamido)ethyl]maleimide
[^{18}F]FPy-TFP	6-[^{18}F]Fluoronicotinic acid 2,3,5,6-tetrafluorophenyl ester
[^{18}F]SFB	*N*-Succinimidyl 4-[^{18}F]fluorobenzoate
18-crown-6	1,4,7,10,13,16-Hexaoxacyclooctadecane
2-[^{18}F]F-Tyr	2-[^{18}F]Fluoro-L-tyrosine
6-[^{18}F]FDOPA	L-3,4-Dihydroxy-6-[^{18}F]fluorophenylalanine
6-[^{18}F]FMT	6-[^{18}F]Fluoro-*m*-tyrosine
6-[^{18}F]OMFD	3-*O*-Methyl-6-[^{18}F]-fluoro-L-DOPA
AADC	Aromatic acid decarboxylase
Aβ	β-Amyloid
AD	Alzheimer's disease
BBB	Blood-brain barrier
Boc	*tert*-Butyloxycarbonyl
Bu	Butyl
COMT	Catecholamine-*O*-methyltransferase
CT	Computed tomography
DBU	1,8-Diazabicyclo(5.4.0)undec-7-ene
DCM	Dichloromethane
Dioxane	1.4-Dioxane
DLB	Dementia with Lewy bodies
DMA	Dimethylacetamide
DMF	Dimethylformamide
DMSO	Dimethyl sulfoxide
dppf	1,1′-Bis(diphenylphosphino)ferrocene
Et	Ethyl
EtOAc	Ethyl acetate
EWG	Electron withdrawing group
Hex	Hexyl
HPLC	High-performance liquid chromatography
K222	4,7,13,16,21,24-Hexaoxa-1,10-diazabicyclo[8.8.8]hexacosane
LG	Leaving group

MA	Molar activity
m-CPBA	3-Chloroperoxybenzoic acid
Me	Methyl
MRI	Magnetic resonance imaging
MS	Mass spectroscopy
Mes	Mesitylene
MSA	Multiple system atrophy
NMF	*N*-Methylformamide
NMP	*N*-Methyl-2-pyrrolidone
NMR	Nuclear magnetic resonance
OMs	Methanesulfonate
OTf (triflate)	Trifluoromethanesulfonate
PCC	Pyridinium chlorochromate
PD	Parkinson´s disease
Pen	Pentyl
PET	Positron emission tomography
Ph	Phenyl
Pr	Propyl
Propylene carbonate	PC
py	Pyridine
RCP	Radiochemical purity
RCY	Radiochemical yield
RP	Reversed-phase
SA	Specific activity
TFE	Trifluoroethanol
TMU	Tetramethylurea
Ts (tosyl)	4-Methylbenzenesulfonyl

1 Introduction

Applications of radioactive nuclides in biochemistry and physiology provided first insights into the dynamics of biochemical processes in living systems.[5] Substantially, the rapid growth of medical imaging techniques was a pivotal event in clinical practice. These techniques enabled objective and quantitative measurements of *in vivo* phenomena, extending a deeper understanding of biological processes, and provoked new discoveries in the pathophysiology of diseases and the development of new diagnostic methods.[6] As a result of molecular processes, morphological imaging visualizes structural and physiological alterations in tissue. Usually these events lead to activation or inhibition of enzymes, receptors or signal transduction pathways. In contrast, molecular imaging exploits the interaction of probes with targets involved in biochemical processes *in vivo* to directly visualize these processes. In 1950´s first concepts utilizing radionuclides for medical imaging were developed[7] and the first examples of the applications of positron emission tomography (PET) were reported.[8]

1.1 PET principle

PET and related hybrid methods like PET/CT (computed tomography) and PET/MRI (magnetic resonance imaging) belong to the most important techniques in medical imaging. These techniques play a major rule in research, nuclear medicine and drug development. In PET target-specific tracers labeled with positron emitter nuclide are applied. Since γ–ray penetrating radiation is emitted, direct external monitoring of this radiation is possible making PET a noninvasive technique. Another advantage of PET imaging is that only very small tracer amounts are required (less than 1 ng) to generate a signal with sufficient intensity. Thereby, the generation of pharmacological effects and a toxicological risk for the patient is very unlikely. Only the radiation exposure of the living organism should be taken into account.[9] PET exploits the physical properties of positrons to make an accurate quantitation of regional radioactivity *in vivo* possible. An emitted positron interacts with an electron after deceleration in tissue resulting in the annihilation of both particles. This annihilation creates two photons that travel antiparallel to each other. A pair of external radiation detectors positioned on either side of a positron-emitting source will register these photons at almost the same time (Figure 1.1). This detector pair is connected by a coincidence processing unit that records only signals from two simultaneously arrived photons. The spatial resolution of a pair of annihilation coincidence detectors is nearly uniform for most of the region located between the two

detectors.[10] Therefore, only two photons arising from one positron annihilation event will be recorded.

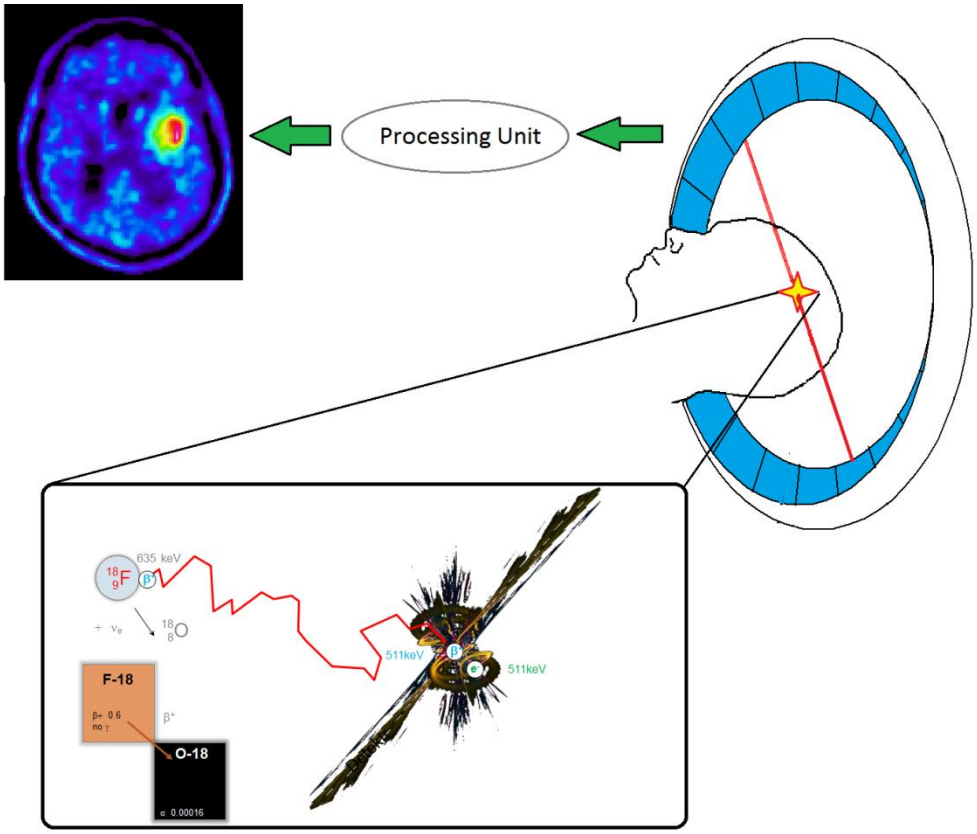

Figure 1.1 Principle of positron emission tomography.

The choice of a suitable PET isotope for medical diagnostics is affected by different independent constraints. Many aspects have to be considered for its selection, such as the intended production route, half-life, chemical reactivity, image resolution, radiation exposure and the desired structural design of the PET tracer that must meet certain physicochemical and pharmaceutical requirements.[9]

Metabolic products and endogenous compounds consist mainly of C-, H-, N-, O-, P- and S-atoms in different combinations. The number of radionuclides with appropriate nuclear properties, which can be produced at small cyclotrons, is limited. Only the "organic" positron emitters like ^{11}C, ^{13}N and ^{15}O can fulfill the requirement of substitution of the stable nuclide by its radioactive isotope that does not alter its pharmacokinetic behavior. Unfortunately, these radionuclides have very short half-lives which limit its practical application with respect to complex preparation procedures and radiotracer application.

Consequently, only easily accessible [^{15}O]H_2O and [^{13}N]NH_4OH are used as tracers for the study of regional blood flow and myocardial tissue vitality, respectively. ^{11}C-Labeled tracers are utilized in the majority of cases for brain imaging. However, the application of ^{11}C-tracers need on-site production of the tracer because of the short half-life of ^{11}C.[9,11]

Nonetheless, ^{18}F is the radionuclide with the highest impact in PET owing to its excellent decay properties, easy accessibility in the form of $^{18}F^-$ at a small cyclotron (Table 1.1). Moreover, a relatively long half-life of ^{18}F ($t_{1/2}$=109 min) enables multistep radiosynthesis and allows transportation of radiofluorinated probes to distant clinic.[9,11,12]

Table 1.1 Decay properties and methods of production of short-lived positron emitters.[13,14]

Nuclide	Half life	Decay	E_{max} of positron	Production
^{11}C	20.4 min	β^+ 99.9%, EC 0.1%	0.960 MeV	^{14}N(p,α)^{11}C
^{13}N	10 min	β^+ 100%	1.199 MeV	^{16}O(p,α)^{13}N
^{15}O	2 min	β^+ 99.9%, EC 0.1%	1.732 MeV	^{14}N(d,n)^{15}O ^{15}N(p,n)^{15}O
^{18}F	109.8 min	β^+ 97%, EC 3%	0.634 MeV	^{18}O(p,n)^{18}F ^{20}Ne(d,α)^{18}F

1.2 Radiolabeling with Fluorine-18

Fluorine chemistry is a steadily expanding research area owing to its impact in clinical and molecular imaging and at not least in drug discovery. Fluorine has a small van der Waals radius (1.47 Å) and is the most electronegative element in the periodic table (3.98 Pauling scale). Additional factors for the design of fluorine-containing pharmaceuticals are: stability of the C–F bond; and the higher lipophilicity of fluorine substituted compounds compared with unsubstituted ones.[17] Therefore, fluorine substitution has a profound effect on small organic molecules.[15,16] Introduction of fluorine has been extensively investigated in drug research as a means of enhancing biological activity and increasing chemical or metabolic stability.

In molecular imaging ^{18}F is of particular importance since it represents the nuclide with the highest impact in PET research: It is easily accessible at a small cyclotron in the form of $^{18}F^-$. Decay characteristics of ^{18}F make it to an ideal PET nuclide with respect to half-life and resolution.[11,18] The maximum positron energy of 634 keV is the lowest of the commonly used PET nuclides and the positron path ($\leq$ 2 mm in water) is in the same

range as the highest spatial resolution achievable with modern PET scanners (about 2 mm).[18]

^{18}F can be produced at a small cyclotron using different nuclear reactions (Table 1.1). The method used to produce ^{18}F depends on the subsequent chemical transformation. For nucleophilic radiofluorination $^{18}F^-$ is produced in aqueous media as $^{18}F^-$ whereas for electrophilic radiofluorination ^{18}F is produced in the form of [^{18}F]F_2. In order to obtain [^{18}F]fluoride for nucleophilic substitutions, the ^{18}O(p,n)^{18}F nuclear process on highly enriched ^{18}O-water target is mainly used (Table 1.1). Application of this nuclear reaction usually leads to product with high specific activities (SA).[19] [^{18}F]F_2 for electrophilic fluorination can be produced by the ^{20}Ne(d,α)^{18}F nuclear reaction. In this case, stable fluorine needs to be added to the neon gas target to prevent adsorption of reactive atomic ^{18}F on the target walls. However, addition of F_2 leads to low specific activities of the labeled products.

1.2.1 Electrophilic substitution

Electrophilic ^{18}F-fluorination is characterized by the reaction of highly polarized ^{18}F with an electron rich reactant, like an aromatic system, an alkene, or a carbanion. [^{18}F]fluorine, the simplest electrophilic fluoro species, is obtained directly from the irradiated target. However, electrophilic fluorination with [^{18}F]fluorine produces a mixture of products because of the high reactivity of [^{18}F]fluorine. The use of metal substituted substrates for radiolabeling directs the [^{18}F]fluorine attack to the electron rich C-M bond and improves the regioselectivity.[20–26] Aromatic *ipso*-^{18}F-fluorodemetalation of aryl trialkyl crystallogens (group IVb) and ^{18}F-fluorodemercuration were widely studied under different conditions.[20–26] Electrophilic carrier-added ^{18}F-fluorodestannylation was found to be the best method to produce ^{18}F-labeled aromatics with high radiochemical yield (RCY) within short preparation time. This reaction is used currently for the preparation of radiolabeled analogues of non-toxic endogenous compounds, such as brain tumor tracers: 3-*O*-methyl-6-[^{18}F]-fluoro-L-DOPA (6-[^{18}F]OMFD) and 2-[^{18}F]fluoro-L-tyrosine (2-[^{18}F]F-Tyr);[27,28] and dopaminergic metabolism tracers: 6-[^{18}F]fluoro-*m*-tyrosine (6-[^{18}F]FMT), L-3,4-dihydroxy-6-[^{18}F]fluorophenylalanine (6-[^{18}F]FDOPA) (Figure 1.2).[29,30]

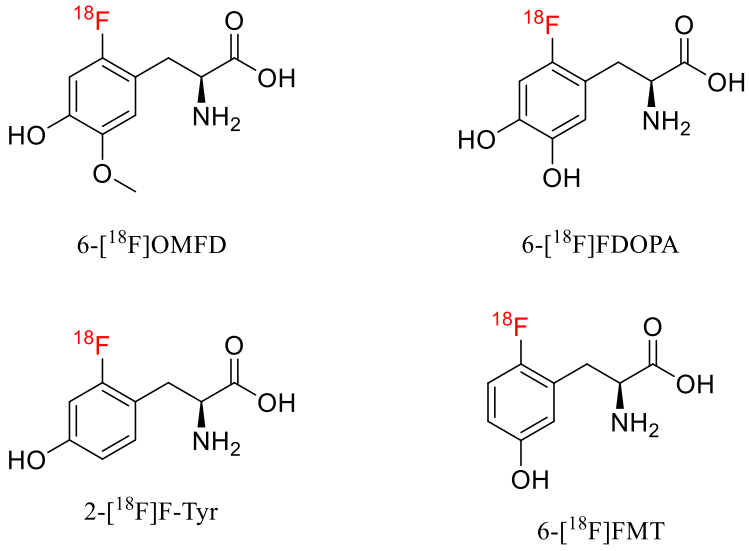

Figure 1.2 Amino acids derivatives prepared using electrophilic radiofluorinaiton.

However, electrophilic ^{18}F-fluorination is less favored nowadays, especially, with regard to the toxicity of some fluoroaromatic amino acid derivatives[31] since products with low SA are obtained.

1.2.2 Nucleophilic substitution

[^{18}F]Fluoride is commonly produced by the nuclear reaction ^{18}O(*p*,*n*)^{18}F in aqueous solution using highly enriched ^{18}O-water target in highly solvated form.[19] In order to activate [^{18}F]fluoride, anion-exchange cartridges (Figure 1.3) are used to retain [^{18}F]fluoride and remove/recover a bulk of ^{18}O-water. Thereafter, aqueous solutions of tetraalkyl ammonium bicarbonates or alkali metal carbonates/bicarbonates/hydroxides together with crown ethers or cryptands are used to elute [^{18}F]fluoride from the cartridge. Crown ethers or cryptands are used to enhance [^{18}F]fluoride nucleophilicity by capturing alkali metal cation and to enable the better solubilization of [^{18}F]fluoride ion in polar aprotic solvents.[18] Water is generally removed by azeotropic distillation with acetonitrile, to produce anhydrous alkali metal or tetraalkyl ammonium [^{18}F]fluoride.[32]

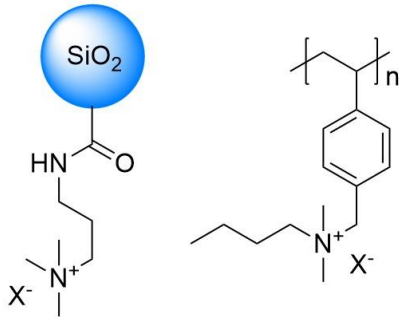

Figure 1.3 Silica based (left) and polymer based (right) anion exchange cartridge resins.

Azeotropic drying is time consuming and causes high losses of radioactivity on the vessel walls during the multiple azeotropic distillation steps (up to four times). Therefore, alternative methods were developed to rapidly prepare reactive [^{18}F]fluoride.[33] For

example according to the "minimalist" approach, methanol was used to wash the anion-exchange cartridge after fixation of [^{18}F]fluoride. Subsequently, [^{18}F]fluoride was eluted from the cartridge with a methanolic solution of an onium salt (like ammonium, iodonium and sulfonium precursors[33] or tetraalkyl ammonium or phosphonium salts[33–35]). Low-boiling MeOH was removed within 3 min to produce anhydrous [^{18}F]fluoride onium salt ready to use for nucleophilic substitution reactions.

For nucleophilic substitution reactions, appropriate leaving groups (LG) are required. Typical examples for leaving groups used in aliphatic ^{18}F-fluorination are iodide, bromide, chloride, tosylate, triflate, mesylate or nosylate. In aromatic systems leaving groups like NO_2, F, Cl, Br, I, $(CH_3)_3N^+$, Ar_2S^+, ArI^+ are used. For all these leaving groups except for iodonium and sulfonium salts the presence of activating substituents (electron withdrawing group [EWG]), such as CN, CHO, COR, COOR, and NO_2 at the *ortho*- or *para*-position of the leaving group are mandatory to obtain the radiolabeled product in reasonable yields (Figure 1.4).[19]

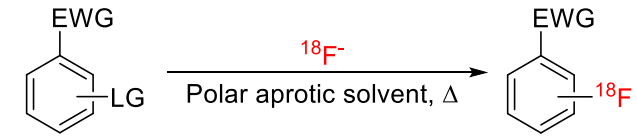

EWG: CN, CHO, COR, COOR, NO_2
LG: 2 or 4-NO_2, -F, -Cl, -Br, -I, Me_3N^+, Me_2S^+, Ar_2S^+, ArI^+

Figure 1.4 Nucleophilic aromatic [^{18}F]fluorination (S_NAr-[^{18}F]fluorination).

Labeling of electron rich aromatic systems using ^{18}F-nucleophilic substitution is challenging and very low RCY are usually obtained.[36] To overcome this problem multistep syntheses starting from activated aromatic compounds have been developed. This multistep syntheses enabled the cGMP production of tracers like 6-[^{18}F]DOPA and 2-[^{18}F]F-Tyr in fair RCYs using mainly custom-made automated synthesis modules.[37]

Radiofluorination via prosthetic groups

Direct ^{18}F-fluorination methods are seldom applicable for labeling of complex molecules (like peptides and proteins) which can be sensitive to heat, organic solvents and/or contain acidic protons which interfere with ^{18}F-labeling.[11,38] In this case, milder indirect ^{18}F-labeling methods have to be used. Three strategies may be applied for labeling of sensitive bioorganic compounds.

The first method uses ^{18}F-labeled small building blocks with a reactive functional group (prosthetic groups). Such building blocks are divided into:

- Amine-reactive prosthetic groups introduced via ^{18}F-fluoroacylation and ^{18}F-fluoroalkylation reactions, like active esters: *N*-succinimidyl 4-[^{18}F]fluorobenzoate ([^{18}F]SFB), 6-[^{18}F]fluoronicotinic acid 2,3,5,6-tetrafluorophenyl ester ([^{18}F]FPy-TFP) and aldehydes: 4-[^{18}F]fluorobenzaldehyde (4-[^{18}F]**4a**).[39,38]
- Thiol-reactive prosthetic groups for labeling cysteine containing peptides via ^{18}F-fluoroalkylation reactions, like maleimides: *N*-[2-(4-[^{18}F]-fluorobenzamido)ethyl]maleimide ([^{18}F]FBEM).[39,38]
- Carboxyl-reactive prosthetic groups targeting carboxyl residues by ^{18}F-fluoroamidation.[40]

The second method employs the high affinity of heteroatoms like silicon, aluminum or boron for fluoride to form stable M-F bonds. Notwithstanding, the specific activity can be increased by reducing the precursor amount below the µg range.[38] The feasibility of this method was exemplified by labeling different organosilico-bombesin derivatives using silicon-fluorine-acceptor (SiFA) technology.[41,42]

Another method utilizes biorthogonal reactions like copper catalyzed click chemistry. This method benefits from the selectivity of the reaction between the appropriately functionalized biomolecules and the corresponding prosthetic group in aqueous media.[38]

1.3 Transition-metal mediated aromatic radiofluorination

Electrophilic ^{18}F-fluorination allows labeling of aromatic compounds only with low SA. On the other hand, nucleophilic ^{18}F-fluorination yields products with high SA but aromatic nucleophilic radiofluorination is limited to activated aromatic compounds. Recently, the concept of late-stage transition-metal mediated ^{18}F-fluorination was reported.[2–4,43–48] This approach allowed to introduce the ^{18}F-label into aromatic compounds regardless of their electronic properties.

1.3.1 Pd- and Ni-mediated aromatic ^{18}F-fluorination

Pd-mediated ^{18}F-fluorination was the first reported method for the transition metal catalyzed synthesis of ^{18}F-labeled arenes. The procedure consists of the reaction of a [^{18}F]Pd(IV) complex prepared in advance which serves as a electrophilic fluorination agent in the reaction with an appropriate Pd(II)–aryl compound. After ^{18}F-transfer the

resulting aryl substituted Pd-complex delivers the ^{18}F-labeled arene via reductive elimination (Figure 1.5 **A**).[49]

A further development of this method involves a one-step oxidative ^{18}F-fluorination of a Ni(II)-aryl complex with a ^{18}F-fluorination agent generated *in situ* from a hypervalent iodine oxidant and [^{18}F]fluoride (Figure 1.5 **B**).[43] The advantage of the Ni-mediated method is the use of only one Ni-complex instead of two Pd-complexes in the Pd-mediated radiofluorination and less starting material. Thereby, the synthesis time is significantly reduced. Unfortunately, the high sensitivity of the oxidant to humidity hampers so far widespread application of this radiolabeling procedure.[50]

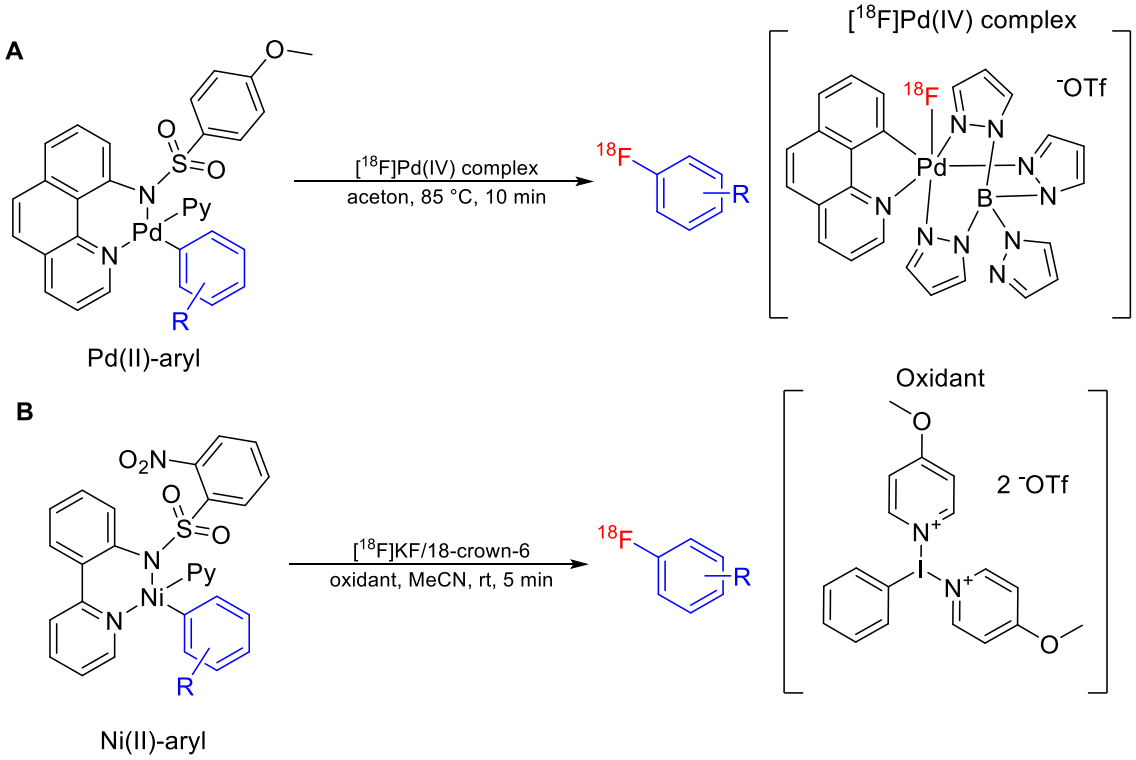

Figure 1.5 A. Pd-mediated ^{18}F-fluorination; B. Ni-mediated ^{18}F-fluorination.

1.3.2 Copper-mediated ^{18}F-fluorination

Numerous Cu-mediated reactions are intensively used in organic preparative chemistry for more than a century since the discovery of Ullmann reaction in 1901. This reaction enables synthesis of symmetric biaryls via copper-catalyzed coupling of arylhalogenides.[51]

In the last few years the copper-mediated fluorination of aryl halides[52], aryl boron reagents (trifluoroborates, aryl boronic acids, aryl boronic acid pinacol esters)[53], aryl

stannanes[54], and (mesityl)(aryl)iodonium salts[55] with fluoride under relatively mild conditions has been reported.

Moreover, some of these procedures were translated to ^{18}F-chemistry (Figure 1.6). The reported copper-mediated ^{18}F-fluorination protocols were applied to produce various radiofluorinated arenes containing electron-donating, -withdrawing and -neutral substituents using substrates with different leaving groups. No special precautions were necessary and ^{18}F-fluorinations could be carried out under air. However, these pioneering methods for copper-mediated ^{18}F-fluorination turned out to be only efficient in small-scale experiments, but were not well-suited for the production of PET tracers on a practical scale (low RCYs or low SAs).[35]

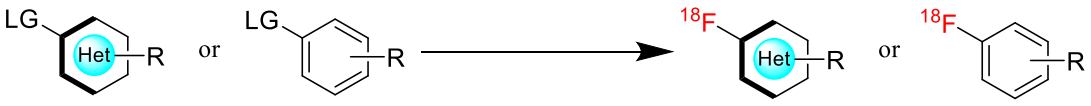

LG: Bpin; $K^{18}F$, $(Py)_4CuOTf_2$, DMF, 110 °C, 20 min
LG: BPin, $B(OH)_2$ or $K^+BF_3^-$; $K^{18}F$, $CuOTf_2$, pyridine, DMF, 110 °C, 20 min
LG: SnR_3; $K^{18}F$, $CuOTf_2$, pyridine, DMF or DMA, 140 °C, 30 min
LG: $I^+Mes\ BF_4^-$, $K^{18}F$, $(MeCN)_2CuOTf$, DMF, 85 °C, 20 min
LG: I; $Ag^{18}F$, $(t$BuCN$)_2CuOTf$, tBuCN/MeCN, 140 °C, 60 min

Figure 1.6 Late-stage copper-mediated ^{18}F-fluorination.

1.3.2.1 ^{18}F-Fluorination of (mesityl)(aryl)iodonium salts

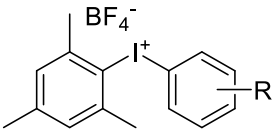

Conventional fluorination of asymmetric diaryliodonium salts directs the addition of [^{18}F]fluoride predominantly to the more electron-poor arene.[56,57] This reaction needs high temperatures (over 100 °C) and provides only low RCYs. Regardless of its electronic properties, copper-mediated nucleophilic substitution of (mesityl)(aryl)iodonium salts undergo sterically-controlled oxidative addition of a nucleophile to the less sterically hindered aryl group while mesityl iodide is eliminated.[55] This copper mediated method was translated to ^{18}F-chemistry by Scott *et. al.*.[46] The preparation of diverse radiofluorinated arenes via copper-mediated ^{18}F-fluorination of (mesityl)(aryl)iodonium salts using [^{18}F]KF/18-crown-6 proceeded at 85 °C within 20 min under air.[46] The disadvantage of this method is the low stability and difficult accessibility of the precursors.

The hypothesized mechanism for such copper-mediated ^{18}F-fluorinations is illustrated in Figure 1.7. It is postulated that the reaction proceeds via a $Cu^{I/III}$ catalytic cycle. Anion metathesis delivers Cu^{I}-F (**A**), which affords after oxidation with iodonium salt a

Cu^{III}-aryl intermediate (**B**). Subsequently, reductive elimination provides a π-complex species **C** that affords the ^{18}F-fluorinated product and the regenerated Cu^{I} catalyst.[46,53,58]

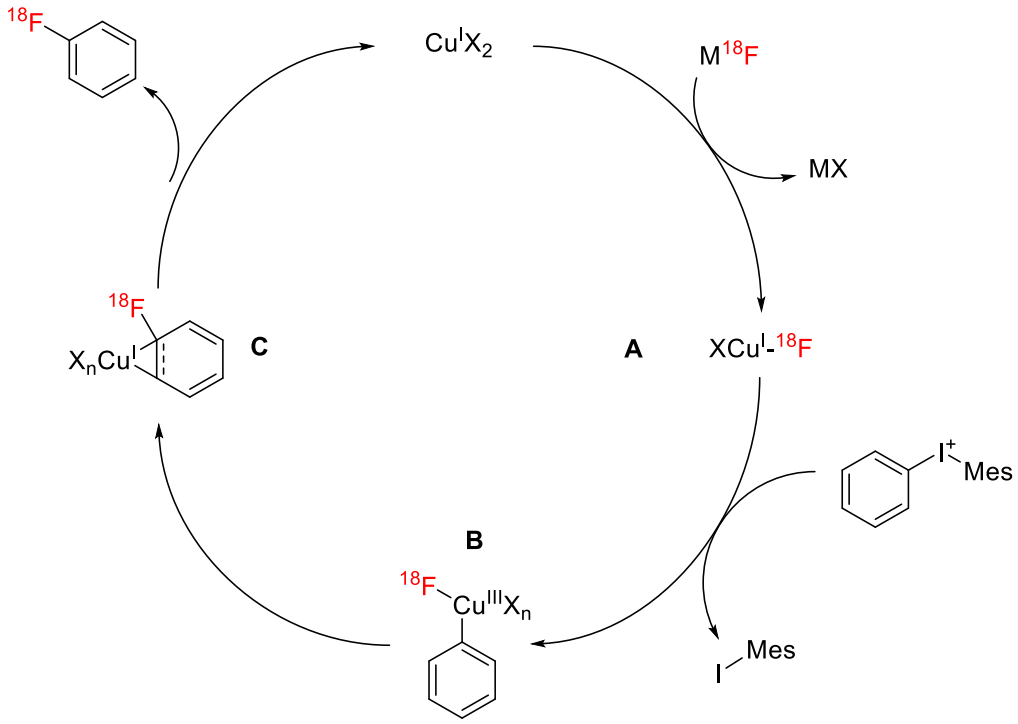

Figure 1.7 Proposed mechanism of copper-mediated fluorination of (mesityl)(aryl)iodonium salts.

1.3.2.2 ^{18}F-Fluorination of aryl boron reagents

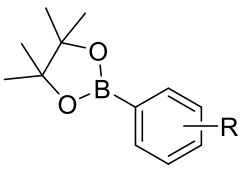

The first protocol for ^{18}F-fluorodeborylation was reported by Gouverneur *et al.*.[45] Accordingly, arylboronic acid pinacol esters were reacted with small aliquots of preliminary azeotropically dried K_2CO_3/[^{18}F]KF/K222 and tetrakispyridinecopper(II) triflate [$Cu(OTf)_2(py)_4$].[53,54] Unfortunately, if the procedure was used for a one-pot synthesis, RCYs decreased dramatically. This was attributed to the instability of the Cu complex under basic reaction conditions.[35] Consequently, low base protocol was developed. Alternatively, potassium oxalate doped with traces of potassium carbonate and higher amounts of $Cu(OTf)_2(py)_4$ were used to obtain reasonable RCYs.[4] However, the improved procedures suffer from the disadvantage of multiple azeotropic distillation steps, which increase radioactivity losses and syntheses time.

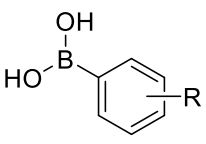

Scott *et al.* demonstrated that aryl boronic acids are suitable substrates for Cu-mediated radiofluorination.[47] According to the radiolabeling protocol KOTf/K_2CO_3/[^{18}F]KF, pyridine and copper(II) triflate [$Cu(OTf)_2$] in DMF were applied to produce the desired ^{18}F-fluorinated

arenes.[47] Again, in this method a low amount of base was used to avoid strong basic conditions. However, the use of the hygroscopic $Cu(OTf)_2$ instead of the bench stable $Cu(OTf)_2(py)_2$ required more precautions. Furthermore, in optimization studies aliquots of previously dried $KOTf/K_2CO_3/[^{18}F]KF$ were used. Therefore, radioactivity losses by the multiple azeotropic steps were not taken into consideration. Moreover, one-pot ^{18}F-fluorodeborylation of arylboronic acids furnished radiolabeled arenes in unexpectedly low RCYs.[59]

1.3.2.3 ^{18}F-Fluorodestannylation

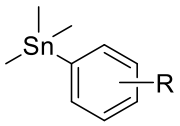

Copper-mediated ^{18}F-fluorodestanylation using copper(II) triflate, potassium triflate doped with potassium carbonate and pyridine was recently reported.[3] Unfortunately, this method suffers from high losses of radioactivity owing to the adsorption of $[^{18}F]$fluoride onto vessel walls of the reactor vial, the high hygroscopicity of copper(II) triflate as well as a complex experimental setup impeding its widespread application.

However, the application of aryl stannanes as precursors for radiofluorination have substantial advantages. These substances are easily accessible (partly commercially available) and already GMP validated for the production of radiopharmaceuticals for human applications.[3] Furthermore, the Sn−C bond tolerates most of functional group manipulations enabling syntheses of complex precursors.

Further copper-mediated ^{18}F-fluorination

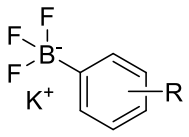

The use of potassium aryl trifluoroborates as substrates for ^{18}F-fluorodeborylation under the same conditions like aryl boronic acids was reported.[2] However, no detailed information about reaction optimization studies and RCYs were presented.

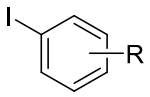

Finally, ^{18}F-fluorodeiodination of aryl iodides was reported recently. This method required preincubation of aryl iodide with $(t\text{-BuCN})_2CuOTf$ in pivalonitrile (*t*-BuCN) for 10 h followed by ^{18}F-fluorination using $[^{18}F]AgF$ in acetonitrile or pivalonitrile at 140 °C for one hour.[2] Deiodination requires long reaction times which are not compatible with the half-life of ^{18}F.

1.4 ^{18}F-Labeled tracers for the diagnosis of neurodegenerative diseases

A hallmark of neurodegenerative diseases is the appearance of misfolded proteins in the brain followed by a progressive and chronic loss of neural tissue in brain systems.[60] Classification of these diseases are based on the most important protein related disorders as tauopathies, α-synucleinopathies, prion diseases, trinucleotide repeat disorders and TDP-43 or FET proteinopathies. The most frequent neurodegenerative disease Alzheimer's disease (AD), is not strictly included in these groups but is defined by both β-amyloid (Aβ) plaques and intracellular tau deposits (Figure 1.8).[61]

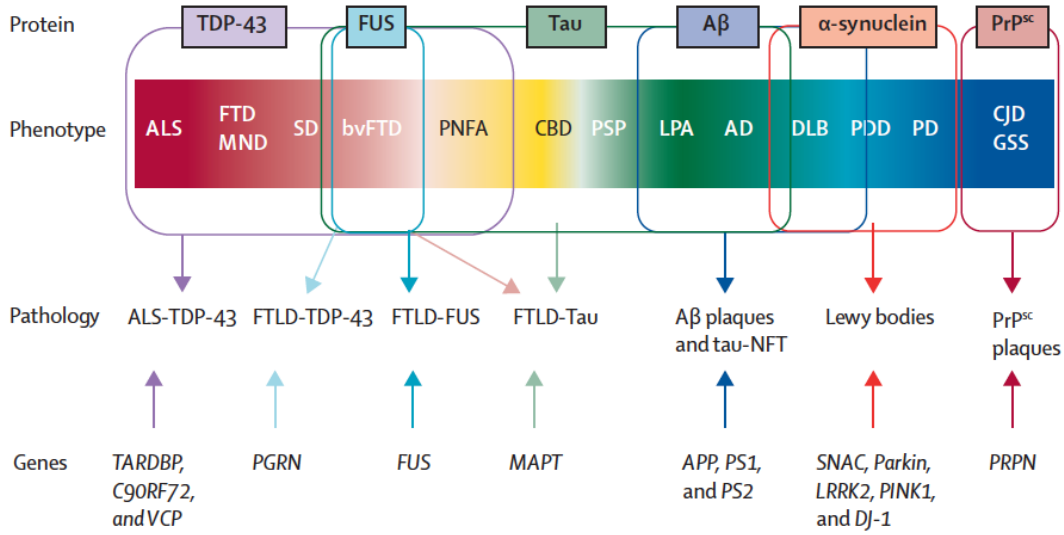

Figure 1.8 Misfolded proteins in neurodegenerative disease; ALS: amyotrophic lateral sclerosis. FTD MND: frontotemporal dementia with motor neuron disease. SD: semantic dementia. bvFTD: behavioral frontotemporal dementia. PNFA: progressive non-fluent aphasia. CBD: corticobasal degeneration. PSP: progressive supranuclear palsy. LPA: logopenic aphasia. PDD: Parkinson's disease dementia. CJD: Creutzfeldt–Jakob disease. GSS: Gerstmann–Sträussler–Scheinker disease. NFT: neurofibrillary tangle.[98]

Neurodegenerative diseases can share similar pathological patterns, for instance, α-synuclein aggregates (PD and dementia with Lewy bodies [DLB]) and dopaminergic deficits (PD and some atypical parkinsonian syndromes).[60] Therefore, accurate differentiation between different neurodegenerative diseases is very important.[60] The contribution of brain PET for differential diagnostics is increasingly gaining importance.

For example, amyloid imaging agents like [^{18}F]florbetaben and [^{11}C]PiB bind selectively to Aβ plaques fibrils in AD (Figure 1.9). These compounds enable to visualize Aß plaques *in vivo* and provide an important tool to study this disease and to bring AD diagnosis to a higher level.

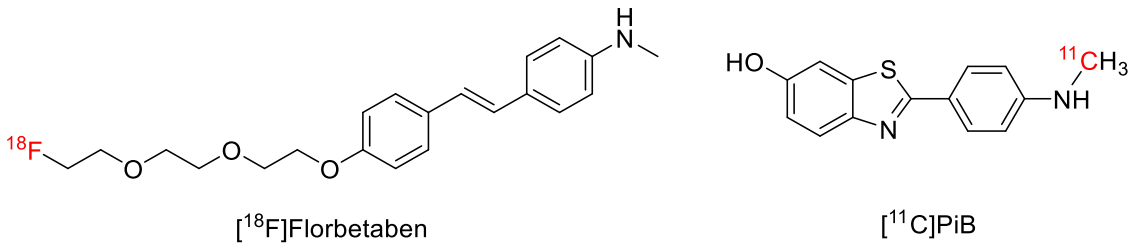

Figure 1.9 AD specific tracers.

In contrast, tracers binding selectively to α-synuclein oligomers which form pathological deposits in PD are still unknown.[62,63] Therefore, the dopamine precursor tracer 6-[^{18}F]FDOPA is used as a surrogate marker for clinical routine purposes to examine dopamine terminal function in α-synucleinopathies. 6-[^{18}F]FDOPA is used to examine the availability of presynaptic dopamine transporters, the activity of aromatic acid decarboxylase (AADC) and the enzyme converting L-DOPA to dopamine (Figure 1.10).[62]

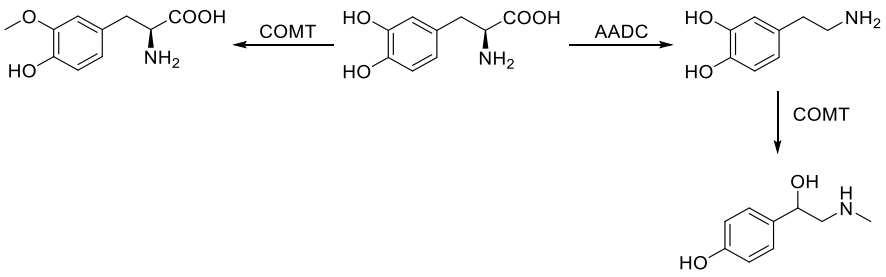

Figure 1.10 DOPA metabolism.

6-[^{18}F]FDOPA PET can demonstrate adaptive changes to putamen dopamine terminal dysfunction, detecting internal rises in AADC activity in early PD, which declines later with disease progression. In DLB, putamen dopaminergic loss is more symmetrical than in PD. However, imaging the pattern of loss of presynaptic dopaminergic function has not been proven to be possible as a reliable tool to differentiate PD and multiple system atrophy (MSA).[62]

The disadvantage of this method is that the enzyme catecholamine-*O*-methyltransferase (COMT) transforms 6-[^{18}F]FDOPA into 6-[^{18}F]OMFD (Figure 1.10). 6-[^{18}F]OMFD can also cross the blood-brain barrier (BBB), distributes widely in brain and compromises image contrast. To overcome this problem, 6-[^{18}F]FMT which is a substrate for AADC but not COMT was developed. 6-[^{18}F]FMT provided better visual contrast and reduced the need for complex multi-compartment kinetic modeling.[29] In turn, 6-[^{18}F]OMFD was applied to visualize brain tumors.[28]

1.5 Comparison of different synthetic routes to 6-[^{18}F]FDOPA

6-[^{18}F]FDOPA is used routinely for the diagnosis of Parkinson´s disease (PD) and other central motor disorders even in their prodromal stage.[64] Therefore, many labeling strategies were developed to produce this valuable tracer. Table 1.2 summarizes different 6-[^{18}F]FDOPA synthesis routes based on conventional and transition metal-mediated ^{18}F-fluorination methods. The conventional electrophilic ^{18}F-fluorination method is used for routine production of 6-[^{18}F]FDOPA. The main disadvantage of this method is the low RCY and molar activity (MA) of the product. In contrast, conventional three step nucleophilic ^{18}F-fluorination synthesis of 6-[^{18}F]FDOPA produced higher yields and MA. The Ni-mediated radiofluorination method delivered very low RCYs. Copper-mediated methods showed different results depending on the leaving group.

Table 1.2 Synthesis of 6-[^{18}F]DOPA with different methods.

	RCY [%]	**ee [%]**	**Starting dose [GBq]**	**MA [GBq/µmol]**	**Time [min]**	**remarks**
Electrophilic "conventional"[65]	33±4 (*n*=13)	No racemization	2.2	10.6±2.3	45	Automated
Nucleophilic "conventional"[37]	36±3 (*n*=8)	98.2±0.6	185	740-1850	62	Automated multistep synthesis
Ni-mediated[50]	7±1	No racemization	6.3	175	50	manual
Cu-mediated (LG=Bpin)[4]	40±4 (*n*=3)	>95	5	-	96	Automated
Cu-mediated (LG=I^{+}Mes)[46]	1.64	-	55.5	10.73	66	Automated, not optimized

2 Aims and scope

A hallmark of Parkinson's disease (PD), prion diseases, dementia with Lewy bodies (DLB) and multiple system atrophy (MSA) is the occurrence of pathological protein aggregates. Recently a series of small molecules was reported to bind selectively to prion proteins and α-synuclein aggregates which have a key responsibility for disease development and progression. Furthermore, [3-(benzo[*d*][1,3]dioxol-5-yl)-5-(3-bromophenyl)-1*H*-pyrazole] (**1a**) represents the most effective candidate as it is able to significantly reduce prion protein and α-synuclein aggregates (Figure 2.1).[1,66,67]

The aim of this work was to prepare ^{18}F-labeled analogs of **1a** (Figure 2.1) to evaluate the potential of this compound for diagnostic purposes. These tracers could represent the first imaging agents for visualization of prion and α-synuclein protein aggregates. They would allow to detect these pathologies in a very early state of disease development and enable the development of novel therapeutic strategies for treatment of patients with neurodegenerative diseases.

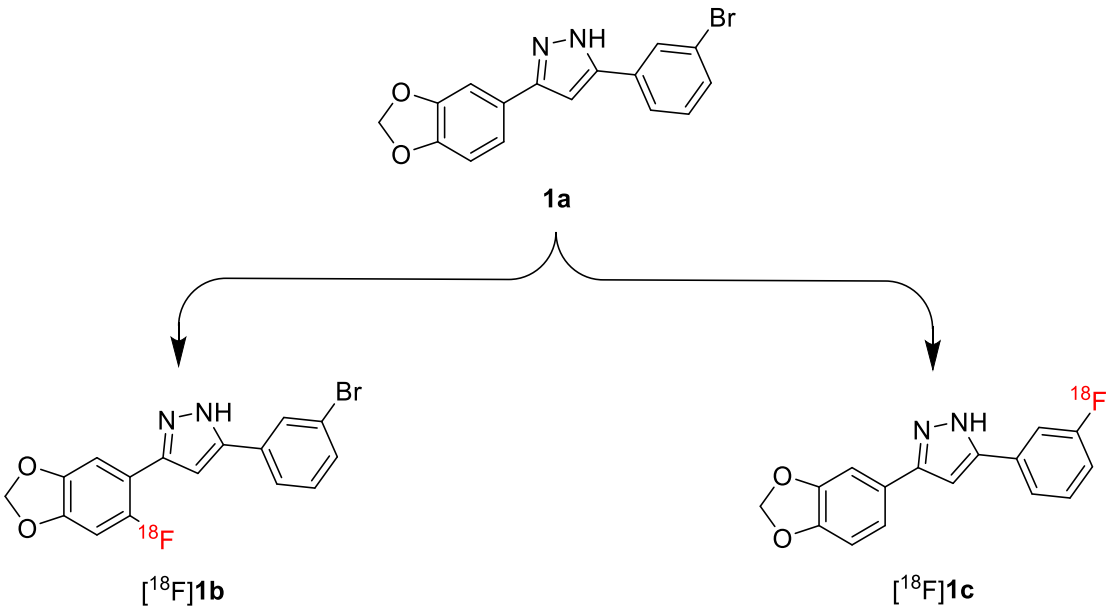

Figure 2.1 potential a-synuclein ^{18}F-tracers.

Initially, [^{18}F]**1b** should be synthesized using 1,3 dipolar cycloaddition between the corresponding radiofluorinated phenyldiazomethane generated *in situ* and 3'-bromophenyl acetylene.

Since multi-step build up synthesis suffered from low yields it was further envisaged to use copper-mediated ^{18}F-fluorination to obtain another α-synuclein targeting compound

[^{18}F]**1c** depicted in Figure 2.1. For this purpose the recently reported Cu-mediated ^{18}F-labeling of aryltrialkylstannanes should be applied.[3]

Since the literature method suffers from severe limitations, a robust, general and efficient protocol for radiofluorination via Cu-mediated ^{18}F-fluorodestannylation should be established. Therefore, this method had to be carefully investigated with respect to distinct reaction parameters using trimethyl(phenyl)tin as a model substrate. These parameters consisted of reaction solvent, temperature, time, water content, and amounts of Cu-complex and precursor. Additionally, the preprocessing of [^{18}F]fluoride had to be adapted and optimized for the subsequent labeling process.

The good amenability to automation should be one of the most important requirements of the novel labeling procedure. This point should be addressed by the implementation of the procedure to the automated production of clinically relevant PET-probes like 6-[^{18}F]FDOPA, 6-[^{18}F]FMT and others from commercially available stannane precursors. Finally, the novel procedure should be used to obtain compound [^{18}F]**1c**.

3 Results and Discussion

3.1 Multistep synthesis of 5-(3-bromophenyl)-3-(6-[^{18}F]fluorobenzo[*d*][1,3]dioxol-5-yl)-1*H*-pyrazole ([^{18}F]**1b**)

The initially developed synthesis of [^{18}F]**1b** comprised 1,3 dipolar cycloaddition between ^{18}F-fluorinated phenyldiazomethane generated *in situ* from the corresponding tosylhydrazone ([^{18}F]**3**) in the presence of a base and 3'-bromophenyl acetylene (**2a**).

This transformation was optimized using 4-[^{18}F]fluorobenzaldehyde (4-[^{18}F]**4a**) to produce [^{18}F]**1d** as a model compound (Figure 3.1).

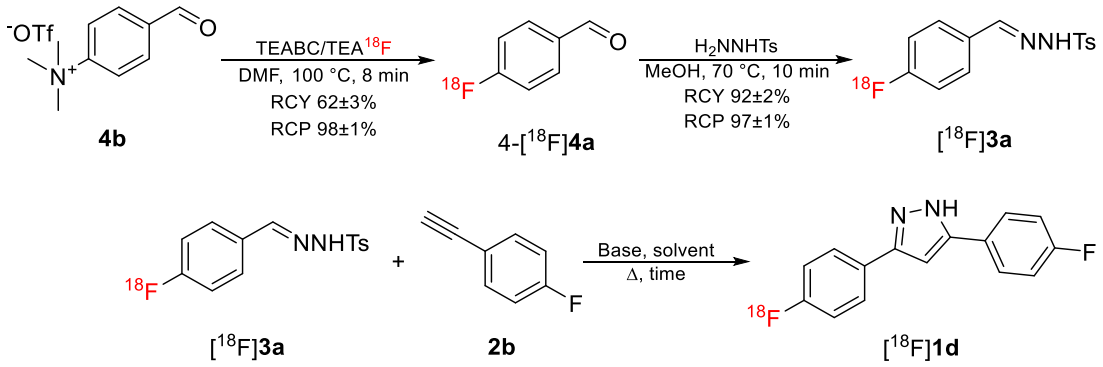

*Figure 3.1 Radiosynthesis of model compound [^{18}F]**1d**.*

The first two steps of the synthesis (^{18}F-fluorination of **4b** and radiosynthesis of [^{18}F]**3a**) were previously optimized.[68] The 1,3 cycloaddition reaction between [^{18}F]**3a** and **2b** was then optimized with respect to solvents, kind of base, reaction time and temperature (c.f. Figure 3.2). Reaction kinetics revealed that the reaction was completed after 25 min at 95 °C and produced [^{18}F]**1d** in good RCY of 66%. A prolongation of the reaction time beyond 25 min did not improve the RCY (Figure 3.2 **B**). Subsequently, the influence of different bases on RCY was determined (Figure 3.2 **A**). Using the alkali bases, potassium carbonate and sodium hydroxide, [^{18}F]**1d** was prepared in 42% and 44% RCY, respectively. 1,8-Diazabicyclo(5.4.0)undec-7-ene (DBU) was less suitable and afforded only a RCY of 33%. The highest RCY of 50% was obtained by using lithium *tert*-butoxide. The dependency of the RCY on the solvent revealed that propylene carbonate (PC) and DMSO were suitable for the preparation of 4-[^{18}F]**4a** and [^{18}F]**3a**. However, the yield of the cycloaddition between [^{18}F]**3a** and **2b** to produce [^{18}F]**1d** was low in DMSO. Yields of >50% were obtained in PC, MeCN and 1,4-dioxane (Figure 3.2 **D**).

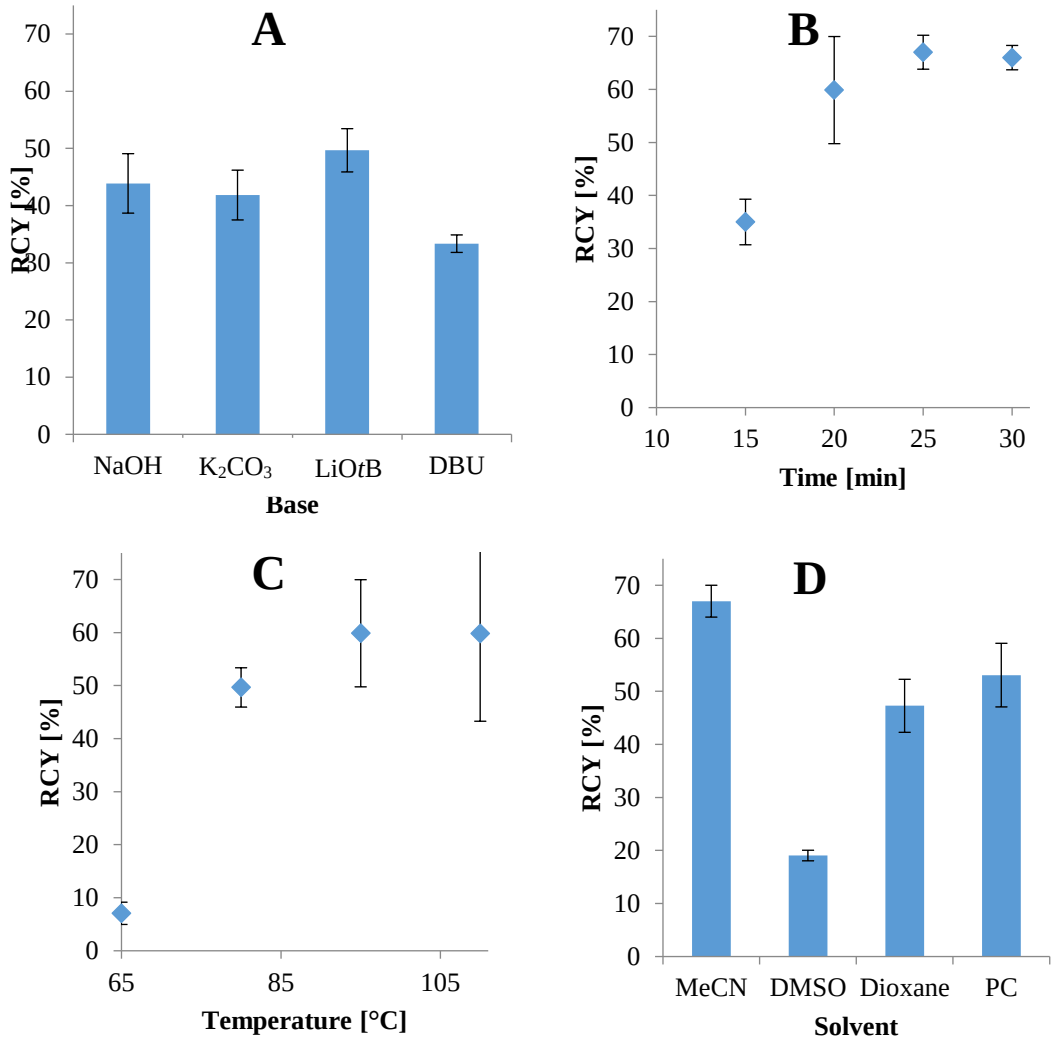

Figure 3.2 ***A.*** *Base optimization;* ***B.*** *Reaction time optimization;* ***C.*** *Reaction temperature optimization;* ***D.*** *Solvent optimization.*

However, the accomplishment of a one pot synthesis in PC as solvent revealed no product formation. In contrast, under optimized conditions using LiO*t*Bu in MeCN for 25 min at 95 °C [^{18}F]**1d** was obtained with RCY 66±3%.

Using optimized conditions [^{18}F]**1b** was synthesized in three steps (Figure 3.3). The building block of this synthesis was commercially available 6-nitropiperonal. Screening experiments to determine the influence of solvents and temperature on the RCY of 6-[^{18}F]fluoropiperonal ([^{18}F]**4c**) showed that DMSO was the most suitable solvent at 130 °C for 10 min reaction time. However, the use of this precursor required HPLC purification to remove 6-nitropiperonal. Without this purification step the RCY of [^{18}F]**3b** was very low and [^{18}F]**1b** was finally not obtained. However, this time-consuming purification step prolongs the synthesis time and decreases the overall RCY significantly. The activity

amount of the obtained product was sufficient for *in vitro* experiments but did not enable to perform *in vivo* examinations. To obviate HPLC purification, excess of 6-nitropiperonal was reduced to 6-aminopiperonal using iron powder and concentrated hydrochloric acid in ethanol at 100 °C for 10 min. After that the product was isolated by solid phase extraction (SPE) chromatography using a reversed-phase (RP) cartridge. First [^{18}F]**4c** was fixed on the cartridge and 6-aminopiperonal was washed from the cartridge with HCl (1 M). However, using this method also low RCYs were obtained and a by-product was detected in the last step having a similar HPLC retention time as [^{18}F]**1b**.

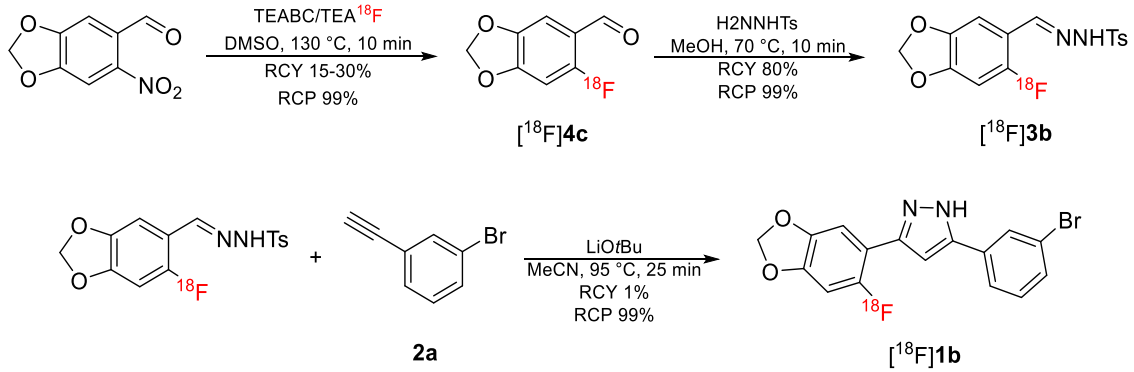

*Figure 3.3 Three steps radiosynthesis of [^{18}F]**1b**.*

Consequently, an onium salt precursor should be used instead of 6-nitropiperonal. This compounds usually allow efficient, time-saving and reliable radiofluorination reactions. The main advantage is that it can be usually easily separated from the labeled product owing to its positive charge using RP SPE purification.[33]

First aryltrimethylammonium triflate salts were selected since these salts are commonly used. To obtain an appropriated onium precursor commercially available 6-bromopiperonal was reacted with an excess of dimethyl amine (40% in water). Unfortunately, this reaction did not produce the corresponding **4d**. This reaction lead to an opening of the methylene bridge in the dioxolane ring forming **4e** (Figure 3.4).

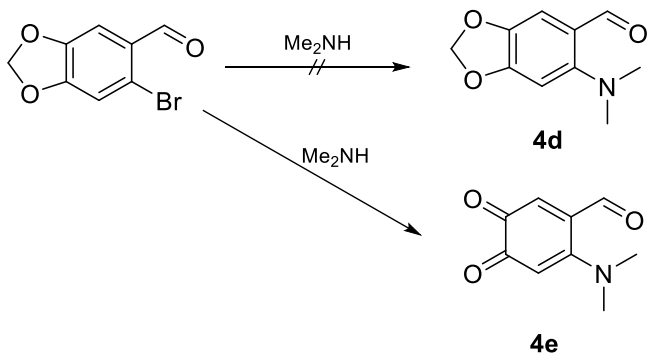

Figure 3.4 Substitution reaction of dimethyl amine with 6-bromopiperonal.

The repetition of the reaction using one equivalent of dimethylamine and one equivalent of potassium carbonate showed again that no product formation occurred after one hour reaction time. The resonance structures shown in (Figure 3.5) could give an explanation for the observed results. In the piperonal ring, the aldehyde group has a strong electron withdrawing effect. In contrast, the dioxolane group is not aromatic, but it disrupts significantly the electron delocalization and impairs the formation of the induced ring current.[69] Therefore, the resonance structures alternates between **II** and **III** (the blue path), rather than between **II** and **IV** (the green path). Consequently, formyl group stabilize resonance structure **III**.[70–73]

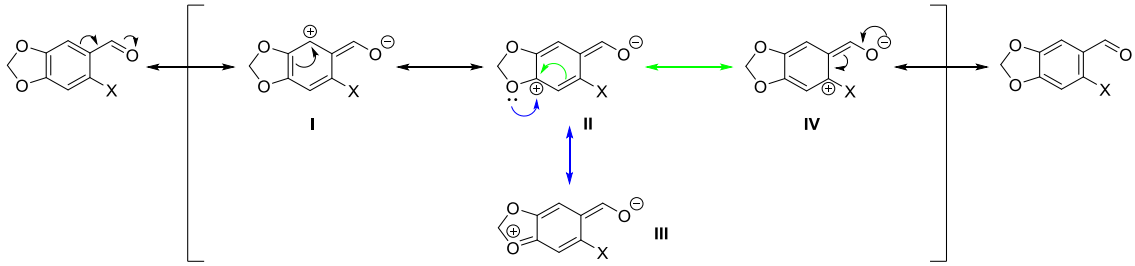

Figure 3.5 Proposed resonance structures of 6-substituted piperonal.

Therefore, a nucleophilic attack on the dioxolane carbon is more likely resulting in the cleavage of dioxolane ring followed by the formation of product **4e** (Figure 3.6).[70–73]

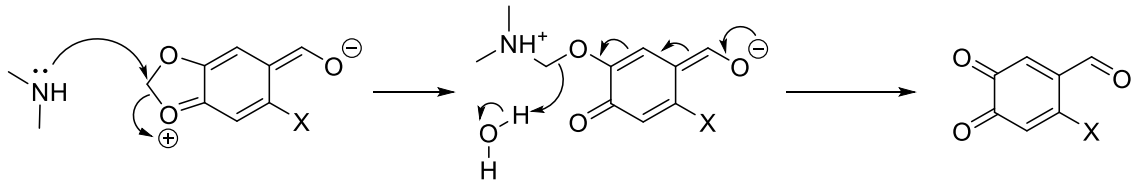

Figure 3.6 Mechanism of dioxolane ring cleavage in piperonal in solution of aqueous dimethylamine.

To avoid the use of nucleophilic reagents and strong basic reaction conditions, direct reductive methylation (Eschweiler-Clarke methylation) of **4f** was investigated (Figure 3.7).[74] **4f** was prepared from 6-nitropiperonal using iron powder and catalytic amounts of concentrated HCl in a water/ethanol mixture in very good yields. The reductive methylation proceeds under acidic conditions using sodium cyanoborohydride as reducing agent (hydride donor).

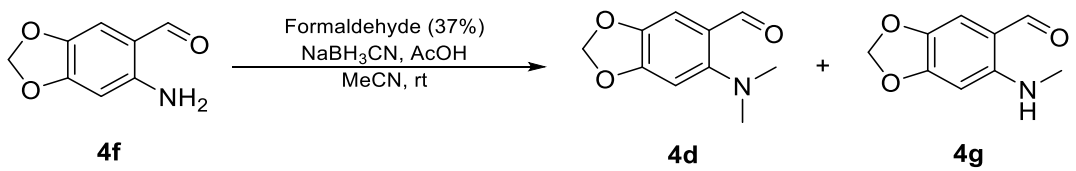

*Figure 3.7 Reductive methylation of **4f**.*

This reaction produced a mixture of mono- and di-methylated products (**4d** and **4g**). The variation of reaction conditions (temperature, time, excess of reagents) delivered a mixture of 95:5 or 70:30 of **4g** and **4d** respectively. This mixture could not be separated with classical flash chromatography. Only preparative HPLC enabled to separate **4d** from **4g**, which was time-consuming and costly due to high solvent consumption (mobile phase). Therefore, this route was not further pursued.

The last method was examined to prepare the desired ammonium salt, was to use nucleophilic substitution with dimethylamine hydrogenchloride ($Me_2NH.HCl$) of fluoride in 6-fluoropiperonal (**4c**). This compound was synthesized according to the literature starting from 6-fluoroveratrol aldehyde (Figure 3.8).[75,76] Demethylation of the aldehyde by boron tribromide produced **4h** in excellent yield. This compound was easily oxidizable under air; therefore, it was alkylated directly with bromochloromethane to yield **4c**. Consequently, the reaction of **4c** with dimethylamine hydrogen chloride in the presence of potassium carbonate delivered **4d** as the only product in this transformation. However, the quaternization under inert conditions of **4d** did not deliver the desired salt. Methyl iodide as a methylation agent in acetone or in ethyl acetate (EtOAc) did not react with **4d**, which was always quantitatively recovered. In contrast, the reaction of methyltriflate with **4d** in dichloromethane (DCM) produced a white precipitate which consisted of a product mixture (c.f. Appendix II). Unfortunately, purification of this mixture using flash chromatography did not succeed. Moreover, the analysis of the crude mixture did not show any trace of the desired product.

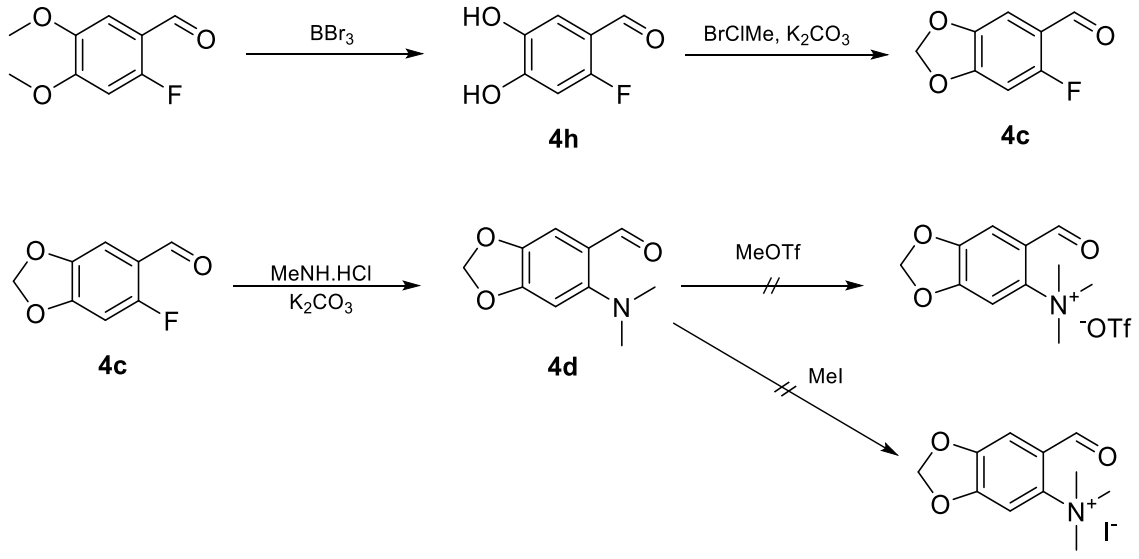

Figure 3.8 Synthesis scheme for 6-N,N,N-trimethylbenzo[d][1,3]dioxol-5-aminium salt.

In a next step, unusual onium salts with piperonal ring system were examined. The first reaction pathway comprised was pyridinium salts that could be prepared by Zincke reaction (Figure 3.9). This reaction proceeds over nucleophilic addition of the amine to the activated *ortho* position in pyridinium derivatives, followed by ring opening. After that amine exchange, and electrocyclic ring closure should take place. However, heating of 6-aminopiperonal and *N*-(2,4-dinitrophenyl)pyridinium chloride (Zincke salt) did not result in product formation.

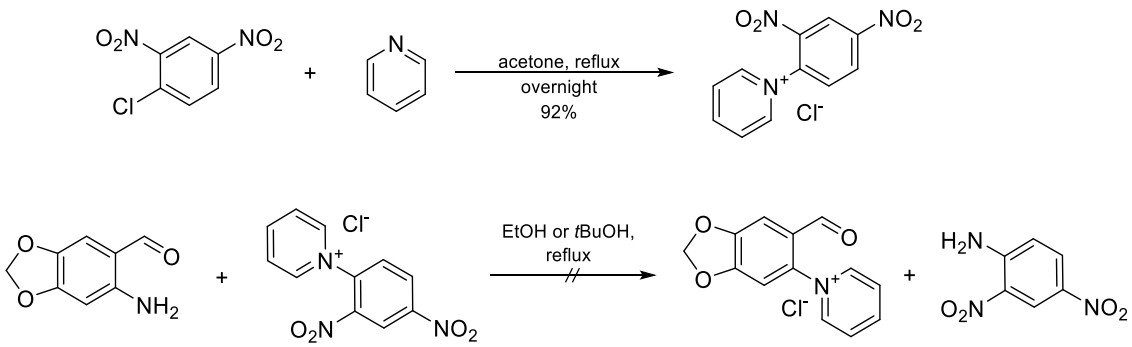

Figure 3.9 Possible synthesis path of 1-(6-formylbenzo[d][1,3]dioxol-5-yl)pyridin-1-ium chloride.

Finally, the synthesis of triphenylphosphonium salts was examined. The reaction of triphenylphosphine with 6-bromopiperonal using tris(dibenzylideneacetone)dipalladium(0) as a catalyst to produce the corresponding phosphonium salt did not work out.

Since the preparation of the onium precursor was not successful the opportunity to use late-stage copper-mediated ^{18}F-fluorination was considered. In this case, 3,5-disubstituted pyrazole with an appropriate leaving group should be synthesized.

3.2 Preparation of precursors for copper-mediated radiolabeling of 3,5-disubstituted pyrazoles

Two methods for the synthesis of 3,5-disubstituted pyrazole derivatives were used (Figure 3.10). The first method employed 1,3-cycloaddition of diazo species – generated *in situ* from tosylhydrazone – with alkynes.[77–79] Tosylhydrazones were easily produced by condensation of tosylhydrazide and the corresponding aldehyde. The second method utilized the condensation of hydrazine hydrate with 1,3-diketones. The later were previously synthesized by the reaction of acid chlorides and ketones.[80]

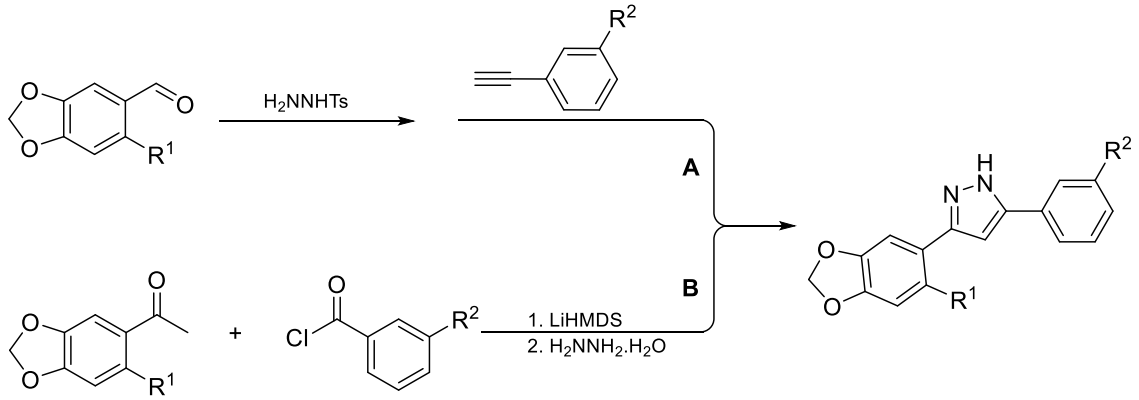

Figure 3.10 methods for the synthesis of 3,5-disubstituted pyrazole derivatives.

3.2.1 Synthesis of aldehydes and ketones

Piperonal derivatives for subsequent radiofluorination were prepared for 1,3-cycloaddition method as following (Figure 3.11): synthesis of **4c** was described earlier. Iodination of piperonal alcohol with iodine and silver trifluoroacetate followed by the oxidation of hydroxyl group with pyridinium chlorochromate (PCC) produced **4i** as described in the literature.[81] **4j** was prepared from the corresponding boronic acid (**4m**) and pinacol. Additionally, treating **4m** with potassium bifluoride produced **4k** in good yield. Finally, 6-bromopiperonal was treated with hexamethylditin using $Pd(PPh_3)_4$ as catalyst to produce **4l**.

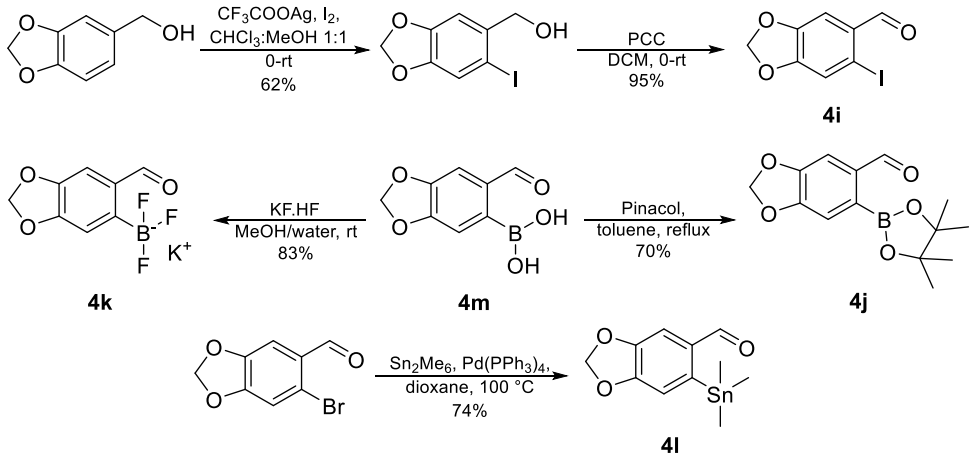

Figure 3.11 Synthesis of different piperonal derivatives for the synthesis of radiofluorinated pyrazole derivatives.

For 1,3-diketones method different acetophenone derivatives were synthesized (Figure 3.12). Methylation of piperonal using methylmagnesium bromide produced the alcohol **5a**, that was iodinated with iodine in the presence of silver trifluoroactate to deliver **5b**. The oxidation of **5b** with PCC produced **6a** in excellent yield. Like piperonal, 6-bromopiperonal was methylated and oxidized to produced **5c** and **6b** respectively.

Bromine in the later was then substituted with trimethyltin using $Pd(PPh_3)_4$ to produce **6c**. Finally, the nitration of 3′,4′-(methylenedioxy)acetophenone with nitric acid (65%) yielded **6d**.

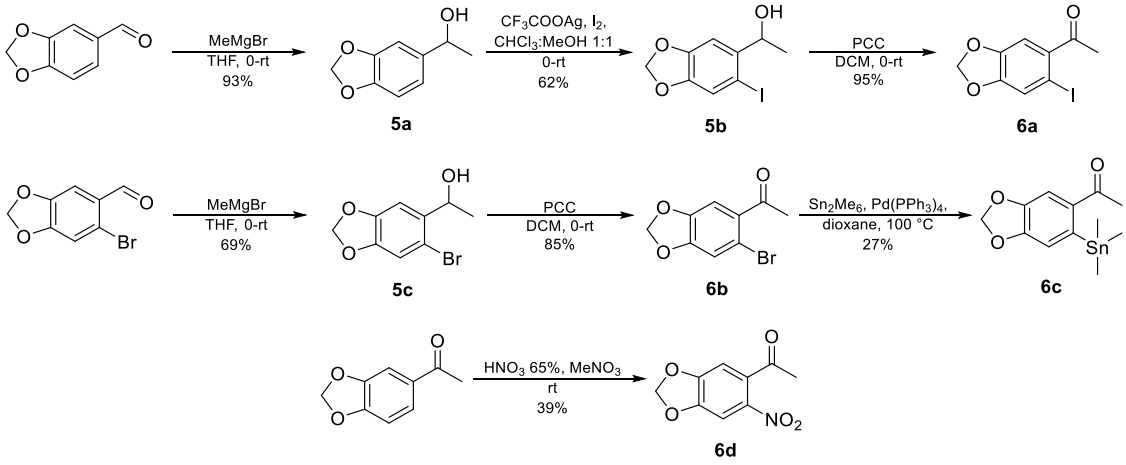

Figure 3.12 Synthesis of different acetophenone derivatives.

3.2.2 Synthesis of acetylene

To prepare **2a** Coery-Fuchs reaction was the method of choice (Figure 3.13 **A**). This reaction included two sequential steps. The addition of 3-bromoaldehyde to a reagent prepared from interaction of zinc dust, triphenylphosphine, and tetrabromomethane produced **7**. However, the reaction of this compound with *n*-BuLi followed by hydrolysis was not successful and did not produce the desired terminal acetylene.

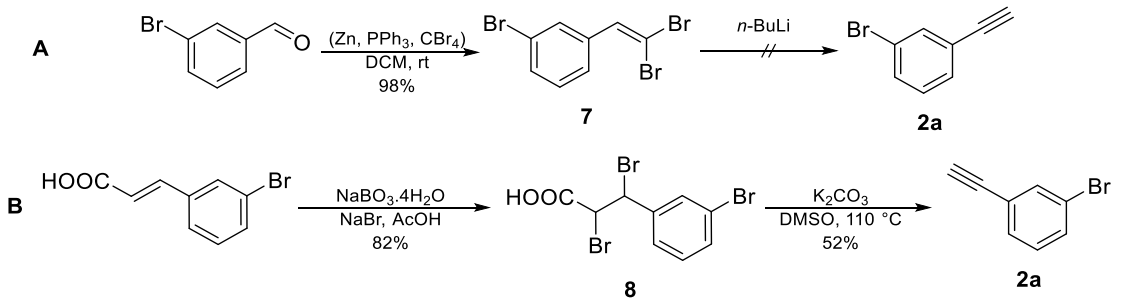

*Figure 3.13 Synthesis of **2a**.*

Another reaction starting from 3-bromocinnamic acid was successful and produced **2a** in 10 g scale (Figure 3.13 **B**). The reaction consists of two steps. The first step includes bromination of 3-bromocinnamic acid with sodium perborate that readily oxidizes sodium bromide to produce compound **8** in good yields. The second and last step was the elimination reaction using potassium carbonate in DMSO. The advantage of this method, that both steps do not require any precautions or inert conditions.

3.2.3 Synthesis of precursor using 1,3-cycloaddition reaction

Primary experiment utilized the procedure reported by Aggrawal *et. al.* to synthesize **1d** (Figure 3.14).[77] This procedure required excess of the acetylene derivative and long reaction time and provided **1d** with low yield.

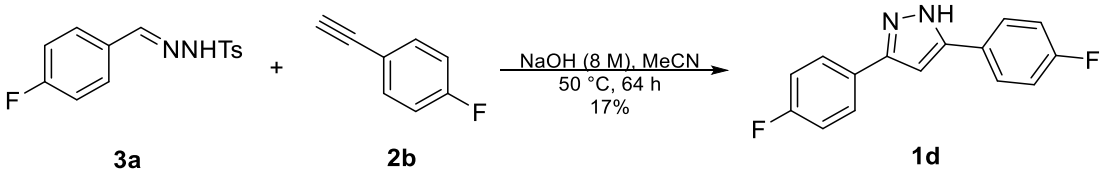

*Figure 3.14 Synthesis of **1d** after Aggrawal et. al. procedure.*

Therefore, the synthesis of **1** were carried out using the optimized conditions from [^{18}F]**1d** synthesis. Thus, **1** were regioselectively produced by 1,3 dipolar cycloaddition of **2a** with *in situ* generated diazo compound (Figure 3.15). The later was promoted from tosylhydrazones **3** in the presence of a base. Tosylhydrazones **3** were synthesized using always the same procedure. Aldehyde **4** was stirred at ambient temperature with tosylhydrazide, after 2 h the product precipitated and was easily filtered off. The yield of **3** was very good but not in the case of **3g**. The product did not precipitate and **4l** was not completely reacted after 24 h. Therefore, chromatography purification was required to isolate the product, which was partly lost during the purification process.

The synthesis of **1** was carried out as one-pot two sequence synthesis starting directly from the aldehyde **4**. This alternative did not affect the yield. Moreover, the use of toluene instead of MeCN at 95 °C produced the same products yield. However, this method produced a lot of by-products that required twice or thrice gravity chromatography purification using different mobile phases or multiple recrystallizations. Consequently, if the reaction was carried out under argon atmosphere and inert conditions some by-products disappeared, but multiple purification steps were always required.

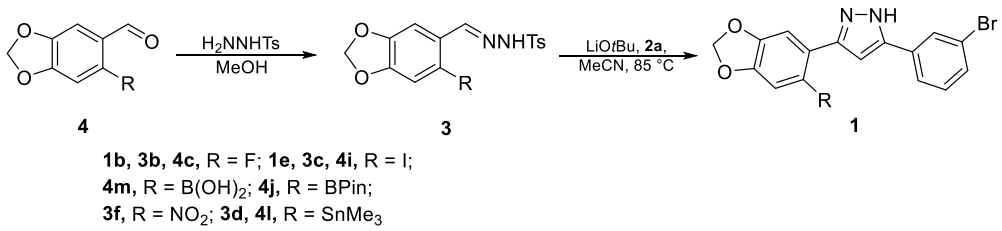

*Figure 3.15 Synthesis of pyrazole **1** over 1,3-cycloaddition of diazo compound and alkyne **2a**.*

In these method aldehydes **4j-m** and tosylhydrazones **3d,e** did not produce the desired pyrazole. Monitoring the reaction with mass spectroscopy (MS) under variation of

reaction conditions (1,4-dioxane instead of MeCN or toluene and the use of DBU or K_2CO_3 instead of LiO*t*Bu) did not show any traces of the desired products.

To synthesize appropriate precursor for copper-mediated ^{18}F-fluorination the substitution of iodine in pyrazole **1e** was tested (Figure 3.16). First, Miyaura borylation reaction was carried out with **1f** using Pd(dppf)Cl_2. This transformation did not proceed and **1f** was quantitative recovered. Then the oxidation of **1f** with 3-chloroperoxybenzoic acid (*m*-CPBA) in DCM produced precipitate of **1e**. The use of **1g** did improve the results and did not produce the desired iodonium salt.

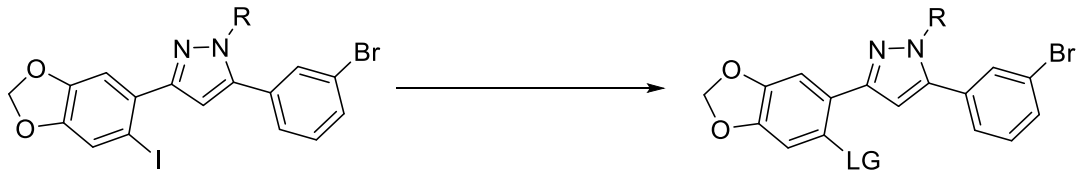

1e, R = H; **1f**, R = Boc; **1g**, R = Tos
LG= Bpin, I^+Mes, $SnMe_3$

*Figure 3.16 Substitution of iodine in **1e-g** with a leaving group.*

Additionally, the substitution of **1e** with hexamethylditin using Pd(PPh_3)$_4$ as catalyst produced the protonated pyrazole **1a**. The reaction was repeated under more precautions and adding molecular sieve to the reaction mixture. Consequently, the product was detected in MS of the reaction crude mixture. However, after flash chromatography purification the product decomposed and produced always **1a**. Thus, synthesis of **1h** was then carried out over 1,3-diketones method to overcome flash chromatography purification of **1h**.

3.2.4 Synthesis of precursor using 1,3-diketones/enolate route

To overcome the multi purification steps of **1** synthesized over 1,3-cycloaddition another method was tried. The acetylation of *in situ* generated enolate of **6** was found to be very efficient to produce enolate **9**. This product (**9**) was confirmed by NMR and no 1,3-diketone was detected. Consequently, condensation of the produced enolate **9** with hydrazine mono hydrate produced **1** with excellent purity (Figure 3.17).

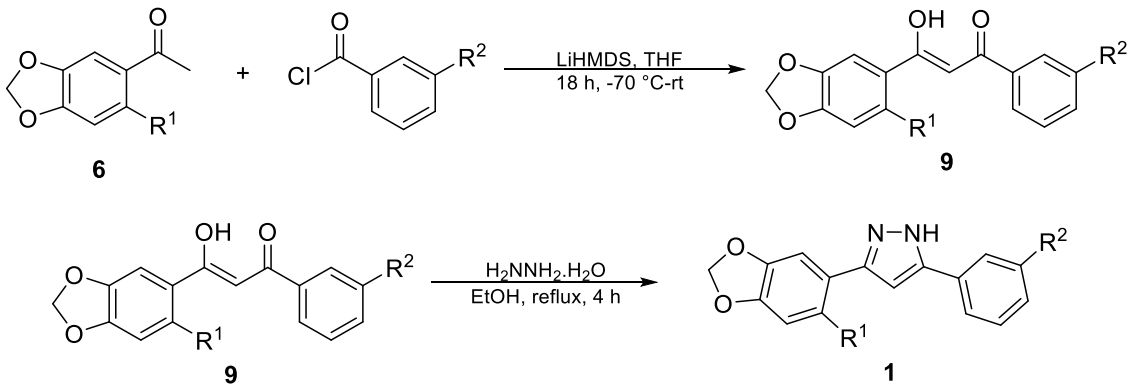

6a, R^1 = I; **6c,** R^1 = $SnMe_3$; **6d,** R^1 = NO_2; **9a,** R^1 = I, R^2 = Br; **9b,** R^1 = $SnMe_3$, R^2 = Br; **9c,** R^1 = H, R^2 = Br; **9d,** R^1 = H, R^2 = F; **1a,** R^1 = H, R^2 = Br; **1c,** R^1 = H, R^2 = F; **1e,** R^1 = I, R^2 = Br; **1h,** R^1 = $SnMe_3$, R^2 = Br; **1i,** R^1 = H, R^2 = $SnMe_3$

*Figure 3.17 Synthesis of pyrazole **1** over 1,3-diketones/enolates.*

This reaction was carried out using literature modified procedure.[80] Subsequently, it proceeded over two steps and delivered pure products. However, this method as the previous one was not tolerant with some functional groups like trimethylstannyl and nitro (**6c, 6d**). In the case of **6c** the second reaction step with hydrazine mono hydrate produced **1h** according to MS of crude mixture (c.f. Appendix II). However, the reaction produced by-products. Thus, the mixture was purified with flash chromatography. The trimethyltin peak in NMR of the isolated fraction disappeared and MS of purified product detected **1a**. That indicate the instability of this compound during purification.

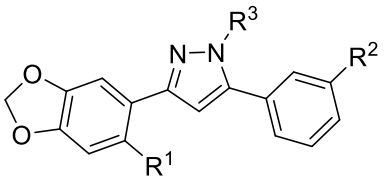

1a, R^1 = H, R^2 = Br, R^3 = H;
1b, R^1 = F, R^2 = Br, R^3 = H;
1c, R^1 = H, R^2 = F, R^3 = H;
1e, R^1 = I, R^2 = Br, R^3 = H;
1f, R^1 = I, R^2 = Br, R^3 = Boc;
1g, R^1 = I, R^2 = Br, R^3 = Tos;
1h, R^1 = $SnMe_3$, R^2 = Br, R^3 = H;
1i, R^1 = H, R^2 = $SnMe_3$, R^3 = H
1j, R^1 = H, R^2 = Br, R^3 = Boc;

Additionally, the implementation of Miyaura borylation on **1f** delivered the same results as before and **1f** was quantitative recovered. This could be attributed to $Pd(dppf)Cl_2$ tendency to bond to pyrazole nitrogen, where Boc rest could play the role of a ligand (Figure 3.18).[82–84] On the other hand, the use of $Pd(PPh_3)_4$ to substitute bromine in **1j** produced always **1i**. The cleavage of Boc protecting group in this reaction support the hypothesis that the used palladium(II) complex with this system could bond to pyrazole nitrogen that restrain the catalytic cycle.

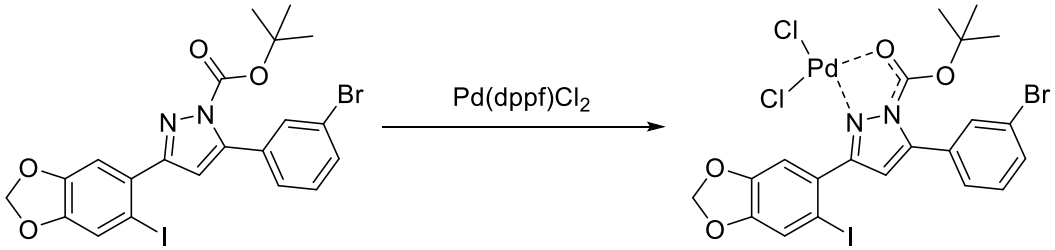

*Figure 3.18 Proposed ligand exchange of $Pd(dppf)Cl_2$ and **1f**.*

3.3 Optimization of copper mediated ^{18}F-fluorination and synthesis of different model compounds and tracers

3.3.1 ^{18}F-Fluorodeborylation

In primary experiments, the feasibility of copper-mediated ^{18}F-fluorodeborylation was examined. ^{18}F-Fluorination of arylboronic acid pinacol ester precursors using $Cu(OTf)_2(py)_4$ and [^{18}F]KF/K222 in DMF at 110 °C for 20 min under air was first described by Gouverneur *et. al.*[45] This procedure afforded [^{18}F]**10**, 4-[^{18}F]**11**, and 3-[^{18}F]**4a** in good RCYs of 66-76% if small aliquots of previously dried [^{18}F]KF/K222 were used. However, under the described conditions in the literature, one-pot radiosynthesis provided [^{18}F]**10**, 4-[^{18}F]**11**, and 3-[^{18}F]**4a** in only 5–7% RCYs. This difference is attributed to the excess of base used in the one-pot procedure. In contrast, reducing the base amount (0.06 mg K_2CO_3 instead of 2.8 mg) afforded ^{18}F-labeled model compounds in high RCYs of 41–64% (Table 3.1).[35]

Table 3.1 RCYs using different base amounts.

Product	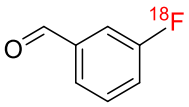 3-[^{18}F]**4a**	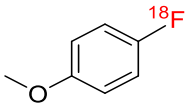 4-[^{18}F]**11a**	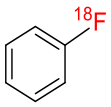 [^{18}F]**10a**
High base RCY [%]	5	7	7
Low base RCY [%]	41	42	64

3.3.2 ^{18}F-Fluorodestannylation

The focus of this work was to improve and optimize copper mediated ^{18}F-fluorodestannylation. The results from optimizing copper mediated ^{18}F-fluorodeborylation confirm that low base amounts should be used in this transformation. Additionally, bench stable $Cu(OTf)_2(py)_4$ should be used instead of hygroscopic $Cu(OTf)_2$. Consequently, optimization of [^{18}F]fluoride preprocessing is very important for this reaction. Moreover, optimization with regard to different solvents, reaction temperature and reaction time is mandatory.

In primary experiments, the elimination of [^{18}F]trimethylfluoride was not detected in the reaction mixture of Et_4N[^{18}F] and trimethyl(4-methoxyphenyl)tin in the presence of $Cu(OTf)_2(py)_4$ in DMA at 100 °C for 10 min. However, the presence of impurities of trimethyltin chloride gave raise to a by-product in the reaction mixture. This by-product disappeared after eliminating any trimethyltin impurities. This indicated that anion

metathesis and disproportionation of copper(II) occurred before the transmetalation step which leads to release of trimethyltin triflate in the proposed mechanism (Figure 3.19). Moreover, the raise of high-valent copper(III) species seems to function as an electron acceptor with higher fluorophilicity than tin which reduces the possibility of eliminating [^{18}F]trimethylfluoride in the transmetalation step. Consequently, the reaction starts with anion metathesis between copper(II) triflate and the ^{18}F-fluorination reagent.[54] Subsequently, disproportionation of Cu(II) to Cu(III) and Cu(I) species proceeds since the reaction is conducted under an air atmosphere.[85] Then, the copper(III) species undergoes transmetalation. Finally, the ^{18}F-fluorinated product is formed after reductive elimination.

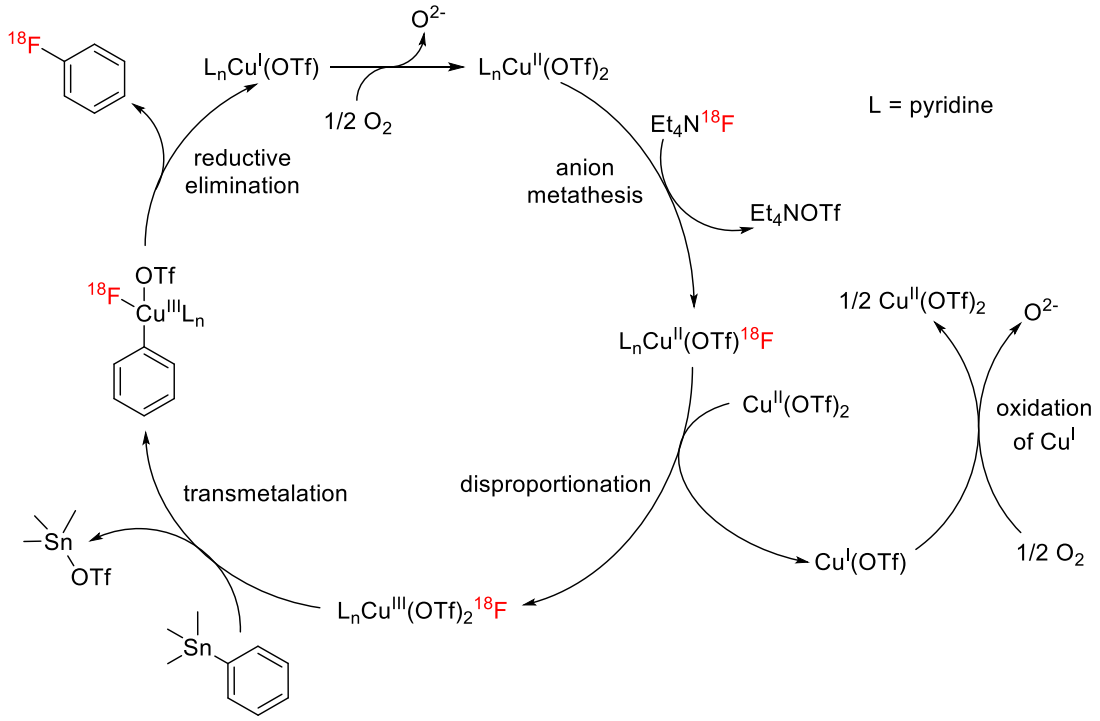

Figure 3.19 Proposed ^{18}F-fluorodestanylation mechanism.

3.3.3 General optimization

The preparation of [^{18}F]fluoride for ^{18}F-fluorodestannylation reaction was first optimized. To accelerate this process MeOH was used instead of water and different tetraethyl ammonium salts (Et_4NX) were used to recover [^{18}F]fluoride from the anion exchange cartridge (QMA-CO_3). After fixing [^{18}F]fluoride on the cartridge, it was rinsed with anhydrous MeOH. Then, various amounts of the salts were utilized to minimize the base contents in the reaction (Figure 3.20). Thus, 2.5 µmol of any tetraethylammonium salt was found to be sufficient to recover over 95% of [^{18}F]fluoride from the cartridge.

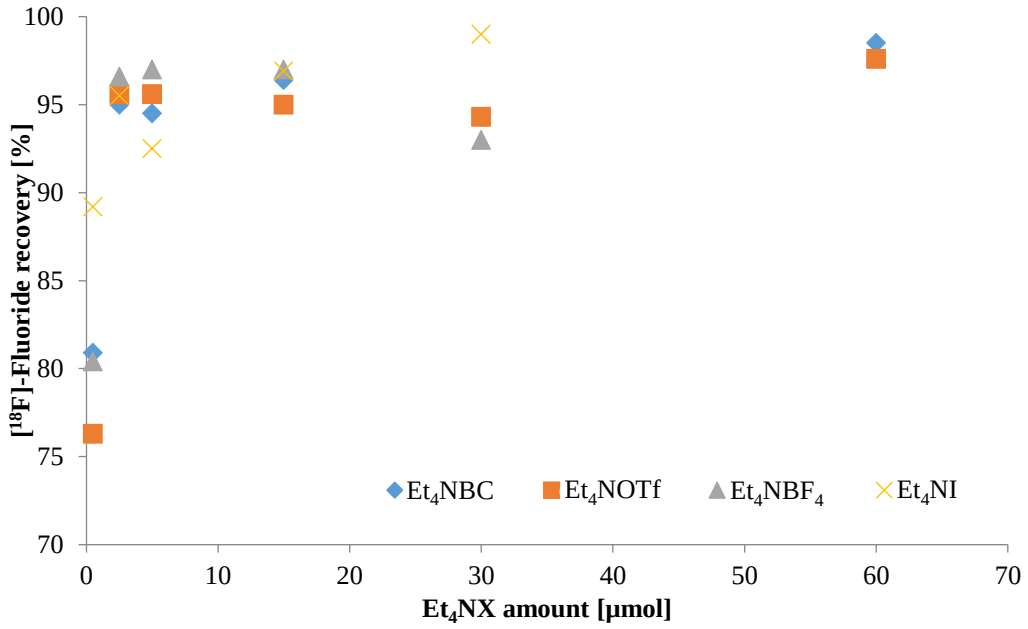

Figure 3.20 [^{18}F]Fluoride recovery using different Et4NX salts.

Subsequently, the reaction of the recovered alcoholic $Et_4N^{18}F$ solution with trimethyl(phenyl)tin (**10b**) and $Cu(OTf)_2(py)_4$ in DMA was considered as a prototype reaction to optimize different parameters (cartridge, fluorination reagent, temperature, solvent, time, water content, precursor and $Cu(OTf)_2(py)_4$ amount).

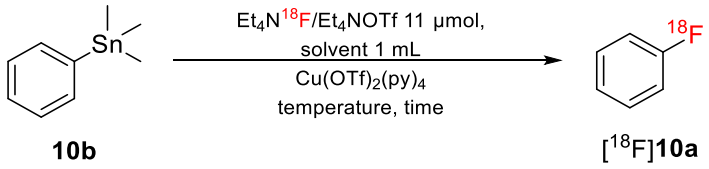

Further investigations in our group showed that copper-mediated ^{18}F-fluorination of arylboronic acid, arylboronic acid pinacol ester or aryltrimethyl tin is tolerant if solvents mixtures of alcohol and DMA are used.[59] This could be explained by the formation of alcohol solvated fluoride "*flexible fluoride*" (Figure 3.21).[86] This fluoride species and alcohol solvated copper (II) triflate accelerated the anion metathesis in the proposed mechanism (Figure 3.19). Moreover, alcohol could assist boron-copper transmetalation, which is an unfavorable reaction.[87,88] This finding has the advantage of performing the labeling reaction after recovering [^{18}F]fluoride from anion exchange cartridge with no need for drying.

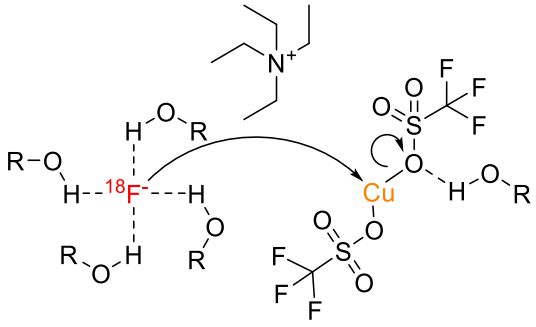

Figure 3.21 The influence of on alcohol anion metathesis.

Therefore, alcohol screening to confirm this finding in ^{18}F-fluorodestannylation was performed. Accordingly, *n*-butanol and *n*-pentanol produced high RCYs that decreased if alcohols with decreased chain length like MeOH or EtOH was used. Reciprocally, the use of *n*-butanol or *n*-pentanol produced lower [^{18}F]fluoride recovery (15-20% activity loss on the anion exchange cartridge) compared to alcohols with shorter chain length like MeOH (Figure 3.22).

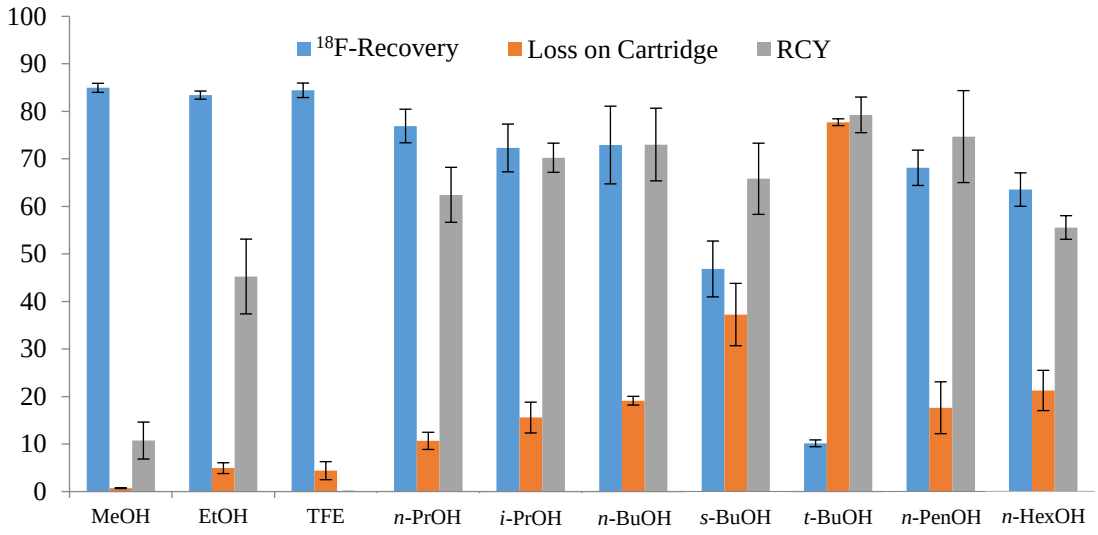

Figure 3.22 Alcohol screening.

After base and alcohol optimization, different anion exchange cartridges with different counter ion were tested. Three commercially available anion exchange cartridges were tested (Figure 3.23). [^{18}F]Fluoride recovery from silica based QMA-CO_3 cartridge was comparable with polymer based StrataX and Chromafix. While carbonate as counter ion on StrataX produced higher [^{18}F]fluoride recovery but lower RCY compared to bicarbonate as a counter ion. However, the best recovery and RCY was obtained using QMA-CO_3. Moreover, other ^{18}F-fluorination reagents were also compared with tetraethyl

ammonium bicarbonate and triflate. The recovery of [^{18}F]fluoride was comparable between KOTf, Bu_4POMs, Et_4NBC and Et_4NOTf. But the best RCYs was obtained in the case of Et_4NOTf.

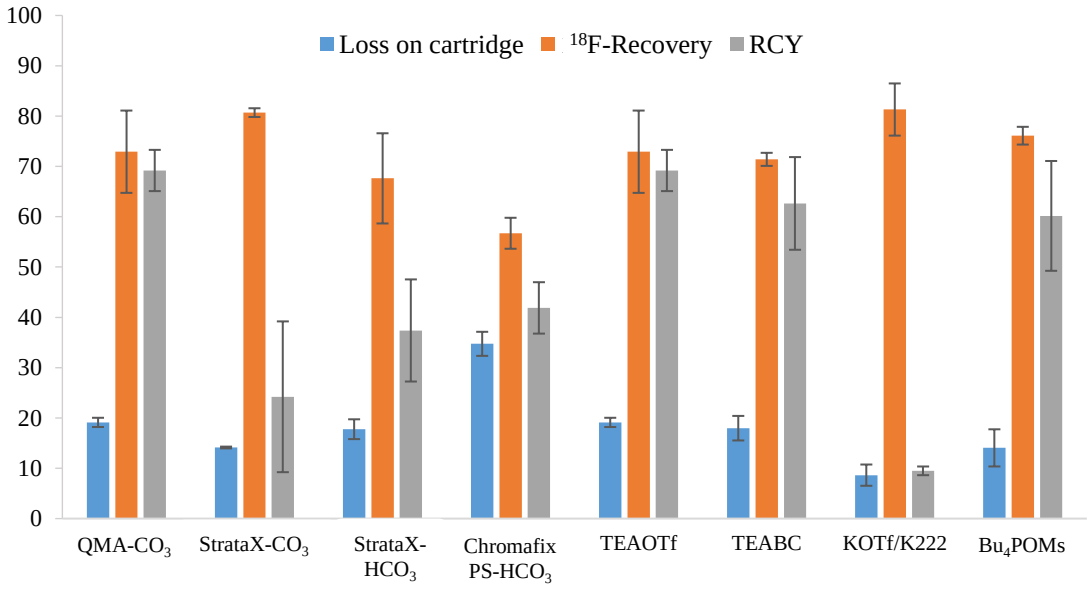

Figure 3.23 Testing different anion exchange cartridges with different counter ion and different ^{18}F-fluorination reagents.

After that, the kinetics of this reaction was studied. Interestingly, ^{18}F-fluorodestannylation proceeded just after 5 min at 100 °C and no significant change in RCY was noticed even after prolonging the reaction time (Figure 3.24 **A**). Raising the reaction temperature from 80 °C to 100 °C increased the RCY considerably. Nevertheless, a reaction temperature higher than 100 °C did not improve the RCY (Figure 3.24 **B**). After that, different solvents mixtures were tested. The mixtures consisted always from three parts *n*-BuOH and seven parts of an aprotic solvent (Figure 3.24 **C**). The reaction did not proceed if pyridine, *N*-methylformamide (NMF) or *t*-BuOH was used. The use of anhydrous DMF and DMSO produced less than 10% RCY. Moreover, the incubation using commercial tetramethylurea (99% pure) produced less than 30% RCY. Only anhydrous *N*-methyl-2-pyrrolidone (NMP) and DMA produced over 70% RCY. Consequently, the water content in the reaction mixture was examined (Figure 3.24 **D**). The contamination of the reaction mixture (*n*-BuOH:DMA 3:7, 1 mL) with water (5 µL) halved the RCY. Moreover, increasing the amount of water (10 µL) further halved the RCY.

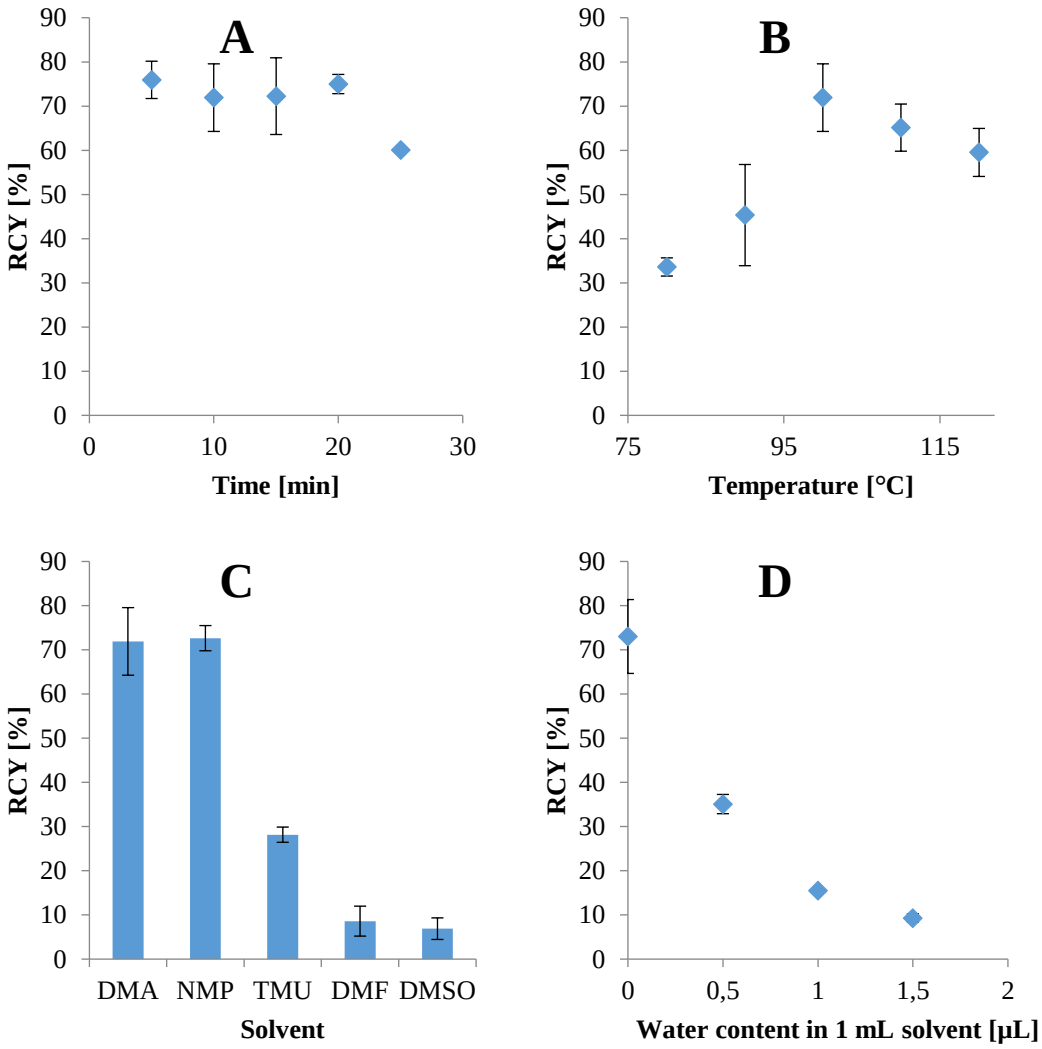

*Figure 3.24 Screening of reaction time (**A**), reaction temperature (**B**), aprotic solvents (**C**) and water content (**D**).*

Then the ratio of *n*-BuOH to DMA was varied to examine the influence of *n*-BuOH on ^{18}F-fluorodestannylation (Figure 3.25). Methanolic Et_4NBC was used to recover [^{18}F]fluoride. Then the incubation in pure DMA delivered RCY of 80%. A mixture of *n*-BuOH:DMA (1:9) show a comparable RCY, if [^{18}F]fluoride was recovered with *n*-BuOH. Moreover, the higher the *n*-BuOH fraction in the solvents mixture, the lower was the RCY of [^{18}F]**10a**. Additionally, the experiments were repeated using always methanol to recover [^{18}F]fluoride. Consequently, the use of DMA, *n*-BuOH:DMA (1:9) or *t*-BuOH:DMA (1:9) produced the similar RCY. However, MeOH as a protic solvent to recover [^{18}F]fluoride was superior to *n*-BuOH. Furthermore, activity loss on the anion exchange cartridge was reduced. MeOH was found to be the best alcoholic solvent for [^{18}F]fluoride recovery and DMA was the best solvent for ^{18}F-fluorodestannylation.

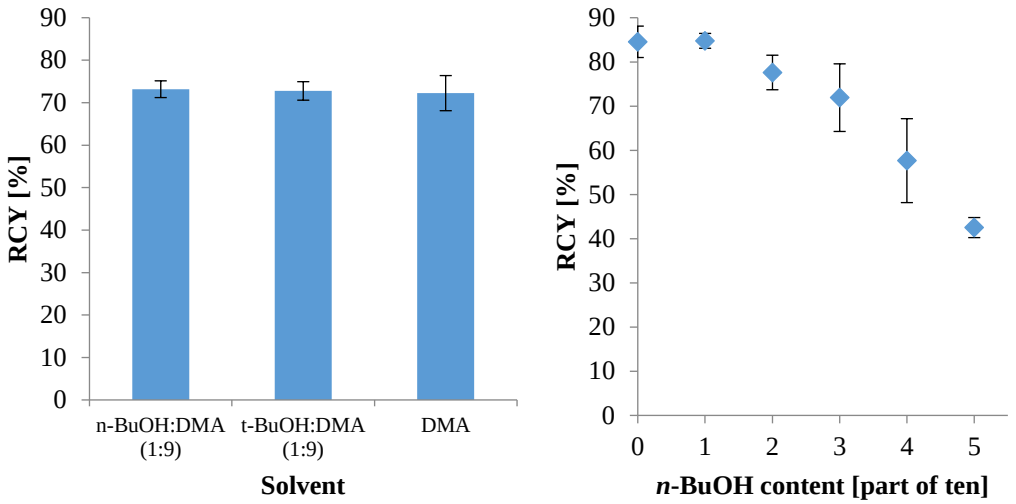

Figure 3.25 Influence of n-BuOH on RCY.

Finally, the amount of precursor and $Cu(OTf)_2(py)_4$ concentration in the reaction mixture was reduced (Figure 3.26). Reduction of precursor simplifies later purification steps of the labeled product and decreases the radiosynthesis costs. The RCY was over 70% if precursor concentration remained beyond 30 mM. Also, the amount of $Cu(OTf)_2(py)_4$ solution should not drop below 30 mM. Reduction of precursor concentration below 20 mM under the same conditions, reduced the RCY to about 10%. Further reduction to 10 µmol produced 20% less RCY.

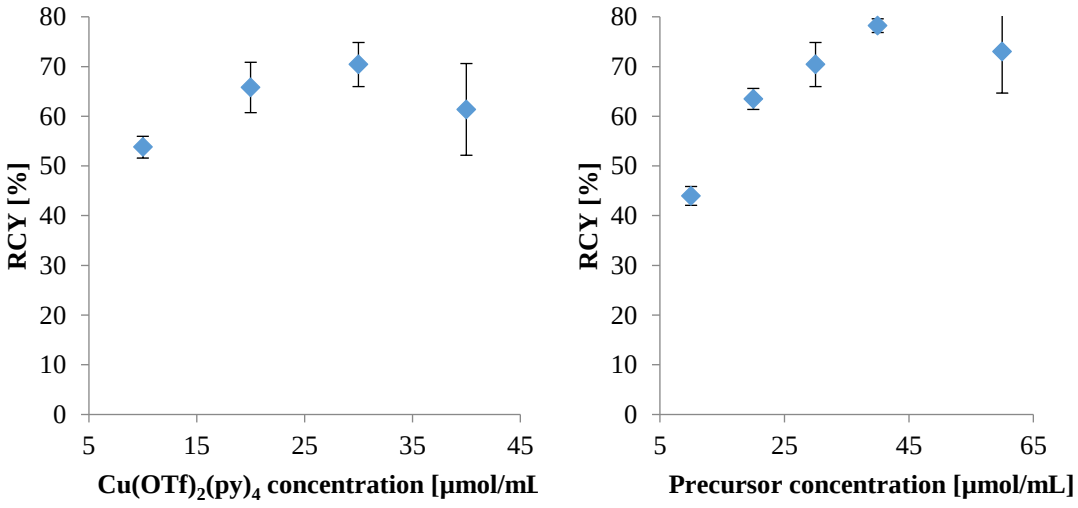

Figure 3.26 Optimization of $Cu(OTf)_2(py)_2$ and precursor concentration.

The variation of $Cu(OTf)_2(py)_4$ using 30 mM precursor showed similar results. The use of 20-40 mM $Cu(OTf)_2(py)_4$ solution produced RCY of >60%. However, loss of more than 10% was noticed if lower amounts of 10 mM $Cu(OTf)_2(py)_4$ were used.

3.3.4 Synthesis of ^{18}F labeled model compounds and [^{18}F]**1c**

Utilizing these results different model compounds and novel tracers were prepared under optimized reaction conditions (DMA, 100 °C, 10 min). It was found that the use of *tert* butyl, trimethylsilyl or trimethyl germane as leaving groups under these optimized conditions did not produce the desired labeled compounds. Only trimethyl tin derivatives afforded the desired labeled compounds in good yields (Table 3.2). The use of tributylstannyl and trimethylstannyl precursors afforded different RCY using different compounds. In the synthesis of [^{18}F]**10a** with the tributylstannyl precursor higher RCYs were obtained compeered to trimethylstannyl derivative. On the contrary, the trimethylstannyl precursor afforded better RCY than the tributylstannyl precursor if 4-[^{18}F]**11a** was prepared. Additionally, *ortho* substituted compounds were not easily accessible using this method. 2-[^{18}F]**11a** was produced in RCY of 16%, while [^{18}F]**4c** and [^{18}F]**3b** could not be prepared by this method. Furthermore, ^{18}F-fluorodestannylation was not suitable to label small electron rich heterocycles like pyridine, furan and thiophene.

Table 3.2 ^{18}F-Fluorinated model compounds, conventional commercially available and novel potential tracers.

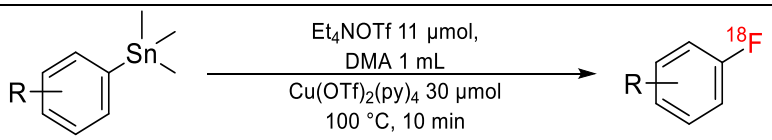

30 µmol

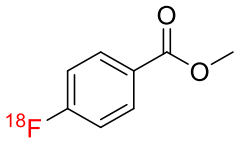

34±2% ($SnMe_3$)

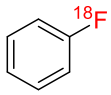

72±4% ($SnMe_3$)

88±1% ($SnBu_3$)

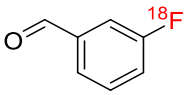

17±1% ($SnMe_3$)

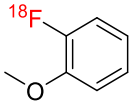

16±1% ($SnMe_3$)

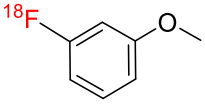

84±2% ($SnMe_3$)

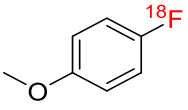

59±3% ($SnMe_3$)

44±2% ($SnBu_3$)

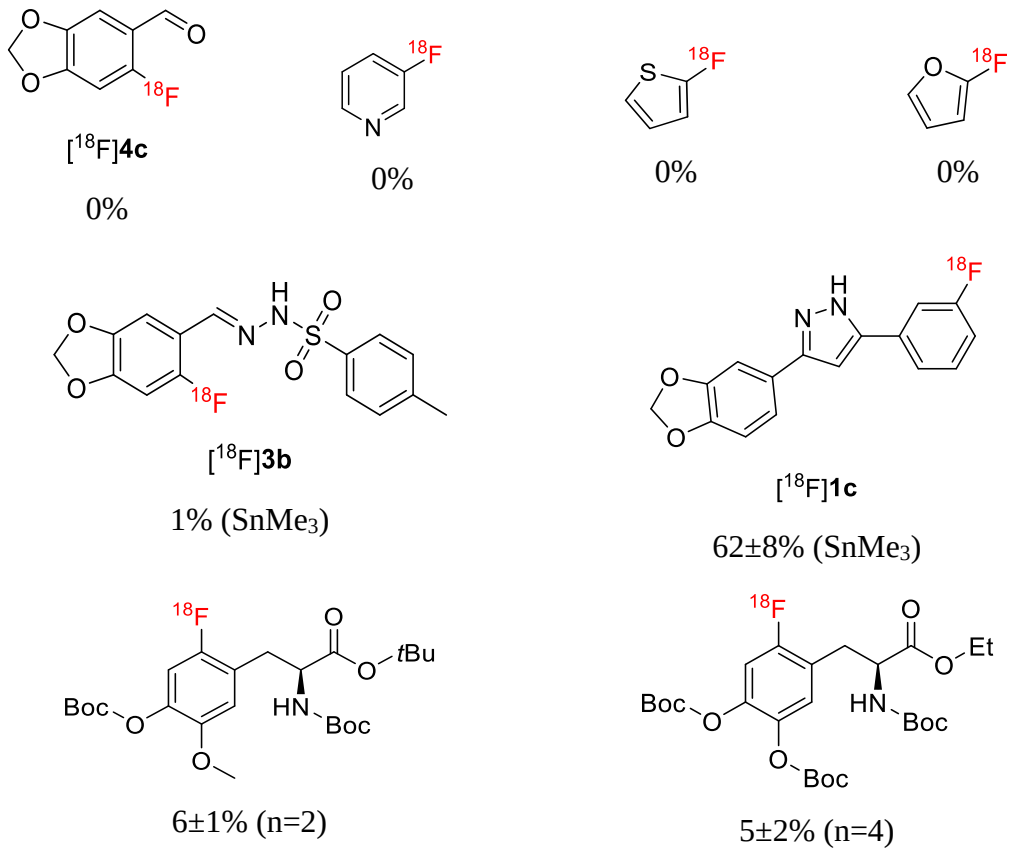

3.3.5 Synthesis of [^{18}F]**4c** as a building block for the synthesis of [^{18}F]**1b**

Copper-mediated ^{18}F-fluorination of **4j-m** did not produce [^{18}F]**4c** (Figure 3.27). The variation of reaction time and solvent did not afford any traces of [^{18}F]**4c**. Only metal-free ^{18}F-fluorination of 6-nitropiperonal was an appropriate method to synthesize [^{18}F]**4c** in good RCY.

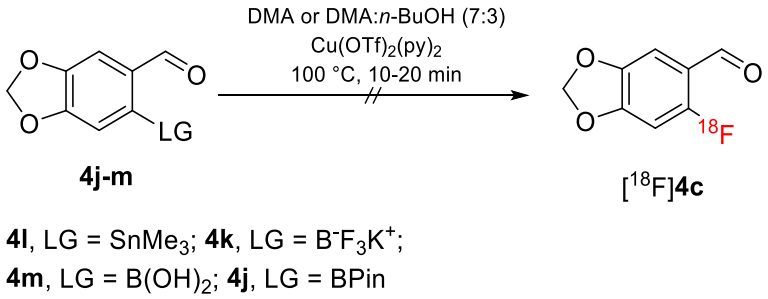

*Figure 3.27 Copper-mediated ^{18}F-fluorination of **4j-m**.*

Therefore, the only synthetic route of [^{18}F]**1b** was found to proceed over three a step synthesis described in the first part of this work.

3.3.6 Optimization of ^{18}F-fluorodestannylation of amino acid derivatives

^{18}F-Fluorodestannylation of commercially available stannylated amino acid precursors afforded only a poor RCYs (5-6%). Therefore, further optimization studies using these precursors were performed. Synthesis of 6-[^{18}F]OMFD was optimized with respect to solvents and $Cu(OTf)_2(py)_4$ concentration (Figure 3.28). The commercially available precursor is di-Boc protected with a free proton on the amine group. This proton could suppress the nucleophilicity of [^{18}F]fluoride and reduce the RCY. Therefore, tri-Boc protected precursor was also tested under the same conditions.

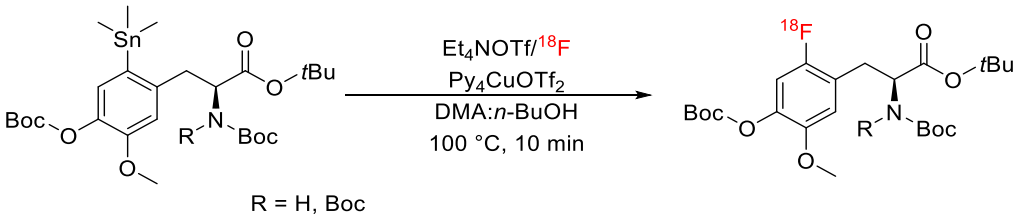

Figure 3.28 ^{18}F-fluordestannylation of OMFD precursor.

If the di-Boc protected precursor was used with *n*-BuOH:DMA (3:7) mixture as solvent the RCY was improved to 22%. Furthermore, an improvement of 2% and 5% in RCY was obtained if excess of $Cu(OTf)_2(py)_4$ 1.5 eq. and 2 eq. were used, respectively. However, tri-Boc protected precursor produced higher RCYs if 1 eq. of $Cu(OTf)_2(py)_4$ was used in DMA. This high RCY decreased if *n*-BuOH was added to the reaction mixture (Figure 3.29).

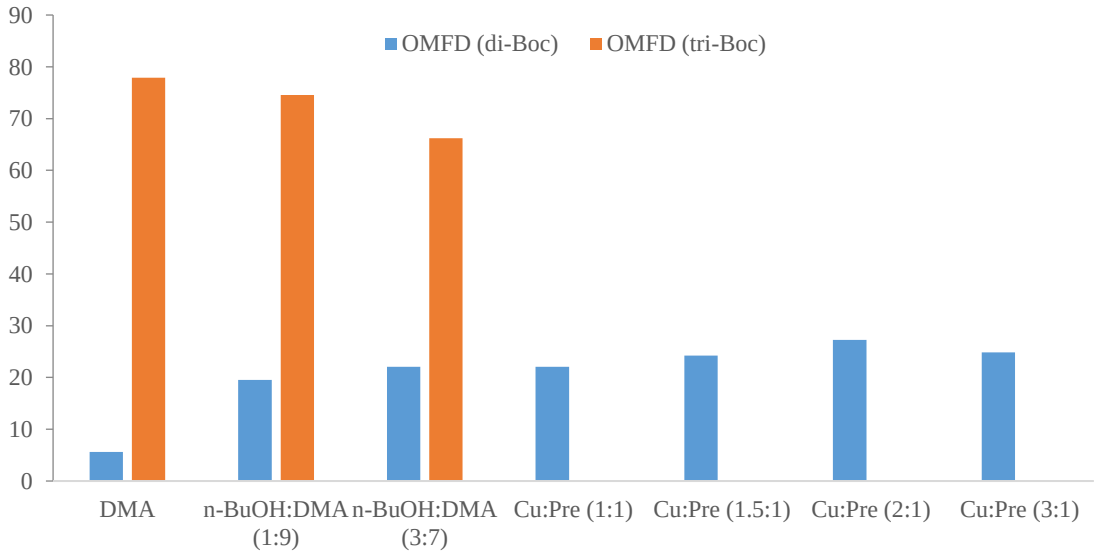

Figure 3.29 Influence of solvent and the concentration of $Cu(OTf)_2(py)_4$.

The increased RCY in ^{18}F-fluorodestannylation of di-Boc protected precursor if *n*-BuOH was added could be assigned to the formation of alcohol solvated fluoride "*flexible fluoride*" that reduce the interaction between the amine proton and [^{18}F]fluoride.[89,86]

After this optimization, commercially available amino acid derivatives were further protected with a Boc group and then radiolabeled followed by hydrolysis. The RCY was very high; however, the deprotection of ethylester precursors was only feasible by using concentrated hydrobromic acid (48%) at 130 °C (Figure 3.30). Subsequently, the manual radiosynthesis was transferred to an automated module to test the ^{18}F-fluorodestannylation procedure using higher radioactivity amounts.

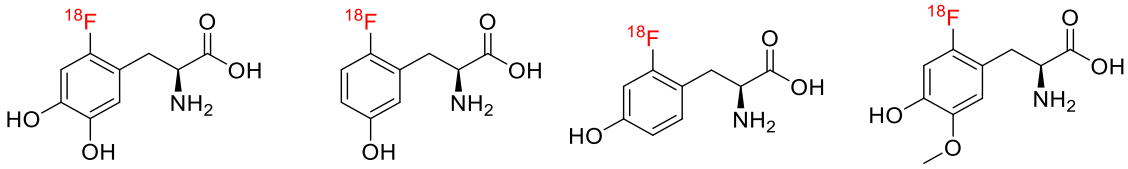

Figure 3.30 HPLC determined RCY of different amino acid derivatives.

3.3.7 Automation radiosynthesis of amino acid derivatives

The automation of amino acid derivatives radiolabeling was carried out in a two reactor apparatus. Figure 3.31 below shows a sketch of the module used in the synthesis. [^{18}F]Fluoride was loaded on to a QMA-CO_3 cartridge from the female side through V2 (Valve 2) and V4. After that the cartridge was rinsed with anhydrous MeOH using the same path. In the reverse direction, [^{18}F]fluoride was recovered using methanolic solution of Et_4NOTf over V3-V4 to the first reactor. After removing methanol under reduced pressure of dry air the corresponding precursor and $Cu(OTf)_2(py)_4$ was added over V32 without precooling. After the incubation, the mixture was cooled and quenched with water. This step produced a precipitate of the hydrophobic precursor. Thus, the transfer of this heterogenous mixture to Sep-Pak C18 Plus Long cartridge was slow and caused 30% radioactivity loss on the reactor wall in the 6-[^{18}F]OMFD synthesis. The cartridge was then rinsed with water to remove DMA, $Cu(OTf)_2(py)_4$ and Et_4NOTf/$Et_4N^{18}F$. The retained activity was then recovered with DCM into the second reactor. DCM was removed under reduced pressure of helium followed by the addition of concentrated HBr (or HCl in the case of OMFD). The use of FFKM valves (from Christian Bürkert GmbH & Co. KG, Ingelfingen, Germany) enabled the use of concentrated acids without causing

any problems. After hydrolysis, the mixture was cooled and diluted with NaOH and HPLC mobile phase. Finally, the diluted mixture was loaded onto the preparative HPLC for purification. No racemization was detected in the product.

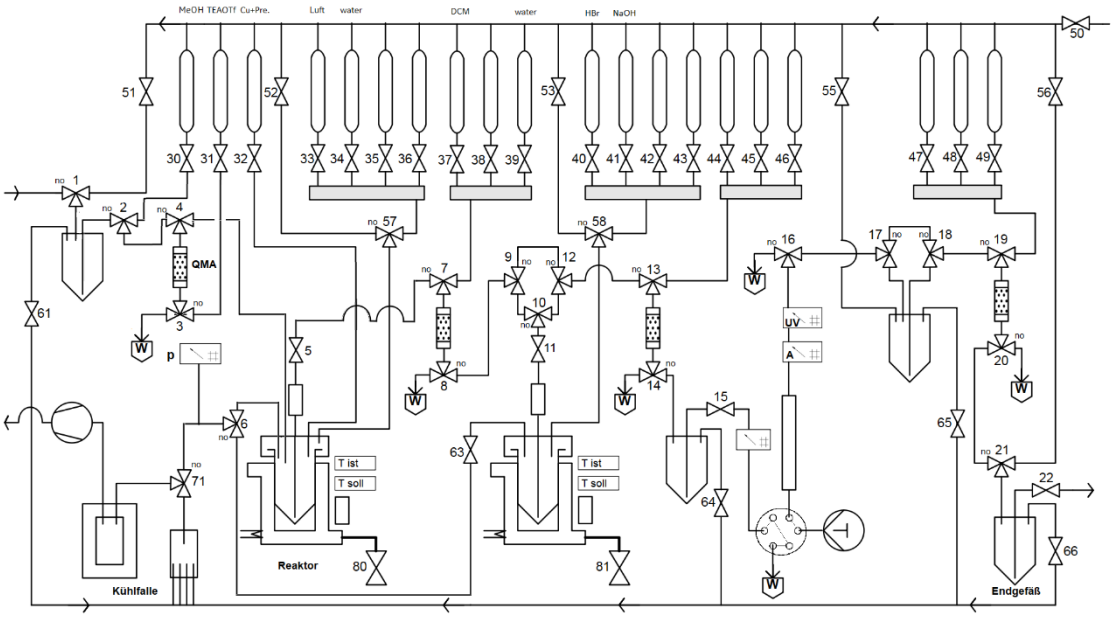

Figure 3.31 Sketch of synthesis module.

The purification was carried out using Synergi™ Hydro-RP (250×10) HPLC column. The separation was acceptable but the use of Synergi™ Hydro-RP (150×21.2) HPLC column allowed better separation and delivered products with very high chemical purity.

In this module 6-[^{18}F]DOPA, 6-[^{18}F]FMT and 2-[^{18}F]F-Tyr were successfully produced in high RCY, over 99% RCP and very good chemical purity. The synthesis of 6-[^{18}F]OMFD produced very low RCY because of its high lipophilicity. Therefore, the automated synthesis of 6-[^{18}F]OMFD should be further optimized.

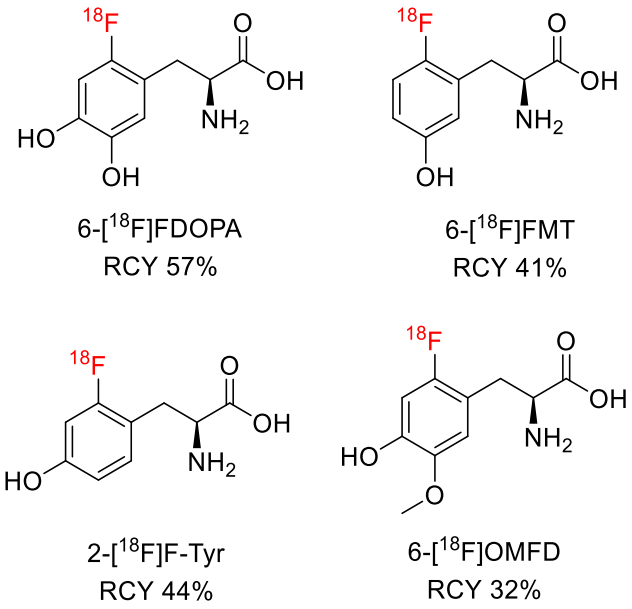

Figure 3.32 Isolated RCY of amino acid derivatives.

The MA of isolated amino acid derivatives were determined. Furthermore, copper and tin content in the isolated solution was also summarized in Table 3.3. Copper content in 6-[^{18}F]DOPA and 2-[^{18}F]F-Tyr was very high. Therefore, after loading the reaction mixture on C18 cartridge more water was used (10 mL instead of 5 mL) to wash out the excess of copper complex. Thus, the copper content in 6-[^{18}F]OMFD and 6-[^{18}F]FMT was much lower.

Table 3.3 Molar activity and Cu and Sn content of amino acid derivatives solution.

	6-[^{18}F]DOPA	6-[^{18}F]FMT	2-[^{18}F]F-Tyr	6-[^{18}F]OMFD
MA [GBq/µmol]		39	50	27
Sn [ng/mL]	324±16	65.8±3	292±8	50.4±1.2
Cu [ng/mL]	2560±120	71.8±2.8	4220±220	208±12

4 Conclusion

One of the aims of this study was the preparation of 5-(3-bromphenyl)-3-(6-[^{18}F]fluoropiperonyl)pyrazol ([^{18}F]**1b**) and 5-(3-[^{18}F]fluorophenyl)-3-(piperonyl)pyrazol ([^{18}F]**1c**) as tracers potentially suitable for the visualization of the deposition of pathological α-synuclein oligomers in Parkinson's disease.

For the preparation of [^{18}F]**1b**, 1,3 cycloaddition between a diazo species generated *in situ* from ^{18}F-labeled tosylhydrazone and an acetylene derivative was optimized. Under optimized conditions the reaction of tosylhydrazone ([^{18}F]**3b)** and 3'-bromophenyl acetylene (**2a**) produced [^{18}F]**1b** in 27–34% RCY. However, the overall RCY of [^{18}F]**1b** the starting from [^{18}F]fluoride was only 1% on three steps.

The second probe, [^{18}F]**1c**, was prepared using Cu-mediated nucleophilic ^{18}F-fluorodestannylation of easily accessible 5-(3-trimethylstannylphenyl)-3-(piperonyl)pyrazol (**1i**). The preliminary meticulous optimization of ^{18}F-fluoride preprocessing and different reaction parameters (reaction time, reaction temperature, solvents, water content, amounts of Cu-complex and stannane precursor) carried out for several model compounds allowed to prepare them in 16–88% RCY. The newly developed protocol enabled the one step preparation of [^{18}F]**1c** in 48% RCY.

With optimized conditions for Cu-mediated ^{18}F-fluorodestannylation in hands the feasibility of the preparation of ^{18}F-fluorinated aromatic amino acids from commercially available stannane precursors was evaluated. Using the novel radiolabeling protocol mono *N*-Boc protected $SnMe_3$-substituted aromatic amino acid derivatives were successfully ^{18}F-fluorinated although in low 5–6% RCY. Additional optimization of the radiolabeling conditions enabled to prepare 6-[^{18}F]OMFD, 6-[^{18}F]FDOPA, 2-[^{18}F]F-Tyr and 6-[^{18}F]FMT after subsequent deprotection in 9–16% RCYs in two steps. In contrast, *N*,*N*-di-Boc protected stannyl substrates were radiolabeled using the developed protocol affording after deprotection the desired PET tracers in 37-78% RCYs. These substrates were prepared in one step from the respective mono-*N*-Boc protected stannyl substituted amino esters.

Finally, the implementation of the optimized procedure for Cu-mediated ^{18}F-fluorodestannylation on a synthesis module enabled the cGMP preparation of clinical doses of 6-[^{18}F]OMFD, 6-[^{18}F]FDOPA, 2-[^{18}F]F-Tyr and 6-[^{18}F]FMT in 32–57% RCY within 1 h. Especially, 6-[^{18}F]FDOPA, the most widely used PET-tracer for

neuroimaging, was prepared in RCY of 57% which is far above the RCYs reported in the literature.

5 Experimental

5.1 Synthesis of precursors and HPLC reference compounds

5.1.1 General procedure

All chemicals and solvents were used in synthesis were purchased from Sigma-Aldrich GmbH (Steinheim, Germany), Fluka AG (Buchs, Switzerland), TCI EUROPE N.V. (Zwijndrecht, Belgium), ChemPUR GmbH (Karlsruhe, Germany), Merck KGaA (Darmstadt, Germany) and ABCR GmbH (Karlsruhe, Germany) and used without special processing or purification. Dry solvents were purchased in sufficient purity from Sigma-Aldrich GmbH (Steinheim, Germany) and were stored under argon.

5.1.1.1 Nuclear magnetic resonance (NMR)

^{1}H-NMR spectra: Bruker DPX Avance 200 (200 MHz), Bruker Avance II 300 (300 MHz) and Varian INOVA 400 (400 MHz). ^{1}H chemical shifts are reported in ppm relative to residual peaks of deuterated solvents. The observed signal multiplicities are characterized as follows: s = singlet, d = doublet, t = triplet, m = multiplet, and br = broad. Coupling constants (*J*) were reported in Hertz (Hz).

^{13}C-NMR spectra [additional APT (Attached Proton Test)]: Bruker DPX Avance 200 (50 MHz), Bruker Avance II 300 (75 MHz) and Varian INOVA 400 (101 MHz). ^{13}C chemical shifts are reported relative to residual peaks of deuterated solvents.

^{19}F-NMR spectra: Bruker DPX Avance 200 (188 MHz).

5.1.1.2 Mass spectroscopy (MS)

High-resolution mass spectrometry (HR-MS) were carried out on LTQ FT Ultra from Thermo Fisher Scientific Inc. (Bremen, Germany). The measuring mode was ESI positive (+) or negative (−).

Inductively coupled plasma mass spectrometry (ICP-MS) was carried out using Agilent 7900 ICP-MS from Gilent Technologies, Santa Clara, United States.

Low-resolution mass spectra were obtained in electrospray ionization (ESI) positive mode with a Thermo Finnigan Surveyor mass spectrometer (Thermo Fisher Scientific GmbH, Dreieich).

5.1.1.3 Miscellaneous Information

All moisture-sensitive or oxygen-sensitive reactions were carried out under atmosphere of argon. The reaction vessels used for this purpose were dried for at least 2 hours at

140 °C and purged with argon 5.0 (> 99.999%, Air Liquide GmbH) thrice using Schlenk line. Before introducing the protective gas into the apparatus, it is purified by a Hydrosorbpatrone from Linde AG (Pullach, Germany; Specification <20 ppb H_2O residual impurity). The vacuum was achieved by a rotary pump RZ 6 (up to 4×10^{-4} mbar) of the company Vacuubrand GmbH (Wertheim, Germany).

In column chromatography silica gel technical grade (w/Ca, ~0.1%), 60 Å, 230-400 mesh particle size, Ca 0.1-0.3% from Sigma-Aldrich GmbH (Steinheim, Germany) for the purification of aryl stannanes. Merck silica gel, grade 60, 230–400 mesh was used for other compounds. Solvent proportions are indicated in a volume/volume ratio.

Thin layer chromatography (TLC) was performed using aluminum finish ALUGRAM® SIL G / UV254 from Macherey-Nagel GmbH (Düren, Germany) or Merck precoated sheets, 0.25 mm Sil G/UV254. The chromatograms were viewed under UV light 254 nm.

5.1.2 3-(Benzo[*d*][1,3]dioxol-5-yl)-5-(3-bromophenyl)-1*H*-pyrazole (**1a**)

General procedure A: A solution of **9c** (2.4 g, 6.91 mmol) and hydrazine monohydrate (1 mL, 98%, 13.83 mmol, 2 eq.) in ethanol (30 ml) was refluxed for 3 h. Water was added to the clear yellow solution and resulting precipitate was collected by filtration, washed with water and dried under vacuum to provide the title compound.

Yield	2 g, 84%
Appearance	white solid
Molecular formula	$C_{16}H_{11}BrN_2O_2$
Molar mass	343.18000
TLC	R_f = 0.31 (EtOAc/petroleum ether, 1:4)
^{1}H-NMR	(200 MHz, DMSO-d_6 + DCl): δ [ppm] = 7.97 (s, 1H), 7.79 (d, *J* = 7.6 Hz, 1H), 7.49 (d, *J* = 8.0 Hz, 1H), 7.34 (t, *J* = 9.2 Hz, 4H), 6.89 (d, *J* = 8.6 Hz, 1H), 5.96 (s, 2H).
^{13}C-NMR	(50 MHz, DMSO-d_6 + DCl): δ [ppm] = 148.94, 148.55, 147.18, 146.64, 132.67, 131.93, 131.75, 129.01, 125.66, 123.08, 122.73, 121.20, 109.56, 106.84, 102.31, 101.64, 12.33.
HRMS	m/z: $[M + H]^+$ calcd for $C_{16}H_{12}BrN_2O_2^+$: 343.00767; found: 343.00781. Correct isotopic pattern.

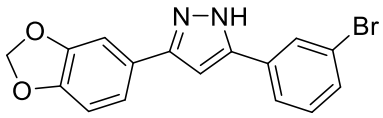

5.1.3 5-(3-Bromophenyl)-3-(6-fluorobenzo[*d*][1,3]dioxol-5-yl)-1*H*-pyrazole (**1b**)

Lithium *tert*-butoxide (214 mg, 2.7 mmol, 3 eq.) was added to **3b** (300 mg, 0.9 mmol) at room temperature in toluene under argon and stirred for 15 min. After that, **2a** (420 mg, 2.3 mmol, 3 eq.) was added to the mixture and stirred for 48 h at 95 °C. The volatiles were removed under reduced pressure, and the residue was dissolved in EtOAc (50 mL) and washed with water (30×3 mL) and brine (30 mL). The combined organic phases were dried over $MgSO_4$. After filtration and removal of the solvent under reduced pressure, the residue was purified by gravity chromatography.

Yield	140 mg, 43%
Appearance	white solid
Molecular formula	$C_{16}H_{10}BrFN_2O_2$

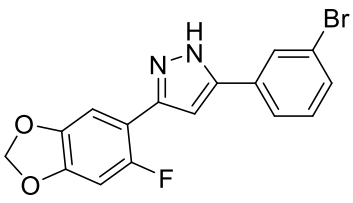

Molar mass	361.17040
TLC	R_f = 0.30 (ethyl acetate/petroleum ether, 1:4)
^{1}H-NMR	(200 MHz, DMSO-d_6): δ [ppm] = 13.41 (s, 1H), 8.03 (s, 1H), 7.83 (d, *J* = 7.1 Hz, 1H), 7.51 (d, *J* = 7.1 Hz, 1H), 7.39 (t, *J* = 6.1 Hz, 2H), 7.06 (s, 2H), 6.11 (s, 2H).
^{13}C-NMR	(50 MHz, DMSO-d_6 + DCl): δ [ppm] = 156.62, 151.80, 148.12, 147.83, 146.25, 144.27, 144.23, 141.37, 134.09, 131.28, 130.67, 127.77, 124.42, 122.46, 111.31, 111.01, 106.13, 106.03, 102.56, 102.36, 99.14, 98.53.
^{19}F-NMR	(188 MHz, DMSO-d_6 + DCl): δ [ppm] = -119.92.
HRMS	m/z: $[M + H]^+$ calcd for $C_{16}H_{11}BrFN_2O_2^+$: 360.99824; found: 360.99823, Correct isotopic pattern.

5.1.4 3-(Benzo[*d*][1,3]dioxol-5-yl)-5-(3-fluorophenyl)-1*H*-pyrazole (**1c**)

The title compound was synthesized according to general procedure A using **9e** (335 mg, 1.17 mmol) and hydrazine monohydrate (1.3 eq.).

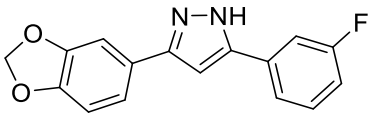

Yield	735 mg, 84%
Appearance	yellow solid
Molecular formula	$C_{16}H_{11}FN_2O_2$
Molar mass	282.27440
TLC	R_f = 0.32 (EtOAc/petroleum ether, 1:4)
^{1}H NMR	(200 MHz, DMSO-d_6 + DCl): δ [ppm] = 7.60 (s, 2H), 7.41 (d, *J* = 6.4 Hz, 1H), 7.28 (d, *J* = 11.6 Hz, 3H), 7.14 (d, *J* = 8.7 Hz, 1H), 6.85 (d, *J* = 8.3 Hz, 1H), 5.94 (s, 2H).
^{13}C NMR	(50 MHz, DMSO-d_6 + DCl): δ [ppm] = 165.50, 160.65, 148.95, 148.50, 147.24, 146.84, 146.78, 131.98, 131.80, 131.59, 131.42, 122.78, 122.61, 121.23, 113.53, 113.07, 109.48, 106.79, 102.28, 101.65.
^{19}F NMR	(188 MHz, DMSO-d_6 + DCl): δ [ppm] = -112.07.

HRMS m/z: $[M + H]^+$ calcd for $C_{16}H_{12}FN_2O_2^+$: 283.08773; found: 283.08775.

5.1.5 3,5-bis(4-fluorophenyl)-1*H*-pyrazole (**1d**)

4-fluorobenzaldehyde (100 µL, 0.94 mmol) was added to a solution of *p*-toluenesulfonyl hydrazide (193 mg, 1 mmol, 1.1 eq.). After the mixture was stirred for 1 h, a solution of NaOH (50 µL, 8M, 0.94 mmol, 1 eq.) was added and the mixture was stirred for a further 20 min. Then 4´-fluorophenyl acetylene (540 µL, 4.7 mmol, 5 eq.) was added, and the mixture was stirred at 50 °C for 64 h. The volatiles were evaporated under reduced pressure, and the residue was taken with EtOAc (10 mL). The organic phase was washed with water (10 mL) and brine (10 mL) and dried over $MgSO_4$. After removing the solvent under reduced pressure the title compound was obtained after recrystallized from Et_2O/*n*-pentane.

Yield 40 mg, 17%

Appearance yellow solid

Molecular formula $C_{15}H_{10}F_2N_2$

Molar mass 256.25581

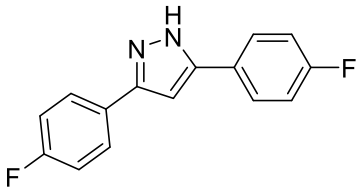

TLC R_f = 0.33 (petroleum ether/EtOAc, 3:1)

^{1}H-NMR (300 MHz, DMSO-d_6): δ [ppm] = 13.32 (s, 1H), 7.86 (dd, *J* = 8.7, 5.5 Hz, 4H), 7.30 (t, *J* = 8.8 Hz, 4H), 7.16 (s, 1H).

^{13}C-NMR (75 MHz, DMSO-d_6): δ [ppm] = 163.86, 163.84, 160.62, 160.61, 127.63, 127.52, 116.32, 116.03, 100.08.

5.1.6 5-(3-Bromophenyl)-3-(6-iodobenzo[*d*][1,3]dioxol-5-yl)-1*H*-pyrazole (**1e**)

In flame dried flask **4i** (1 g, 3.62 mmol) and *p*-toluenesulfonyl hydrazide (0.681 g, 3.66 mmol, 1.01 eq.) were stirred in anhydrous MeCN (50 mL) at 85 °C for 1 h. After that lithium *tert*-butoxide (7.25 mL, 1M in THF, 7.25 mmol, 2 eq.) was added to the mixture and stirred for 15 min. Then, **2a** (1.312 g, 7.25 mmol, 2 eq.) was added to the mixture. After 24 h the reaction mixture was allowed to cool to room temperature, then MeCN was removed under reduced pressure, and the residue was dissolved in EtOAc (50 mL) and washed with water (3×80 mL) and brine (80 mL). The organic layer was separated and dried over $MgSO_4$. After filtration and removal of the solvent, the crude

material was purified by gravity chromatography (twice: EtOAc:petroleum ether 1:4 and EtOAc:DCM 1:15) to deliver the title compound

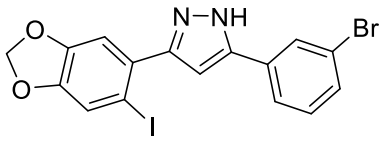

Yield	800 mg, 47%
Appearance	white solid
Molecular formula	$C_{16}H_{10}BrIN_2O_2$
Molar mass	469.07647
TLC	R_f = 0.28 (EtOAc/petroleum ether, 1:4)
	R_f = 0.48 (EtOAc/DCM, 1:15)
^{1}H-NMR	(200 MHz, DMSO-d_6 + DCl): δ [ppm] = 7.99 (s, 1H), 7.88 – 7.62 (m, 2H), 7.42 (dd, *J* = 15.4, 7.9 Hz, 2H), 6.97 (dd, *J* = 16.9, 8.1 Hz, 2H), 6.06 (s, 2H).
^{13}C-NMR	(50 MHz, DMSO-d_6 + DCl): δ [ppm] = 159.12, 154.26, 150.37, 150.07, 144.64, 144.60, 143.79, 140.06, 139.95, 136.15, 130.17, 129.91, 128.22, 127.48, 113.93, 113.70, 102.86, 102.82, 102.79, 98.60, 98.00, 21.31, 21.21.
HRMS	m/z: $[M + H]^+$ calcd for $C_{16}H_{11}BrIN_2O_2^+$: 468.90431; found: 468.90467. Correct isotopic pattern.

Another method was tried to synthesize the title compound. A solution of **9a** (1.8 g, 3.81 mmol) and hydrazine monohydrate (2 mL, 98%, 41.86 mmol, 11 eq.) in ethanol (20 ml) was refluxed for 3 h. Water was added to the clear yellow solution and resulting precipitate was collected by filtration, washed with water and dried to provide the title compound (1.2 g, 67%).

5.1.7 *tert*-Butyl 5-(3-bromophenyl)-3-(6-iodobenzo[*d*][1,3]dioxol-5-yl)-1*H*-pyrazole-1-carboxylate (**1f**)

1e (200 mg, 0.4 mmol) was stirred with di-*tert*-butyl dicarbonate (200 mg, 0.9 mmol, 2.2 eq.) and 4-dimethylaminopyridine (15.6 mg, 0.12 mmol, 0.3 eq) in THF (5 mL) at ambient temperature for 2 h. After that the reaction mixture was diluted with EtOAc (10 mL) and washed with water (3×5 mL) and brine (5 mL) then dried over $MgSO_4$. After removing the solvents under reduced pressure, the residue was purified with flash chromatography.

Yield	210 mg, 89%
Appearance	white solid
Molecular formula	$C_{21}H_{18}BrIN_2O_4$
Molar mass	569.19347

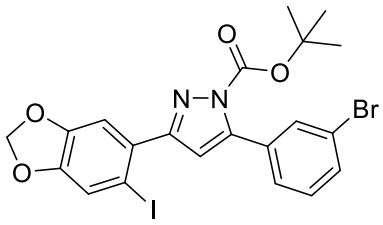

TLC	R_f = 0.30 (Et_2O/petroleum ether, 1:4)
^{1}H-NMR	(200 MHz, DMSO-d_6): δ [ppm] = 8.12 (s, 1H), 7.95 (d, *J* = 7.9 Hz, 1H), 7.63 (d, *J* = 8.8 Hz, 1H), 7.51 (d, *J* = 4.8 Hz, 1H), 7.43 (d, *J* = 7.8 Hz, 1H), 7.10 (d, *J* = 2.9 Hz, 2H), 6.12 (s, 2H), 1.32 (s, 9H).
^{13}C-NMR	(50 MHz, DMSO-d_6): δ [ppm] = 150.97, 148.60, 147.94, 147.68, 146.63, 146.21, 133.79, 131.78, 131.12, 130.45, 128.28, 124.87, 122.31, 117.48, 110.49, 108.96, 102.11, 89.45, 85.57, 85.00, 84.35, 26.86.
HRMS	m/z: $[M + H]^+$ calcd for $C_{21}H_{19}BrIN_2O_4^+$: 568.95674; found: 568.95783. Correct isotopic pattern.

5.1.8 5-(3-Bromophenyl)-3-(6-iodobenzo[*d*][1,3]dioxol-5-yl)-1-tosyl-1*H*-pyrazole (**1g**)

1e (170 mg, 0.36 mmol, 1 eq.) was stirred with NaH (26 mg, 1 mmol, 3 eq.) in anhydrous THF (5 mL) at 0 °C. Then 4-methylbenzenesulfonyl chloride (207 mg, 1 mmol, 3 eq.) was added. After 24 h that the reaction mixture was diluted with EtOAc (10 mL) and washed with water (3×5 mL) and brine (5 mL) then dried over $MgSO_4$. After removing the solvents under reduced pressure, the residue was purified with flash chromatography (EtOAc/petroleum ether, 1:9).

Yield	175 mg, 77%
Appearance	White solid
Molecular formula	$C_{23}H_{16}BrIN_2O_4S$
Molar mass	623.25947

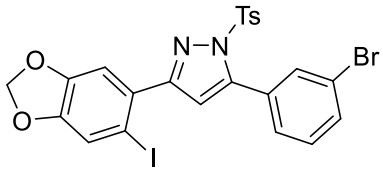

^{1}H NMR	(200 MHz, $CDCl_3$): δ [ppm] = 8.06 (t, *J* = 1.6 Hz, 1H), 7.99 – 7.66 (m, 3H), 7.65 – 7.45 (m, 1H), 7.33 (d, *J* = 7.7 Hz, 4H), 6.87 (s, 1H), 6.62 (s, 1H), 6.11 (d, *J* = 3.2 Hz, 2H), 2.44 (s, 3H).

^{13}C NMR (50 MHz, $CDCl_3$): δ [ppm] = 152.79, 149.51, 149.07, 147.91, 145.85, 134.56, 133.50, 132.14, 130.29, 129.90, 129.33, 128.76, 127.92, 125.04, 122.92, 118.32, 111.48, 109.60, 102.31, 88.99, 21.83.

HRMS m/z: $[M + H]^+$ calcd for $C_{23}H_{17}BrIN_2O_4S^+$: 622.91316; found: 622.91365. Correct isotopic pattern.

5.1.9 *tert*-Butyl 3-(benzo[*d*][1,3]dioxol-5-yl)-5-(3-bromophenyl)-1*H*-pyrazole-1-carboxylate (**1j**)

1a (1.9 g, 5.5 mmol, 1 eq.) was stirred with di-*tert*-butyl dicarbonate (2.54 g, 11.6 mmol, 2.1 eq.) and 4-dimethylaminopyridine (0.2 mg, 1.7 mmol, 0.3 eq) in THF (5 mL) at ambient temperature for 18 h. After removing THF under vacuum the residue was purified with flash chromatography.

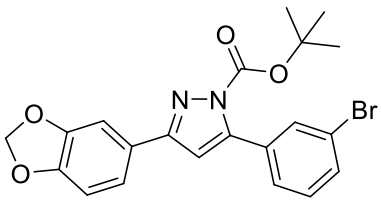

Yield 2.2 g, 90%

Appearance white solid

Molecular formula $C_{21}H_{19}BrN_2O_4$

Molar mass 443.29700

TLC R_f = 0.35 (Et_2O/petroleum ether, 1:4)

^{1}H-NMR (200 MHz, DMSO-d_6) δ 8.08 (d, *J* = 1.6 Hz, 1H), 7.92 (d, *J* = 7.8 Hz, 1H), 7.75 – 7.52 (m, 1H), 7.43 (t, *J* = 7.9 Hz, 1H), 7.24 – 7.05 (m, 2H), 7.00 (d, *J* = 7.9 Hz, 1H), 6.93 (dd, *J* = 8.0, 1.6 Hz, 1H), 6.08 (s, 2H), 1.36 (s, 9H).

^{13}C-NMR (50 MHz, DMSO-d_6): δ [ppm] = 150.92, 147.69, 147.39, 147.09, 146.93, 133.98, 131.75, 131.14, 128.37, 124.94, 124.68, 122.87, 122.32, 109.73, 108.64, 107.91, 101.40, 84.79, 27.15, 11.58.

HRMS m/z: $[M + H]^+$ calcd for $C_{21}H_{20}BrN_2O_4^+$: 443.06009; found: 443.06089. Correct isotopic pattern.

5.1.10 3-(Benzo[*d*][1,3]dioxol-5-yl)-5-(3-(trimethylstannyl)phenyl)-1*H*-pyrazole (**1i**)

General procedure B: In flame dried flask **1a** (550 mg, 1.6 mmol), $Pd(PPh_3)_4$ (185 mg, 0.16 mmol, 0.1 eq.) were purged thrice with argon using Schlenck line technique. Anhydrous 1,4-dioxane (2 mL) was bubbled with a stream of argon for 30 min, then it

was added to the reagents at room temperature. Hexamethylditin (830 µL, 4 mmol, 2.5 eq.) was added via syringe, and the mixture was heated to 100 °C for 18 h. The mixture was filtered through a plug of Celite and TBAF (2 mL, 1M in THF) was added to the filtrate, and the mixture was stirred for 30 min. The filtrate was washed with water (50 mL) and with brine (50 mL). After drying the solution over magnesium sulfate, it was concentrated under vacuum. The crude product was purified via flash column chromatography. The resulted yellow oil was recrystallized from DCM/Hexane (DCM was removed under reduced pressure).

Yield	566 mg, 83%
Appearance	white solid
Molecular formula	$C_{19}H_{20}N_2O_2Sn$
Molar mass	427.09100
TLC	R_f = 0.30 (EtOAc/petroleum ether, 1:4)
^{1}H-NMR	(200 MHz, DMSO-d_6): δ [ppm] =13.20 (s, 1H), 7.93 (s, 1H), 7.74 (s, 1H), 7.60 – 7.22 (m, 5H), 7.12 (s, 1H), 6.99 (d, *J* = 7.7 Hz, 1H), 6.06 (s, 2H), 0.31 (s, 9H).
^{13}C-NMR	(50 MHz, DMSO-d_6): δ [ppm] = 147.74, 146.86, 132.25, 128.28, 125.03, 118.82, 108.59, 105.60, 101.12, 99.30, -9.29.
HRMS	m/z: $[M + H]^+$ calcd for $C_{19}H_{21}N_2O_2Sn^+$: 429.06195; found: 429.06286. Correct isotopic pattern.

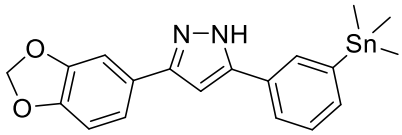

5.1.11 1-Bromo-3-ethynylbenzene (**2a**)[90]

8 (35 g, 90.5 mmol) and K_2CO_3 (37.5 g, 271 mmol, 3 eq.) in DMSO (200 mL) was stirred at 115 °C for 18 h. After being cooled to ambient temperature, water was added to the heterogeneous mixture till it turned homogeneous. Then it was extracted using Et_2O (3×150 mL). The organic layers were combined, rinsed with brine, and dried over $MgSO_4$. Removals of solvent afford the title compound (10 g, 61%) as yellow oil.

If pentane was used instead of Et_2O and the resulted residue was purified over flash chromatography (pentane 100%), the product was obtained as colorless oil (8.5 g, 52%).

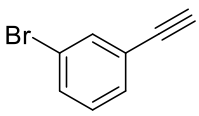

Yield	8.5 g, 52%

Appearance	colorless oil turned yellow after two months at 5 °C
Molecular formula	C_8H_5Br
Molar mass	181.03200
TLC	R_f = 0.5 (pentane)
^{1}H-NMR	(200 MHz, $CDCl_3$): δ [ppm] = 7.64 (t, 1H), 7.44 (m, 2H), 7.20 (t, 1H), 3.12 (s, 1H).

5.1.12 *N'*-((6-Fluorobenzo[*d*][1,3]dioxol-5-yl)methylene)-4-methylbenzenesulfonohydrazide (**3b**)

General procedure C: 4c (300 mg, 1.8 mmol) was stirred at room temperature with *p*-toluenesulfonyl hydrazide (400 mg, 2.1 mmol, 1.2 eq.) in MeOH (10 mL) for 4 h. The resulted precipitate was filtered and dried under vacuum to afford the title compound.

Yield	400 mg, 67%
Appearance	white solid
Molecular formula	$C_{15}H_{13}FN_2O_4S$
Molar mass	336.33740

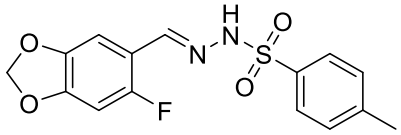

^{1}H-NMR	(200 MHz, DMSO-d_6): δ [ppm] = 11.42 (s, 1H), 7.96 (s, 1H), 7.76 (d, *J* = 8.2 Hz, 2H), 7.40 (d, *J* = 8.0 Hz, 2H), 7.04 (d, *J* = 5.9 Hz, 1H), 6.98 (d, *J* = 10.3 Hz, 1H), 6.09 (s, 2H), 2.36 (s, 3H).
^{13}C-NMR	(50 MHz, DMSO-d_6): δ [ppm] = 149.66, 149.37, 143.92, 142.94, 139.56, 139.45, 135.85, 129.02, 126.93, 102.86, 101.85, 97.43, 96.85, 20.96.
^{19}F-NMR	(188 MHz, DMSO-d_6): δ [ppm] = -126.43.
HRMS	m/z: $[M + H]^+$ calcd for $C_{15}H_{14}FN_2O_4S^+$: 337.06528; found:337.06535.

5.1.13 *N'*-((6-Iodobenzo[*d*][1,3]dioxol-5-yl)methylene)-4-methylbenzenesulfonohydrazide (**3c**)

The title compound was synthesized according to general procedure C using **4i** (1.8 g, 6.5 mmol).

Yield	2.65 g, 91%
Appearance	white solid
Molecular formula	$C_{15}H_{13}IN_2O_4S$
Molar mass	444.24347
^{1}H-NMR	(200 MHz, DMSO-d_6): δ [ppm] = 11.54 (s, 1H), 8.02 (s, 1H), 7.76 (d, *J* = 8.3 Hz, 2H), 7.41 (d, *J* = 7.0 Hz, 2H), 7.11 (s, 1H), 6.09 (s, 2H), 2.36 (s, 3H).
^{13}C-NMR	(101 MHz, $CDCl_3$): δ [ppm] = 150.64, 148.96, 144.55, 129.90, 128.74, 128.15, 119.61, 118.68, 109.07, 107.15, 102.82, 102.29, 21.78.
HRMS	m/z: $[M + H]^+$ calcd for $C_{15}H_{14}IN_2O_4S^+$: 444.97135; found: 444.97144.
Anal.	Calcd for $C_{15}H_{13}IN_2O_4S$: C, 40.56; H, 2.95; N, 6.31; Found: C, 39,79±0.26; H, 2.94±0.02; N, 6.55±0.04.

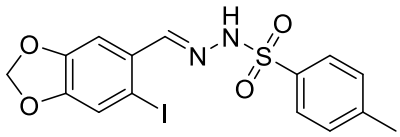

5.1.14 4-Methyl-*N'*-((6-(trimethylstannyl)benzo[*d*][1,3]dioxol-5-yl)methylene)benzenesulfonohydrazide (**3d**)

The title compound was synthesized according to general procedure C using **4l** (400 mg, 1.3 mmol) and stirred for 18 h. After that MeOH was removed under vacuum and the residue was purified with flash chromatography EtOAc:petroleum ether (1:4).

Yield	170 mg, 28%
Appearance	yellow oil
Molecular formula	$C_{18}H_{22}N_2O_4SSn$
Molar mass	481.15400
^{1}H NMR	(200 MHz, DMSO-d_6): δ [ppm] = 11.45 (s, 1H), 7.93 (s, 1H), 7.72 (d, *J* = 8.3 Hz, 2H), 7.40 (d, *J* = 8.0 Hz, 2H), 7.11 (s, 1H), 6.92 (s, 1H), 6.02 (s, 2H), 2.35 (s, 3H), 0.17 (s, 9H).
^{13}C NMR	(50 MHz, DMSO-d_6): δ [ppm] = 149.07, 148.66, 148.14, 143.42, 136.39, 135.91, 133.51, 129.72, 127.12, 115.15, 108.12, 101.23, 21.00, -7.12.

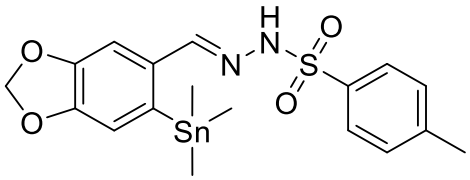

HRMS m/z: $[M - CH_3]^+$ calcd for $C_{17}H_{19}N_2O_4SSn^+$: 467.00820; found: 467.00877. Correct isotopic pattern.

5.1.15 4-Methyl-*N'*-((6-nitrobenzo[*d*][1,3]dioxol-5-yl)methylene)benzenesulfonohydrazide (**3f**)

The title compound was synthesized according to general procedure C using 6-nitropiperonal (1.8 g, 6.5 mmol).

Yield 2.65 g, 91%

Appearance yellow solid

Molecular formula $C_{15}H_{13}N_3O_6S$

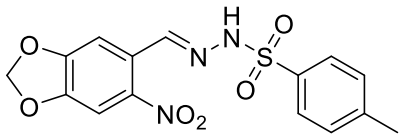

Molar mass 363.34400

^{1}H-NMR (200 MHz, DMSO-d_6): δ [ppm] = 11.92 (s, 1H), 8.38 (s, 1H), 7.88 (d, *J* = 8.2 Hz, 2H), 7.71 (s, 1H), 7.52 (d, *J* = 8.0 Hz, 2H), 7.25 (s, 1H), 6.36 (s, 2H), 2.47 (s, 3H).

^{13}C-NMR (50 MHz, DMSO-d_6): δ [ppm] = 151.78, 148.93, 143.67, 142.80, 142.42, 136.02, 129.79, 127.22, 125.02, 104.95, 103.86, 21.02.

HRMS m/z: $[M + H]^+$ calcd for $C_{15}H_{14}N_3O_6S^+$: 364.05978; found: 364.05989.

5.1.16 6-Fluorobenzo[*d*][1,3]dioxole-5-carbaldehyde (**4c**)[76]

In flame dried flask under inert atmosphere of argon 6-fluoroveratraldehyde (1 g, 5.4 mmol) was dissolved in anhydrous DCM (10 mL). The mixture was placed in acetone and dry ice bath (-80 °C), then BBr_3 (10 mL of a 1M solution in DCM) was added dropwise. The reaction mixture was allowed to warm to room temperature and stirred for 18 h. After that, methanol was added to the resulting mixture at -80 °C, and stirred at ambient temperature for 1 h. Then solvents were removed. This process was repeated three times. The residue was purified with column chromatography (DCM/EtOAc, 5:1) to afford 2-fluoro-4,5-dihydroxybenzaldehyde (700 mg, 83%) as yellow solid R_f = 0.33 (DCM/EtOAc, 5:1). This compound is directly used in the next step.

In flame dried flask under inert atmosphere of argon bromochloromethane (680 mg, 5.3 mmol, 1.5 eq.) was added to a stirred suspension of 2-fluoro-4,5-dihydroxybenzaldehyde (550 mg, 3.5 mmol) and cesium carbonate (2.65 g, 10.6 mmol,

3 eq.) in anhydrous DMF (20 mL). The resulting mixture was heated at 110 °C for 18 h. After cooling to room temperature, water (50 mL) was added and the aqueous layer was extracted with EtOAc (3×50 mL). The organic layers were combined, washed with water, brine and dried over $MgSO_4$. Evaporation of the solvents left a residue, which was purified by flash column chromatography petroleum ether:Et_2O (3:1).

Yield	450 mg, 76%
Appearance	white solid
Molecular formula	$C_8H_5FO_3$
Molar mass	168.12340
^{1}H-NMR	(200 MHz, $CDCl_3$): δ [ppm] = 10.17 (s, 1H), 7.21 (d, *J* = 5.6 Hz, 1H), 6.63 (d, *J* = 9.7 Hz, 1H)., 6.07 (s, 2H).
^{13}C-NMR	(50 MHz, $CDCl_3$): δ [ppm] = 185.58, 162.71, 154.16, 144.97, 118.02, 105.11, 103.00, 98.09.
^{19}F-NMR	(188 MHz, $CDCl_3$): δ [ppm] = -126.08.

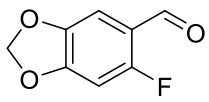

5.1.17 6-(Dimethylamino)benzo[*d*][1,3]dioxole-5-carbaldehyde (**4d**)

4c (1 g, 5.9 mmol), dimethylaminehydrochloride (0.63 g, 7.7 mmol, 1.3 eq.) and potassium carbonate (1.07 g, 7.7 mmol, 1.3 eq.) were stirred and heated to reflux (130 °C) in a mixture of DMSO (10 ml) and water (4 ml). Saturated aqueous potassium carbonate (20 ml) was added to the cooled solution, which was twice extracted with Et_2O (30 mL). The combined organic phases were washed with brine (50 mL) dried on $MgSO_4$. The yellow oil obtained after filtration and evaporation was purified with flash chromatography to deliver the title compound.

Yield	780 mg, 68%
Appearance	yellow solid
Molecular formula	$C_{10}H_{11}NO_3$
Molar mass	193.20200
TLC	R_f = 0.30 (Et_2O/petroleum ether, 1:4)
^{1}H-NMR	(200 MHz, $CDCl_3$): δ [ppm] = 10.15 (s, 1H), 7.23 (s, 1H), 6.63 (s, 1H), 5.97 (s, 2H), 2.83 (s, 6H).

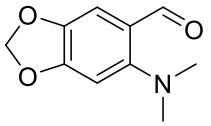

^{13}C-NMR	(50 MHz, $CDCl_3$): δ [ppm] = 189.74, 153.50, 122.43, 107.44, 101.93, 99.80, 46.65.
HRMS	m/z: $[M + H]^+$ calcd for $C_{10}H_{12}NO_3^+$: 194.08117; found: 194.08204.

5.1.18 6-Aminobenzo[*d*][1,3]dioxole-5-carbaldehyde (**4f**)[91]

To 6-nitropiperonal (3.5 g, 17.9 mmol) dissolved in EtOH/H_2O (3:1, 150 mL) iron powder (10 g, 179.4 mmol, 10 eq.) and HCl (38%, 100 µL) was added. The mixture was stirred at 70 °C for 3 h. after cooling to room temperature the mixture was filtered over Celite and the filtrate was dried under reduced pressure. The residue was dissolved in DCM and dried over MgSO4. Then DCM was removed to deliver the title compound.

Yield	2.6 g, 88%
Appearance	yellow solid
Molecular formula	$C_8H_7NO_3$
Molar mass	165.14800
^{1}H-NMR	(200 MHz, $CDCl_3$): δ [ppm] = 9.61 (s, 1H), 6.82 (s, 1H), 6.36 (br, 2H), 6.14 (s, 1H), 5.93 (s, 2H).

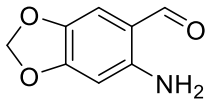

5.1.19 6-Iodobenzo[*d*][1,3]dioxole-5-carbaldehyde (**4i**)

To a solution of (6-iodobenzo[*d*][1,3]dioxol-5-yl)methanol (2 g, 7.2 mmol) in anhydrous DCM (50 mL) at 0 ºC under argon pyridinium chlorochromate (3.1 g, 14.4 mmol, 2 eq.) was added portionwise. The resulting mixture stirred at ambient temperature for 18 h. After this time, the solids were removed by filtration over a plug of silica that was subsequently washed with DCM (50 mL). The combined filtrates were concentrated under reduced pressure to afford a pale-yellow oil that was purified by column chromatography to provide the title compound.

Yield	1.88 g, 95%
Appearance	off-white solid
Molecular formula	$C_8H_5IO_3$
Molar mass	276.02947
TLC	R_f = 0.72 (DCM)

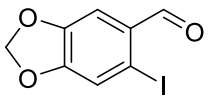

^{1}H-NMR	(200 MHz, $CDCl_3$): δ [ppm] = 9.88 (s, 1H), 7.37 (s, 1H), 7.33 (s, 1H), 6.08 (s, 2H).

Another method was tried to synthesize the title compound.[92] To a solution of (6-formylbenzo[*d*][1,3]dioxol-5-yl)boronic acid (240 mg, 1.2 mmol) in dry acetonitrile (10 mL) *N*-iodosuccinimide (418 mg, 1.9 mmol, 1.5 eq.) was added and the mixture was stirred at 80 °C for 18 h in darkness. After that, the reaction mixture was extracted thrice with petroleum ether (50 mL) and the combined extracts were washed with aqueous $NaHCO_3$ (5%, 50 mL), distilled water, brine and finally dried over $MgSO_4$. The residue obtained by evaporation of the solvent was purified by column chromatography. The spectroscopic data of the product matched to those of the first method. Yield (285 mg, 83%).

5.1.20 6-(4,4,5,5-Tetramethyl-1,3,2-dioxaborolan-2-yl)benzo[*d*][1,3]dioxole-5-carbaldehyde (**4j**)

(6-Formylbenzo[*d*][1,3]dioxol-5-yl)boronic acid (0.5 g, 2.58 mmol) and pinacol (347 µL, 2.84 mmol, 1.1 eq.) was refluxed in toluene (10 mL) for 18 h. After cooling, the mixture was filtered through a pad of Celite and a pad of Na_2SO_4. The solvent was then removed in vacuum by adding MeOH (2×10 mL) to remove toluene. The residue was recrystallized from petroleum ether to yield the title compound.

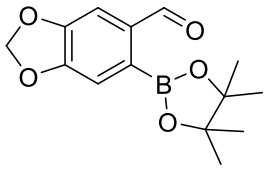

Yield	500 mg, 70%
Appearance	white solid
Molecular formula	$C_{14}H_{17}BO_5$
Molar mass	276.0950
^{1}H-NMR[93]	(400 MHz, $CDCl_3$): δ [ppm] = 10.50 (s, 1H), 7.46 (s, 1H), 7.31 (s, 1H), 6.04 (s, 1H), 1.36 (s, 12H).
^{13}C-NMR	(101 MHz, $CDCl_3$) δ [ppm] = 193.00, 151.88, 150.47, 138.28, 114.89, 106.84, 102.03, 84.54, 24.98.
HRMS	m/z: $[M + H]^+$ calcd for $C_{14}H_{18}BO_5^+$: 277.12418; found: 277.12432.
Anal.	Calcd for $C_{14}H_{17}BO_5$: C, 60.90; H, 6.21. Found: C, 60.88 ± 0.02; H, 6.25± < 0.01.

5.1.21 Potassium trifluoro(6-formylbenzo[*d*][1,3]dioxol-5-yl)borate (**4k**)

(6-Formylbenzo[*d*][1,3]dioxol-5-yl)boronic acid (200 mg, 1 mmol) was stirred with potassium bifluoride (240 mg, 3.1 mmol, 3 eq.) in a mixture of MeOH (4 ml) and water (2 ml) for 2 h at ambient temperature. After that, the solvents were removed under reduced pressure. Acetonitrile was added to the residue and treated in ultrasonic bath then acetonitrile was removed and this process was repeated three times. The acetonitrile phases were combined and dried under reduced pressure to deliver the title compound.

Yield	220 mg, 83%
Appearance	white solid
Molecular formula	$C_8H_5BF_3KO_3$
Molar mass	256.02851
^{1}H-NMR	(200 MHz, DMSO-d_6): δ [ppm] = 10.24 (s, 1H, H-8), 7.14 (s, 1H, H-), 7.01 (s, 1H, H-), 5.99 (s, 2H, H-1).
^{19}F-NMR	(188 MHz, DMSO-d_6): δ [ppm] = -131.83.
HRMS	m/z: $[M - K]^-$ calcd for $C_8H_5BF_3O_3^-$: 217.02893; found: 217.02878.

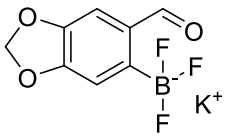

5.1.22 6-(Trimethylstannyl)benzo[*d*][1,3]dioxole-5-carbaldehyde (**4l**)

The title compound was synthesized according to general procedure B using methyl 6-bromopiperonal (2.95 g, 13 mmol), $Pd(PPh_3)_4$ (0.05 eq.) and hexamethylditin (1.2 eq.). The crude mixture was purified with flash chromatography petroleum ether:Et_2O (4:1).

Yield	3 g, 74%
Appearance	white solid
Molecular formula	$C_{11}H_{14}O_3Sn$
Molar mass	312.94000
^{1}H NMR	(200 MHz, $CDCl_3$): δ [ppm] = 9.77 (d, *J* = 0.7 Hz, 1H), 7.31 (dd, *J* = 9.7, 4.1 Hz, 1H), 7.22 – 7.14 (m, 1H), 6.07 (s, 2H), 0.27 (s, 9H).
^{13}C NMR	(50 MHz, $CDCl_3$): δ [ppm] = 191.43, 152.53, 148.57, 141.77, 135.77, 116.41, 114.01, 101.90, -7.55.
HRMS	m/z: $[M - CH_3]^+$ calcd for $C_{10}H_{11}O_3Sn^+$: 298.97247; found: 298.97264. Correct isotopic pattern.

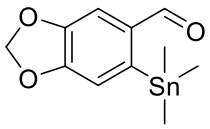

5.1.23 1-(Benzo[*d*][1,3]dioxol-5-yl)ethan-1-ol (**5a**)

General procedure D: To a stirred solution of a piperonal (3 g, 20 mmol) in dry THF (60 mL) methylmagnesium bromide (20 mL of a 3M solution in Et_2O, 3.0 eq.) was added at 0 °C. The reaction mixture was stirred at 0 °C for 30 min and then warmed to room temperature. After stirring overnight, saturated aqueous NH_4Cl (40 mL) was added slowly at 0 °C and then extracted with ethyl acetate (3×40 mL). The combined organic phases was dried over $MgSO_4$. Evaporation of the solvent and purification by column chromatography (EtOAc:petroleum ether, 1:4) afforded the pure product.

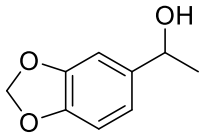

Yield	3.1 g, 93%
Appearance	yellow oil
Molecular formula	$C_9H_{10}O_3$
Molar mass	166.17600
^{1}H NMR	(200 MHz, $CDCl_3$): δ [ppm] = 6.88 (d, *J* = 1.0 Hz, 1H), 6.81 (t, *J* = 4.8 Hz, 1H), 6.76 (d, *J* = 7.9 Hz, 1H), 5.94 (d, *J* = 0.4 Hz, 2H), 4.80 (q, *J* = 6.5 Hz, 1H), 2.03 (s, 1H), 1.45 (d, *J* = 6.4 Hz, 3H).
^{13}C NMR	(50 MHz, $CDCl_3$): δ [ppm] = 147.78, 146.84, 140.05, 118.72, 108.11, 106.09, 101.00, 70.23, 25.17.

5.1.24 1-(6-Iodobenzo[*d*][1,3]dioxol-5-yl)ethan-1-ol (**5b**)

In a darkened fume hood, a solution of molecular iodine (5.10 g, 20 mmol, 1.2 eq.) in MeOH (50 mL) was added, dropwise and via a pressure-equalized dropping funnel, to a magnetically stirred suspension of **5a** (2.8 g, 16.8 mmol) and silver trifluoroacetate (4.46 g, 20 mmol, 1.2 eq.) in $CHCl_3$ (50 mL) maintained at 0 ºC under argon. The resulting suspension was stirred vigorously at ambient temperature for 18 h. The solids formed were removed by filtration through a pad of Celite. The pad was washed with CHCl3 (50 mL), the combined filtrates concentrated under reduced pressure, and the dark-red residue thus obtained was dissolved in DCM (100 mL) and the solution was washed three times with saturated aqueous solution of sodium thiosulfate (50 mL) then brine (50 mL) before being dried over MgSO4, filtered and concentrated under reduced pressure. The residue was purified with flash chromatography (DCM) to provide the title compound.

Yield	2.5 g, 51%
Appearance	off white solid
Molecular formula	$C_9H_9IO_3$
Molar mass	292.07247

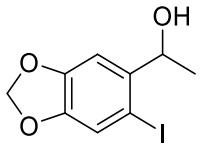

^{1}H NMR	(200 MHz, $CDCl_3$): δ [ppm] = 7.20 (s, 1H), 7.09 (s, 1H), 5.97 (dd, *J* = 3.3, 1.4 Hz, 2H), 5.01 (q, *J* = 6.3 Hz, 1H), 1.99 (s, 1H), 1.40 (d, *J* = 6.3 Hz, 3H).
^{13}C NMR	(50 MHz, $CDCl_3$): δ [ppm] = 148.92, 147.75, 141.20, 118.33, 106.64, 101.69, 84.62, 73.75, 23.84.

5.1.25 1-(6-Bromobenzo[*d*][1,3]dioxol-5-yl)ethan-1-ol (**5c**)[94]

The title compound was synthesized according to general procedure D using 6-bromopiperonal (2 g, 9 mmol). Then it was purified by flash chromatography (EtOAc:petroleum ether, 1:4) afforded the pure product.

Yield	1.5 mg, 69%
Appearance	colorless oil
Molecular formula	$C_9H_9BrO_3$
Molar mass	245.07200

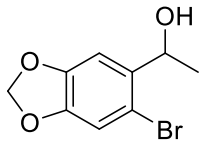

^{1}H-NMR	(200 MHz, $CDCl_3$): δ [ppm] = 7.09 (s, 1H), 6.96 (s, 1H), 5.97 (dd, *J* = 2.8, 1.4 Hz, 2H), 5.17 (q, *J* = 6.2 Hz, 1H), 1.91 (s, 1H), 1.43 (d, *J* = 6.4 Hz, 3H).
^{13}C-NMR	(50 MHz, $CDCl_3$): δ [ppm] = 147.93, 147.58, 138.24, 112.57, 111.91, 106.78, 101.85, 69.23, 23.77.

5.1.26 1-(6-Iodobenzo[*d*][1,3]dioxol-5-yl)ethan-1-one (**6a**)

To a solution of **5b** (2 g, 6.8 mmol) in anhydrous DCM (50 mL) at 0 ºC under argon pyridinium chlorochromate (2.9 g, 13.7 mmol, 2 eq.) was added portionwise. The resulting mixture stirred at ambient temperature for 18 h. After this time, the solids were removed by passing the reaction mixture through a plug of silica that was subsequently washed with DCM (50 mL). The combined filtrates were concentrated under reduced

pressure to afford pale-yellow oil that was purified by flash chromatography (DCM) to provide the title compound.

Yield	1.8 g, 91%
Appearance	yellow solid
Molecular formula	$C_9H_7IO_3$
Molar mass	290.05647
^{1}H NMR	(200 MHz, $CDCl_3$): δ [ppm] = 7.36 (s, 1H), 7.05 (s, 1H), 6.04 (s, 2H), 2.58 (s, 3H).
^{13}C NMR	(50 MHz, $CDCl_3$): δ [ppm] = 199.63, 150.40, 148.27, 136.63, 120.71, 109.23, 102.39, 81.42, 29.29.

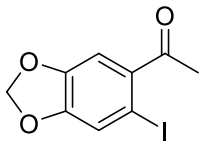

5.1.27 1-(6-Bromobenzo[*d*][1,3]dioxol-5-yl)ethan-1-one (**6b**)

To a solution of **5c** (1.4 g, 6 mmol) in dry DCM (50 mL) at 0 °C pyridinium chlorochromate (2.6 g, 12 mmol, 2 eq.) was added. The mixture was stirred for 2 h and then allowed to warm to room temperature and stirred overnight. The resulted mixture was filtered through silica. DCM was removed under vacuum to deliver the title compound after recrystallization from DCM/hexane.

Yield	1.5 g, 69%
Appearance	White solid
Molecular formula	$C_9H_7BrO_3$
Molar mass	243.05600
^{1}H-NMR[94]	(200 MHz, $CDCl_3$): δ [ppm] = 7.08 – 6.97 (m, 2H)., 6.03 (s, 2H), 2.60 (s, 3H).
^{13}C-NMR	(50 MHz, $CDCl_3$) δ 199.65, 150.50, 147.52, 134.42, 114.02, 112.10, 109.47, 102.56, 30.44.

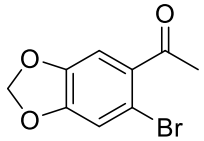

5.1.28 1-(6-(Trimethylstannyl)benzo[*d*][1,3]dioxol-5-yl)ethan-1-one (**6c**)

The title compound was synthesized according to general procedure B using **6b** (1.2 g, 5.1 mmol), $Pd(PPh_3)_4$ (295 mg, 0.3 mmol, 0.05 eq.) and hexamethylditin (1.2 mL, 6.1 mmol, 1.2 eq.). The product was purified with flash chromatography (Et_2O:petroleum ether, 1:9).

Yield	450 mg, 27%
Appearance	white solid
Molecular formula	$C_{12}H_{16}O_3Sn$
Molar mass	326.96700

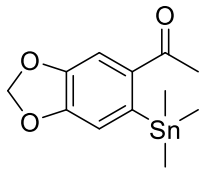

^{1}H-NMR	(200 MHz, $CDCl_3$): δ [ppm] = 7.48 (s, 1H), 7.17 (s, 1H), 6.05 (s, 2H), 2.57 (s, 3H), 0.20 (s, 9H).
^{13}C-NMR	(50 MHz, $CDCl_3$): δ [ppm] = 197.43, 151.73, 148.26, 142.63, 135.34, 116.02, 110.75, 101.86, 26.45, -6.97.
HRMS	m/z: $[M - CH_3]^+$ calcd for $C_{11}H_{13}O_3Sn^+$: 312.98812; found: 312.98846. Correct isotopic pattern.

5.1.29 Methyl 3,4-(methylenedioxy)-6-nitrophenyl ketone (**6d**)

To 3,4-(methylenedioxy)-acetophenone (0.5 g, 3 mmol) in $MeNO_2$ (10 mL) at ambient temperature was added HNO_3 (1 mL, 65%, 18.3 mmol, 6 eq.) dropwise in 10 min. The solution was stirred for additional 2 h. The reaction mixture was carefully neutralized by the addition of saturated aqueous $NaHCO_3$ solution and then extracted with DCM. The combined organic phase was dried over Na_2SO_4. The solvent was removed in vacuum and the residue was purified by flash chromatography to afford the title compound.

Yield	250 mg, 39%
Appearance	yellow solid
Molecular formula	$C_9H_7NO_5$
Molar mass	209.15700
TLC	R_f = 0.48 (EtOAc:petroleum ether 1:2)
^{1}H NMR	(200 MHz, $CDCl_3$): δ [ppm] = 7.51 (s, 1H), 6.73 (s, 1H), 6.17 (s, 2H), 2.47 (s, 3H).
^{13}C NMR	(50 MHz, $CDCl_3$): δ [ppm] = 199.33, 152.83, 148.97, 135.23, 106.29, 104.91, 103.78, 30.32.

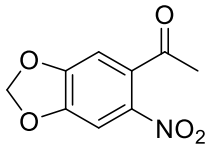

5.1.30 1-Bromo-3-(2',2'-dibromovinyl)benzene (**7**)

3-Bromobenzaldehyde (630 µL, 5.4 mmol,) was added to a reagent prepared from interaction of zinc dust (0.7 g, 10.8 mmol, 2 eq.), triphenylphosphine (2.8 g, 10.8 mmol,

2 eq.), and tetrabromomethane (3.6 g, 10.8 mmol, 2 eq.) in DCM at room temperature for 30 h with a reaction time of 12 h at room temperature. After that DCM was evaporated and the rest was taken with Et_2O (100 mL), washed with water (2×100 mL) and brine (100 mL) and then dried over $MgSO_4$. The organic phase was dried under vacuum and the raw product was purified by column chromatography (petroleum ether) to give the desired product.

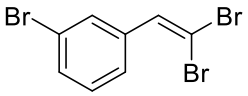

Yield	1.8 g, 98%
Appearance	yellow oil
Molecular formula	$C_8H_5Br_3$
Molar mass	340.84000
^{1}H NMR	(200 MHz, $CDCl_3$): δ [ppm] = 8.23 – 6.01 (m, 5H).

5.1.31 2,3-Dibromo-3-(3-bromophenyl)propanoic acid (**8**)[95]

Sodium bromide (27.2 g, 264 mmol, 2.4 eq.) is added to mixture of sodium perborate tetrahydrate (20.3 g, 132 mmol, 1.2 eq.) and 3-bromocinnamic acid (25 g, 110 mmol) in glacial acetic acid (200 mL) and stirred for 18 h at room temperature. The mixture is then diluted with water, the product extracted into ether and dried over $MgSO_4$. Removals of solvent afford the title compound.

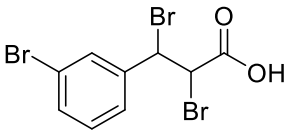

Yield	35 g, 82%
Appearance	white solid
Molecular formula	$C_9H_7Br_3O_2$
Molar mass	386.86500
^{1}H-NMR	(200 MHz, DMSO-d_6): δ [ppm] = 7.93 (t, *J* = 1.6 Hz, 1H), 7.66 (d, *J* = 7.9 Hz, 1H), 7.54 (ddd, *J* = 8.0, 1.9, 1.0 Hz, 1H), 7.42 – 7.20 (m, 1H), 5.57 (d, *J* = 11.8 Hz, 1H), 5.38 (d, *J* = 11.8 Hz, 1H), 4.30 (br, 1H).
^{13}C-NMR	(50 MHz, DMSO-d_6): δ [ppm] = 168.98, 140.99, 131.93, 131.17, 130.83, 127.56, 121.75, 50.27, 46.81.

5.1.32 1-(3-Bromophenyl)-3-hydroxy-3-(6-iodobenzo[*d*][1,3]dioxol-5-yl)prop-2-en-1-one (**9a**)

General procedure E: To a solution of **6a** (1.5 g, 5.2 mmol) in anhydrous THF (20 mL) was added LiHMDS (15.6 mL, 1M in THF, 15.6 mmol, 3 eq.) and the resulting solution stirred for 1 h at -80 °C. The solution was warmed to room temperature and stirred for 2 h before cooling to -80 °C and adding 3-bromobenzoyl chloride (0.68 mL, 5.2 mmol, 1 eq.) dropwise. The solution was allowed to warm to room temperature and stirred for additional 18 h. Then the reaction was quenched with saturated solution of NH_4Cl (50 mL). The pH adjusted to 7.0. Then extracted with EtOAc (3×50 mL). The combined organic layers were washed with brine (100 mL), dried over $MgSO_4$ and then dried under vacuum. The resulted residue was purified with flash chromatography.

Yield	2 g, 84%
Appearance	yellow solid
Molecular formula	$C_{16}H_{10}BrIO_4$
Molar mass	473.06047

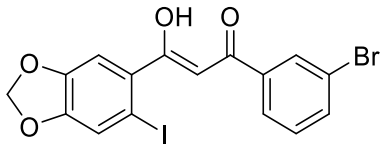

TLC	R_f = 0.53 (Et_2O/petroleum ether, 1:4)
^{1}H NMR	(200 MHz, $CDCl_3$): δ [ppm] = 16.04 (s, 1H), 8.06 (t, J = 1.7 Hz, 1H), 7.96 – 7.75 (m, 1H), 7.66 (ddd, J = 8.0, 1.9, 1.0 Hz, 1H), 7.48 – 7.27 (m, 2H), 7.05 (s, 1H), 6.53 (s, 1H), 6.05 (s, 2H).
^{13}C NMR	(50 MHz, $CDCl_3$): δ [ppm] = 190.73, 181.17, 150.42, 148.56, 136.79, 135.51, 135.44, 130.39, 130.26, 125.77, 123.12, 120.30, 109.67, 102.47, 98.09, 82.78.
HRMS	m/z: $[M - H]^-$ calcd for $C_{16}H_9BrIO_4^-$: 470.87344; found: 470.87396. Correct isotopic pattern.

5.1.33 1-(3-Bromophenyl)-3-hydroxy-3-(6-(trimethylstannyl)benzo[*d*][1,3]dioxol-5-yl)prop-2-en-1-one (**9b**)

The title compound was synthesized according to general procedure E using **6c** (450 mg, 1.4 mmol), LiHMDS (3 eq.) and 3-bromobenzoyl chloride (1 eq). The resulted residue was purified with flash chromatography.

Yield	690 mg, 98%

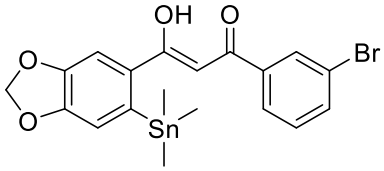

Appearance	yellow solid
Molecular formula	$C_{19}H_{19}BrO_4Sn$
Molar mass	509.97100
TLC	R_f = 0.50 (Et_2O/petroleum ether, 1:4)
^{1}H-NMR	(200 MHz, $CDCl_3$): δ [ppm] = 16.42 (s, 1H), 8.09 (s, 1H), 7.88 (d, *J* = 7.9 Hz, 1H), 7.68 (d, *J* = 7.9 Hz, 1H), 7.48 (d, *J* = 6.5 Hz, 1H), 7.38 (t, *J* = 7.9 Hz, 1H), 7.26 (d, *J* = 11.7 Hz, 1H), 6.74 (s, 1H), 6.09 (s, 2H), 0.29 (s, 9H).
^{13}C-NMR	(50 MHz, $CDCl_3$): δ [ppm] = 191.22, 177.31, 151.56, 148.37, 142.46, 136.52, 135.13, 135.01, 130.35, 129.87, 125.39, 123.07, 116.32, 108.77, 101.88, 93.35, -6.39.
HRMS	m/z: $[M - CH_3]^+$ calcd for $C_{18}H_{16}BrO_4Sn^+$: 496.92280; found: 496.92306. Correct isotopic pattern.

5.1.34 3-(Benzo[*d*][1,3]dioxol-5-yl)-1-(3-bromophenyl)-3-hydroxyprop-2-en-1-one (**9c**)

The title compound was synthesized according to general procedure E using 1-(benzo[*d*][1,3]dioxol-5-yl)ethan-1-one (1.5 g, 9.1 mmol), LiHMDS (3 eq.) and 3-bromobenzoyl chloride (1 eq.).

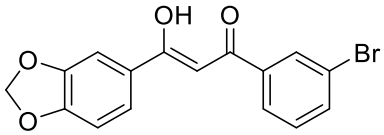

Yield	2.82 g, 89%
Appearance	yellow solid
Molecular formula	$C_{16}H_{11}BrO_4$
Molar mass	347.16400
TLC	R_f = 0.46 (Et_2O/petroleum ether, 1:4)
^{1}H-NMR	(200 MHz, $CDCl_3$): δ [ppm] = 7.88 (q, *J* = 1.7 Hz, 1H), 7.75 – 7.60 (m, 1H), 7.53 – 7.34 (m, 2H), 7.31 – 7.23 (m, 1H), 7.23 – 7.08 (m, 1H), 6.75 – 6.61 (m, 1H), 6.54 (s, 1H), 5.87 (s, 2H).
^{13}C-NMR	(50 MHz, $CDCl_3$): δ [ppm] = 151.34, 147.91, 136.89, 136.87, 134.57, 129.91, 129.50, 125.19, 122.91, 122.42, 107.89, 106.85, 101.61, 92.48.

HRMS m/z: $[M - H]^-$ calcd for $C_{16}H_{10}BrO_4^-$: 344.97679; found: 344.97664. Correct isotopic pattern.

5.1.35 3-(Benzo[*d*][1,3]dioxol-5-yl)-1-(3-fluorophenyl)-3-hydroxyprop-2-en-1-one (**9e**)

The title compound was synthesized according to general procedure E using 1-(benzo[*d*][1,3]dioxol-5-yl)ethan-1-one (500 mg, 3 mmol), LiHMDS (3 eq.) and 3-fluorobenzoyl chloride (1 eq).

Yield 735 mg, 84%

Appearance yellow solid

Molecular formula $C_{16}H_{11}FO_4$

Molar mass 286.25840

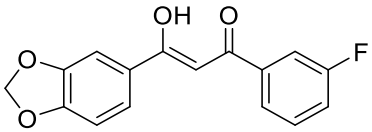

TLC R_f = 0.45 (Et_2O/petroleum ether, 1:4)

1H NMR (200 MHz, $CDCl_3$): δ [ppm] = 16.80 (s, 1H), 7.74 (dd, *J* = 7.8, 1.1 Hz, 1H), 7.63 (ddd, *J* = 10.0, 6.0, 2.2 Hz, 2H), 7.55 – 7.37 (m, 2H), 7.32 – 7.16 (m, 1H), 6.90 (d, *J* = 8.2 Hz, 1H), 6.71 (s, 1H), 6.07 (s, 2H).

13C NMR (50 MHz, $CDCl_3$): δ [ppm] = 186.52, 182.20, 165.36, 160.59, 151.79, 148.44, 130.45, 130.29, 130.02, 123.28, 122.76, 122.70, 119.40, 118.98, 114.28, 113.82, 108.41, 107.41, 102.08, 92.88.

^{19}F NMR (188 MHz, $CDCl_3$): δ [ppm] = -111.97.

HRMS m/z: $[M - H]^-$ calcd for $C_{16}H_{10}FO_4^-$: 285.05686; found: 285.05685.

5.1.36 (6-Iodobenzo[*d*][1,3]dioxol-5-yl)methanol[81]

In a darkened fume hood, a solution of molecular iodine (4.10 g, 16 mmol, 1.2 eq.) in MeOH (75 mL) was added, dropwise and via a pressure-equalized dropping funnel, to a magnetically stirred suspension of 1,3-benzodioxole-5-methanol (2.05 g, 13.48 mmol) and silver trifluoroacetate (3.60 g, 16 mmol, 1.2 eq.) in $CHCl_3$ (75 mL) maintained at 0 ºC under argon. The resulting suspension was stirred vigorously at ambient temperature for 18 h. The solids formed were removed by filtration through a pad of Celite. The pad was washed with $CHCl_3$ (50 mL). The combined filtrates were washed three times with saturated aqueous solution of sodium thiosulfate (100 mL) then brine (100 mL) before

being dried over $MgSO_4$, filtered and concentrated under reduced pressure. The residue was purified with flash chromatography to provide the title compound.

Yield	2.33 g, 62%
Appearance	white solid
Molecular formula	$C_8H_7IO_3$
Molar mass	278.04547
TLC	R_f = 0.37 (EtOAc/petroleum ether, 1:4)
^{1}H-NMR	(200 MHz, $CDCl_3$): δ [ppm] = 7.23 (s, 1H), 6.99 (s, 1H), 5.98 (s, 2H), 4.59 (s, 2H), 1.81 (s, 1H).

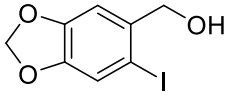

5.1.37 Tetrakis(pyridine)copper(II) bis(trifluoromethanesulfonate)[96]

Copper(II) trifluoromethanesulfonate (5 g, 14 mmol) was dissolved in methanol (25 mL). Pyridine (12 mL, 149 mmol) was added dropwise and stirred for 30 min. The exothermic reaction was allowed to sit in room temperature for one hour and then in fridge (5 °C) overnight. The blue crystalline precipitate was filtrated off. The product was recrystallized from a hot (40 °C) solution of pyridine in methanol (1:4 v/v) and dried under stream of air.

Yield	8.5 g, 91%
Appearance	blue solid
Molecular formula	$C_{22}H_{20}CuF_6N_4O_6S_2$
Molar mass	678.08042
Anal.	Calcd for $C_{22}H_{20}CuF_6N_4O_6S_2$: C, 38.97; H, 2.97; N, 8.26. Found: C, 39.1± < 0.1; H, 3.16±0.09; N, 8.33±0.01.

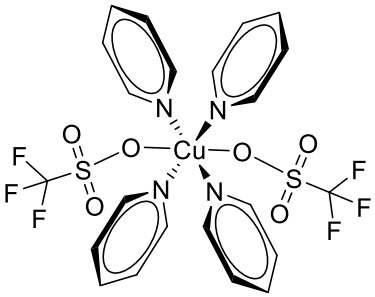

5.1.38 3-(Trimethylstannyl)benzaldehyde

The title compound was synthesized according to general procedure **B** using 3-bromobenzaldehyde (850 mg, 4.6 mmol), $Pd(PPh_3)_4$ (531 mg, 0.5 mmol, 0.1 eq.) and hexamethylditin (1.9 mL, 9.2 mmol, 2 eq.). The product was purified with flash chromatography (Et_2O:petroleum ether, 1:9).

Yield	900 mg, 73%

Appearance	colorless oil
Molecular formula	$C_{10}H_{14}O_3Sn$
Molar mass	268.93100
^{1}H-NMR	(200 MHz, $CDCl_3$): δ [ppm] = 10.03 (s, 1H), 8.19 – 7.89 (m, 1H), 7.89 – 7.64 (m, 2H), 7.52 (t, *J* = 7.4 Hz, 1H), 0.34 (s, 9H).
^{13}C-NMR	(50 MHz, $CDCl_3$): δ [ppm] = 193.18, 143.88, 142.05, 137.09, 135.75, 129.87, 128.61, -9.33.

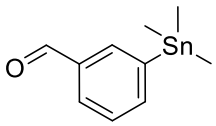

5.1.39 Trimethyl(phenyl)germane

General procedure F: In flame dried flask *n*-BuLi (1 mL 2.5M in , 1.3 eq.) was added to a stirred solution of iodobenzene (219 µL, 2 mmol) in anhydrous Et_2O (2 mL) under argon at -80 °C. After 30 min chlorotrimethylgermane (291 µL, 1.2 eq.) dissolved in anhydrous Et_2O (1 mL) was added at -50 °C. The reaction was stirred for further 30 min and then quenched with $NH_4Cl_{sat.}$ (50 mL). The mixture was extracted with Et_2O (3×10 mL). The organic phase was then washed with brine (50 mL) and dried over Na_2SO_4. The volatiles were then removed under reduced pressure. The resulted residue was used without further purification.

Yield	248 mg, 50%
Appearance	yellow oil
Molecular formula	$C_9H_{14}Ge$
Molar mass	194.84100
^{1}H NMR[97]	(200 MHz, $CDCl_3$): δ [ppm] = 7.55 – 7.28 (m, 5H), 0.39 (s, 9H).

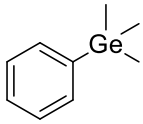

5.1.40 Methyl 4-fluorobenzoate

4-fluorobenzoyl chloride (500 µL, 4.2 mmol) was stirred in MeOH (20 mL) at 40 °C for 2 h. After that, the volatiles were removed under reduced pressure. The residue was used without further purification.

Yield	440 mg, 67%
Appearance	colorless oil
Molecular formula	$C_8H_7FO_2$
Molar mass	154.14040

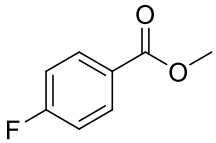

^{1}H NMR (200 MHz, $CDCl_3$): δ [ppm] = 8.17 – 7.95 (m, 2H), 7.21 – 6.97 (m, 2H), 3.92 (s, 3H).

^{13}C NMR (50 MHz, $CDCl_3$): δ [ppm] = 168.41, 166.27, 163.36, 132.34, 132.16, 126.58, 126.52, 115.85, 115.42, 52.31.

^{19}F NMR (188 MHz, $CDCl_3$): δ [ppm] = -105.79.

5.1.41 Methyl 4-(trimethylstannyl)benzoate

The title compound was synthesized according to general procedure B using methyl 4-iodobenzoate (2 g, 7.6 mmol), $Pd(PPh_3)_4$ (0.05 eq.) and hexamethylditin (1.2 eq.). The product was purified with flash chromatography (Et_2O:petroleum ether, 1:9).

Yield 1.9 g, 83%

Appearance yellow oil

Molecular formula $C_{11}H_{16}O_2Sn$

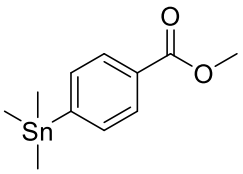

Molar mass 298.85700

^{1}H NMR (200 MHz, $CDCl_3$): δ [ppm] = 8.19 – 7.86 (m, 2H), 7.79 – 7.37 (m, 2H), 3.92 (s, 3H), 0.33 (s, 9H).

^{13}C NMR (50 MHz, $CDCl_3$): δ [ppm] = 167.48, 149.69, 135.82, 135.82, 129.86, 128.55, 128.55, 52.08, -9.50.

5.1.42 *tert*-Butyl (*S*)-2-(bis(*tert*-butoxycarbonyl)amino)-3-(4-((*tert*-butoxycarbonyl)oxy)-5-methoxy-2-(trimethylstannyl)phenyl)propanoate

General procedure F: To a solution of *tert*-butyl (*S*)-2-((tert-butoxycarbonyl)amino)-3-(4-((*tert*-butoxycarbonyl)oxy)-5-methoxy-2-(trimethylstannyl)phenyl)propanoate (220 mg, 0.3 mmol) in dry acetonitrile (3 mL) under argon was added 4-dimethylaminopyridine (DMAP) (17 mg, 0.1 mmol, 0.4 eq.) and di-*tert*-butyl dicarbonate (229 mg, 1 mmol, 3 eq.). The reaction was stirred at room temperature for 48 h, and then concentrated under vacuum. Purification by flash chromatography (Et_2O:petroleum ether, 1:9) afforded the title compound.

Yield	255 mg, 86%
Appearance	yellow oil
Molecular formula	$C_{32}H_{53}NO_{10}Sn$
Molar mass	730.48300

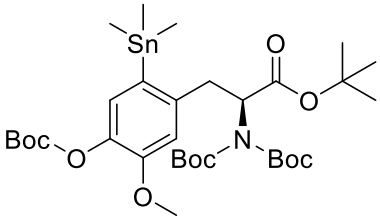

^{1}H NMR	(200 MHz, $CDCl_3$): δ [ppm] = 7.09 (s, 1H), 6.84 – 6.68 (m, 1H), 5.29 (s, 3H), 4.88 (dd, *J* = 9.3, 6.2 Hz, 1H), 3.60 – 3.36 (m, 2H), 1.53 (s, 9H), 1.48 (s, 9H), 1.38 (s, 18H), 0.30 (s, 9H).
^{13}C NMR	(50 MHz, $CDCl_3$): δ [ppm] = 169.01, 152.27, 143.78, 129.41, 114.13, 83.26, 82.84, 81.86, 60.52, 55.74, 28.13, 28.01, 27.77, -8.22.
HRMS	m/z: $[M + Na]^+$ calcd for $C_{32}H_{53}NNaO_{10}Sn^+$: 754.25836; found: 754.25918. Correct isotopic pattern.

5.1.43 Ethyl (*S*)-3-(4,5-bis((*tert*-butoxycarbonyl)oxy)-2-(trimethylstannyl)phenyl)-2-(bis(*tert*-butoxycarbonyl)amino)propanoate

The title compound was synthesized according to general procedure F using ethyl (*S*)-3-(4,5-bis((*tert*-butoxycarbonyl)oxy)-2-(trimethylstannyl)phenyl)-2-((*tert*-butoxycarbonyl)amino)propanoate (200 mg, 0.3 mmol), DMAP (0.4 eq.) and di-*tert*-butyl dicarbonate (3 eq.).

Yield	229 mg, 96%
Appearance	yellow oil
Molecular formula	$C_{34}H_{55}NO_{12}Sn$
Molar mass	788.51900

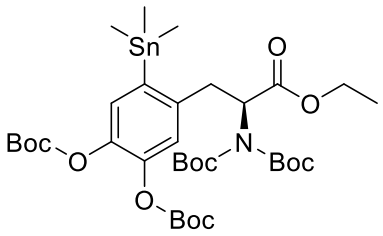

^{1}H NMR	(200 MHz, $CDCl_3$): δ [ppm] = 7.23 (s, 1H), 7.15 – 6.97 (m, 1H), 5.03 (dd, *J* = 9.8, 4.8 Hz, 1H), 4.21 (ddt, *J* = 10.3, 7.0, 3.5 Hz, 2H), 3.52 – 3.18 (m, 2H), 1.52 (d, *J* = 2.5 Hz, 18H), 1.38 (s, 18H), 1.27 (t, *J* = 5.8 Hz, 3H), 0.33 (s, 9H).
^{13}C NMR	(50 MHz, $CDCl_3$): δ [ppm] = 170.17, 152.04, 150.87, 150.72, 143.22, 142.58, 141.37, 140.61, 130.08, 123.94, 83.54, 83.45, 83.19, 61.57, 59.48, 37.93, 29.80, 27.96, 27.72, 14.26, -8.03.

HRMS m/z: $[M + Na - CH_2]^+$ calcd for $C_{34}H_{55}NNaO_{12}Sn^+$: 812.26384; found: 812.26458. Correct isotopic pattern.

5.1.44 Ethyl (*S*)-2-(bis(*tert*-butoxycarbonyl)amino)-3-(5-((*tert*-butoxycarbonyl)oxy)-2-(trimethylstannyl)phenyl)propanoate

The title compound was synthesized according to general procedure F using ethyl (*S*)-2-((*tert*-butoxycarbonyl)amino)-3-(5-((*tert*-butoxycarbonyl)oxy)-2-(trimethylstannyl)phenyl)propanoate (300 mg, 0.5 mmol), DMAP (0.4 eq.) and di-*tert*-butyl dicarbonate (3 eq.).

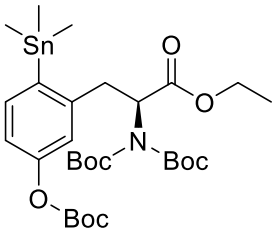

Yield 250 mg, 71%

Appearance yellow oil

Molecular formula $C_{29}H_{47}NO_9Sn$

Molar mass 672.40300

^{1}H NMR (200 MHz, $CDCl_3$): δ [ppm] = 7.37 (t, *J* = 8.4 Hz, 1H), 7.12 – 6.97 (m, 1H), 6.92 (d, *J* = 2.2 Hz, 1H), 5.02 (dd, *J* = 10.4, 4.5 Hz, 1H), 4.22 (qd, *J* = 7.1, 2.7 Hz, 2H), 3.59 – 3.20 (m, 2H), 1.53 (s, 9H), 1.38 (s, 18H), 1.28 (s, 3H), 0.32 (s, 9H).

^{13}C NMR (50 MHz, $CDCl_3$): δ [ppm] = 170.21, 151.98, 151.90, 151.72, 146.34, 140.06, 137.19, 122.32, 118.86, 83.34, 83.09, 61.58, 59.69, 38.42, 29.82, 27.96, 14.28, -8.10.

HRMS m/z: $[M + Na]^+$ calcd for $C_{29}H_{47}NNaO_9Sn^+$: 696.21650; found: 696.21766. Correct isotopic pattern.

5.1.45 Ethyl (*S*)-2-(bis(*tert*-butoxycarbonyl)amino)-3-(4-((*tert*-butoxycarbonyl)oxy)-2-(trimethylstannyl)phenyl)propanoate

The title compound was synthesized according to general procedure F using ethyl (*S*)-2-((*tert*-butoxycarbonyl)amino)-3-(4-((*tert*-butoxycarbonyl)oxy)-2-(trimethylstannyl)phenyl)propanoate (100 mg, 0.2 mmol), DMAP (0.4 eq.) and di-*tert*-butyl dicarbonate (3 eq.)

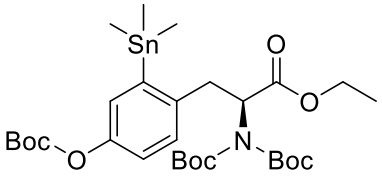

Yield 117 mg, 85%

Appearance yellow oil

Molecular formula $C_{29}H_{47}NO_9Sn$

Molar mass	672.40300
^{1}H NMR	(200 MHz, $CDCl_3$): δ [ppm] = 7.17 (d, *J* = 2.3 Hz, 1H), 7.12 – 6.84 (m, 1H), 4.98 (dd, *J* = 9.7, 5.1 Hz, 1H), 4.21 (qd, *J* = 7.2, 1.9 Hz, 1H), 3.35 (dd, *J* = 7.2, 4.2 Hz, 1H), 1.54 (s, 1H), 1.36 (s, 2H), 1.27 (s, 1H), 0.33 (s, 1H).
^{13}C NMR	(50 MHz, $CDCl_3$): δ [ppm] = 170.19, 151.95, 151.81, 149.48, 144.66, 142.01, 130.20, 128.49, 121.39, 83.39, 83.11, 61.54, 59.89, 37.87, 29.79, 27.97, 27.80, 14.26, -8.10.
HRMS	m/z: $[M + Na]^+$ calcd for $C_{29}H_{47}NNaO_9Sn^+$: 696.21650; found: 696.21700. Correct isotopic pattern.

5.1.46 (2-Methoxyphenyl)trimethylstannane

The title compound was synthesized according to general procedure D using 2-iodoanisol (131 µL, 1 mmol), *n*-BuLi (1.3 eq.) and trimethyltin chloride (2 eq.). The reaction was quenched with TBAF (1 mL, 1M solution in THF).

Yield	150 mg, 55%
Appearance	yellow oil
Molecular formula	$C_{10}H_{16}OSn$
Molar mass	270.94700
^{1}H NMR	(200 MHz, $CDCl_3$): δ [ppm] = 7.35 (ddd, *J* = 9.7, 7.5, 1.7 Hz, 2H), 7.24 – 6.94 (m, 1H), 6.94 – 6.72 (m, 1H), 3.80 (s, 3H), 0.27 (s, 9H).

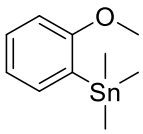

5.1.47 (3-Methoxyphenyl)trimethylstannane

The title compound was synthesized according to general procedure D using 3-iodoanisol (120 µL, 1 mmol), *n*-BuLi (1.3 eq.) and trimethyltin chloride (2 eq.). The reaction was quenched with TBAF (1 mL, 1M solution in THF).

Yield	180 mg, 66%
Appearance	yellow oil
Molecular formula	$C_{10}H_{16}OSn$
Molar mass	270.94700

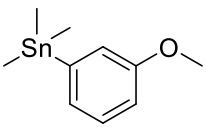

^{1}H NMR (200 MHz, $CDCl_3$): δ [ppm] = 7.45 – 7.18 (m, 1H), 7.18 – 6.97 (m, 2H), 6.89 (ddd, *J* = 8.3, 2.7, 1.1 Hz, 1H), 3.85 (s, 3H), 0.33 (s, 9H).

5.1.48 (4-Methoxyphenyl)trimethylstannane

The title compound was synthesized according to general procedure **D** using 3-iodoanisol (235 mg, 1 mmol), *n*-BuLi (1.3 eq.) and trimethyltin chloride (2 eq.). The reaction was quenched with TBAF (1 mL, 1M solution in THF).

Yield 190 mg, 70%

Appearance yellow oil

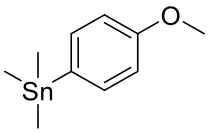

Molecular formula $C_{10}H_{16}OSn$

Molar mass 270.94700

^{1}H NMR (200 MHz, $CDCl_3$): δ [ppm] = 7.64 – 7.20 (m, 2H), 6.94 (ddd, *J* = 6.5, 4.1, 1.9 Hz, 2H), 3.82 (s, 3H), 0.28 (s, 9H).

5.1.49 1-(2,4-Dinitrophenyl)-pyridinium chloride

Pyridine (457 µL, 5.7 mmol, 1.1 eq.) was dissolved in acetone (2.5 mL) and stirred, while 2,4-dinitrochlorobenzene (1 g, 5 mmol, 1 eq.) was added to the reaction mixture. The mixture was heated under reflux 24 h and cooled to room temperature. The precipitate produced was filtered under suction and washed with *n*-hexane to obtain the title compound.

Yield 1.27 g, 91%

Appearance yellow solid

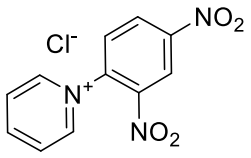

Molecular formula $C_{11}H_8ClN_3O_4$

Molar mass 281.65200

^{1}H NMR (300 MHz, DMSO-d_6): δ [ppm] = 9.48 (dd, *J* = 6.8, 1.2 Hz, 2H), 9.12 (d, *J* = 2.5 Hz, 1H), 9.03–8.90 (m, 2H), 8.58–8.38 (m, 3H).

^{13}C NMR (75 MHz, DMSO-d_6): δ [ppm] = 149.03, 148.73, 146.02, 143.01, 138.64, 131.88, 130.08, 127.94, 121.31.

5.2 Radiochemistry

5.2.1 General procedures

5.2.1.1 Materials and Methods

All labeling experiments were repeated at least 3 times. Standard deviations (SD) were calculated by the least-square method. All experiments were carried out as one-pot procedure and not by using aliquots. The reaction mixture was always quenched with water (2-4 mL) to dissolve any [^{18}F]fluoride on the reaction vessel walls. The loss of radio activity on the reaction vessel walls did not exceed 13±2% from the starting activity (decay corrected) in all experiments. All radiochemical yields (RCY) are decay corrected and radiochemical purities (RCP) were determined after purification. RCY for model compounds and in optimization experiments was determined by HPLC without purification.

5.2.1.2 High-performance liquid chromatography (HPLC)

For manual synthesis, the following system was used:

Ultimate® 3000 HPLC system from Thermo Scientific (Sunnyvale, USA) with Ultimate® 3000 LPG-3400A pump, Ultimate® 3000 VWD-3100 UV/Vis detector and γ-detector Gabi Star from Raytest GmbH (Straubenhardt, Deutschland) were used. The volume of injection was 20 µL. UV-detection was at λ = 210 nm wave length.

The following column were used:

- Chromolith® SpeedROD RP-18 endcapped 50×4.6 mm from Merck KGaA (Darmstadt, Germany).
- ProntoSIL C18 ace-EPS 125×4.6 mm from Bischoff Analysentechnik und -geräte GmbH, Leonberg, Germany.
- Gemini® 5 µm C18 110 Å, LC Column 250×4.6 mm from Phenomenex Inc.
- Gemini® 5 µm C18 110 Å, LC Column 250×10 mm from Phenomenex Inc.

In the automated synthesis, the following system was used:

WellChrom Spectro-photometer K-2501 UV/Vis detector, BlueShadow Pump 80P from KNAUER Wissenschaftliche Geräte GmbH, Berlin, Germany and AD 1422 PIN-photodiode and scintillator detector from Eckert & Ziegler Strahlen- und Medizintechnik AG, Berlin, Germany was connected directly to the automated module.

For automated synthesis, the following C18 with polar endcapping column were used:

- Synergi™ 4 µm Hydro-RP 80 Å, LC Column 250×10 mm from Phenomenex Inc.
- Synergi™ 4 µm Hydro-RP 80 Å, LC Column 150×21.2 mm, AXIA™ Packed from Phenomenex Inc.

5.2.1.3 Solid Phase Extraction Cartridges (SPE) and anion exchange cartridges (AX)

Strata™-X-A 33 µm Polymeric Strong Anion, 30 mg/1 mL, tubes from Phenomenex Inc; Chromafix® (PS-HCO_3) cartridge from Macherey-Nagel GmbH & Co.KG and Sep-Pak® Accell plus QMA Carbonate Plus Light Cartridge from Waters Co. These anion exchange cartridges were preconditioned with 1 mL water before it was dried with a stream of air.

Strata™-X 33 µm Polymeric Reversed Phase, 30 mg/1 mL, tubes from Phenomenex Inc. and Sep-Pak C18 Plus Light Cartridge, 130 mg Sorbent per Cartridge, 55-105 µm Particle Size from Waters Co. were preconditioned with 1 mL ethanol followed by 10 mL water.

Sep-Pak C18 Plus Long Cartridge, 820 mg Sorbent per Cartridge, 55-105 µm Particle Size from Waters Co. was preconditioned with 2 mL ethanol followed by 20 mL water.

5.2.1.4 Solvents and Reagents

HPLC solvents were purchased from Merck KGaA (Darmstadt, Germany). Pure water to precondition the cartridges and purify the labeled products was obtained from Berlin-Chemie AG. MENARINI Group. Other solvents were obtained from Sigma-Aldrich GmbH (Steinheim, Germany) as anhydrous solvents and used without further purification.

5.2.1.5 Miscellaneous Information

Radioactivity was measured with a CRC®-55tR Dose Calibrator from Capintec, Inc or the Curiementor 2 from PTW GmbH (Freiburg, Germany).

5.2.1.6 Production of fluorine-18

No-carrier-added [^{18}F]F^- (2-3 GBq) was produced via the nuclear reaction $^{18}O(p,n)^{18}F$ by bombardment of 0.5-1 mL ^{18}O-enriched water for 2-30 min with a 17 MeV proton beam and 15-35 µA current at the MC 16 cyclotron (Scanditronix, Uppsala, Sweden) of the Max Planck Institute for Metabolic Research, or Baby Cyclotron BC 1710 (Japan Steel Works Ltd. [JSW], Japan) of the institute of nuclear chemistry (INM-5) in Forschungszentrum Jülich.

5.2.2 Screening of pyrazole [^{18}F]**1d** synthesis

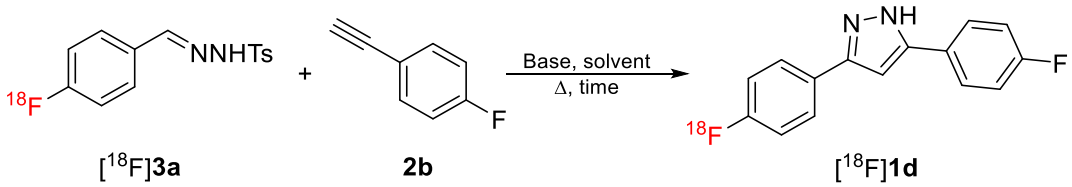

[^{18}F]**3a** **2b** [^{18}F]**1d**

5.2.2.1 Reaction temperature

Reaction conditions: [^{18}F]**3a** (10-50 MBq), **2b** (40 µmol), LiO*t*Bu (12 µmol), 20 min, MeCN, volume (500 µL).

Reaction temperature [°C]	RCY [%]
65	7±2
80	50±4
95	60±10
110	60±17

5.2.2.2 Solvent

Reaction conditions: [^{18}F]**3a** (10-50 MBq), **2b** (40 µmol), LiO*t*Bu (12 µmol), 25 min, 95 °C, volume (500 µL).

Solvent	RCY [%]
MeCN	67±3
DMSO	19±1
Dioxane	47±5
PC	53±6

5.2.2.3 Reaction time

Reaction conditions: [^{18}F]**3a** (10-50 MBq), **2b** (40 µmol), LiO*t*Bu (12 µmol), 95 °C, MeCN, volume (500 µL).

Reaction time [min]	RCY [%]
15	35±4
20	60±10
25	67±3
30	66±2

5.2.2.4 Base

Reaction conditions: [^{18}F]**3a** (10-50 MBq), **2b** (40 µmol), base (12 µmol), 20 min, 80 °C, MeCN, volume (500 µL).

Base	RCY [%]
NaOH	44±5
K_2CO_3	42±4
LiO*t*Bu	50±4
DBU	33±2

5.2.3 Synthesis of 5-(3-bromophenyl)-3-(6-[^{18}F]fluorobenzo[*d*][1,3]dioxol-5-yl)-1*H*-pyrazole ([^{18}F]**1b**)

5.2.3.1 6-[^{18}F]Fluorobenzo[d][1,3]dioxole-5-carbaldehyde

[^{18}F]F$^-$ (1000 MBq) was fixed on QMA anion exchange cartridge. The cartridge was rinsed with MeOH (2 mL) and dried with air stream. [^{18}F]F$^-$ was then eluted using Et_4NBC (5 mg, 26 µmol) in MeOH (1 mL). MeOH was removed under reduced pressure at 100 °C within 5 min. Then a solution of 6-nitropiperonal (5 mg, 25.6 µmol) in DMSO (400 µL) was added to the dry salt. The V-vial was allowed to stir at 130 °C for 10 min. after that the reaction mixture was cooled to room temperature and purified with StrataX RP cartridge. The recovered acetonitrile solution was diluted with water and purified over HPLC (semi prep Gemini 8 mL/min, 18% MeCN). The purified fraction was diluted with water, concentrated on StrataX RP cartridge and eluted with MeOH (300 µL). 6-[^{18}F]fluoropiperonal (131.7 MBq, RCY 22%, RCP 99%).

5.2.3.2 N'-((6-[^{18}F]Fluorobenzo[d][1,3]dioxol-5-yl)methylene)-4-methylbenzenesulfonohydrazide

To the methanolic solution of 6-[^{18}F]fluoropiperonal (131.7 MBq), tosylhydrazide (10 mg, 53.7 µmol) was added and the mixture was stirred at 80 °C for 10 min. after that the reaction mixture was quenched with water (6 mL) and filtered through PTFE filter and purified using StrataX RP cartridge. The cartridge was rinsed with 10 mL water and finally 6-[^{18}F]fluorotosylhydrazone was eluted with MeCN (300 µL). 6-[^{18}F]fluorotosylhydrazone (60.12 MBq, RCY 53%, RCP 99%).

*5.2.3.3 Synthesis of 5-(3-bromophenyl)-3-(6-[^{18}F]fluorobenzo[d][1,3]dioxol-5-yl)-1H-pyrazole ([^{18}F]**1b**)*

LiO*t*Bu (5 mg, 62 µmol) and **2a** (10 µL, 80 µmol) were added to MeCN solution of 6-[^{18}F]fluorotosylhydrazone (60.12 MBq) and stirred at 95 °C for 25 min. then the reaction mixture was cooled to room temperature, diluted with MeCN (50% v/v) and purified over HPLC. The purified fraction was concentrated on StrataX RP cartridge and eluted with

EtOH (300 µL). Then it was purified over HPLC (50% MeCN+0.1% TFA). The purified fraction was concentrated on StrataX RP cartridge and eluted with EtOH (300 µL). The overall RCY was 1%.

5.2.4 Screening ^{18}F-fluorodestannylation

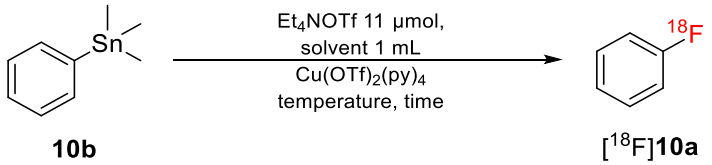

10b [^{18}F]**10a**

5.2.4.1 Recovery of [^{18}F]fluoride from anion exchange cartridge

Recovery conditions: 50 MBq [^{18}F]Fluoride fixed on QMA-CO_3 from the male side, then rinsed with MeOH (1 mL) in the same direction, after that [^{18}F]-fluoride was recovered with methanolic solution of Et_4NX (500 µL).

[µmol]	^{18}F-Recovery [%]			
	Et_4NBC	Et_4NTf	Et_4NBF_4	Et_4NI
60	98	98		
30	94	94	93	99
15	96	95	97	97
5	94	96	97	92
2,5	95	96	97	96
0,5	81	76	80	89

5.2.4.2 Alcohol screening

Reaction conditions: [^{18}F]Fluoride (~50 MBq) was recovered from QMA-CO_3 with alcoholic solution (300 µL) of Et_4NOTf (11 µmol), **10b** (60 µmol), $Cu(OTf)_2(py)_4$ (30 µmol), 100 °C, 10 min, ROH:DMA/3:7 (volume 1 mL).

ROH	RCY [%]	^{18}F Recovered [%]	Rest on cartridge [%]
MeOH	11±4	85±1	1±0
EtOH	45±8	83±1	5±1
TFE	0	84±2	4±2
***n*-PrOH**	62±6	77±4	11±2
***i*-PrOH**	70±3	72±5	16±3
***n*-BuOH**	72±8	73±8	19±1
***s*-BuOH**	66±7	47±6	37±7
***t*-BuOH**	80±4	10±1	78±1

***n*-PenOH**	75±10	68±4	18±5
***n*-HexOH**	55±2	64±4	21±4

5.2.4.3 Anion exchange cartridge

Reaction conditions: [^{18}F]Fluoride (~50 MBq) was recovered from anion exchange cartridge with *n*-BuOH solution (300 µL) of Et_4NOTf (11 µmol), **10b** (60 µmol), $Cu(OTf)_2(py)_4$ (30 µmol), 100 °C, 10 min, *n*-BuOH:DMA/3:7 (volume 1 mL).

	QMA-CO_3	**Strata X-CO_3**	**Strata X-HCO_3**	**Chromafix PS-HCO_3**
Rest on the cartridge [%]	19±1	14±1	18±2	35±2
^{18}F recovery [%]	73±8	81±1	68±9	57±3
RCY [%]	69±4	24±15	37±10	42±5

5.2.4.4 ^{18}F-Fluorination reagents

Reaction conditions: [^{18}F]Fluoride (~50 MBq) was recovered from QMA-CO_3 with *n*-BuOH solution (300 µL) of ^{18}F-Fluorination reagents (11 µmol), **10b** (60 µmol), $Cu(OTf)_2(py)_4$ (30 µmol), 100 °C, 10 min, *n*-BuOH:DMA/3:7 (volume 1 mL). In the case of KOTf, K222 (33 µmol) was added.

	Et_4NOTf	**Et_4NBC**	**KOTf/K222**	**Bu_4POMs**
Rest on the cartridge [%]	19±1	18±2	9±2	14±4
^{18}F recovery [%]	72±8	71±1	81±5	76±2
RCY [%]	69±4	63±9	9±1	60±11

5.2.4.5 Reaction time

Reaction conditions: [^{18}F]Fluoride (~50 MBq) was recovered from QMA-CO_3 with *n*-BuOH solution (300 µL) of Et_4NOTf (11 µmol), **10b** (60 µmol), $Cu(OTf)_2(py)_4$ (30 µmol), 100 °C, *n*-BuOH:DMA/3:7 (volume 1 mL).

Reaction time [min]	**RCY [%]**
5	76±4
10	72±8
15	72±9

20	75±2
25	60±1

5.2.4.6 *Reaction temperature optimization*

Reaction conditions: [^{18}F]Fluoride (~50 MBq) was recovered from QMA-CO_3 with *n*-BuOH solution (300 µL) of Et_4NOTf (11 µmol), **10b** (60 µmol), $Cu(OTf)_2(py)_4$ (30 µmol), 10 min, *n*-BuOH:DMA/3:7 (volume 1 mL).

Reaction temperature [°C]	RCY [%]
80	34±2
90	45±11
100	72±8
110	65±5
120	60±5

5.2.4.7 *Aprotic solvent optimization*

Reaction conditions: [^{18}F]Fluoride (~50 MBq) was recovered from QMA-CO_3 with *n*-BuOH solution (300 µL) of Et_4NOTf (11 µmol), **10b** (60 µmol), $Cu(OTf)_2(py)_4$ (30 µmol), 100 °C, 10 min, *n*-BuOH:solvent/3:7 (volume 1 mL).

Solvent	RCY [%]
DMA	72±8
NMP	73±3
TMU	28±2
DMF	9±3
DMSO	7±2
Pyridine	0
NMF	0
t-BuOH	0

5.2.4.8 *Water content*

Reaction conditions: [^{18}F]Fluoride (~50 MBq) was recovered from QMA-CO_3 with *n*-BuOH solution (300 µL) of Et_4NOTf (11 µmol), **10b** (60 µmol), $Cu(OTf)_2(py)_4$ (30 µmol), 100 °C, 10 min, *n*-BuOH:DMA/3:7 + X µL water (volume 1 mL).

Water content [µL/1 mL]	RCY [%]
0	73±8
5	35±2
10	16±1
15	9±1

5.2.4.9 n-BuOH content

Reaction conditions: [^{18}F]Fluoride (~50 MBq) was recovered from QMA-CO_3 with *n*-BuOH solution (300 µL) of Et_4NOTf (11 µmol), **10b** (60 µmol), $Cu(OTf)_2(py)_4$ (30 µmol), 100 °C, 10 min, *n*-BuOH:DMA/X:Y (volume 1 mL).

***n*-BuOH part from 10**	**RCY [%]**
0	84±4
1	85±2
2	78±4
3	72±8
4	58±9
5	42±2

Reaction conditions: [^{18}F]Fluoride (~50 MBq) was recovered from QMA-CO_3 with MeOH solution (500 µL) of Et_4NOTf (11 µmol), then MeOH was evaporated. **10b** (30 µmol), $Cu(OTf)_2(py)_4$ (30 µmol), 100 °C, 10 min, solvent (volume 1 mL).

Solvents	RCY [%]
n-BuOH:DMA (1:9)	73±2
t-BuOH:DMA (1:9)	73±2
DMA	72±4

5.2.4.10 Precursor concentration

Reaction conditions: [^{18}F]Fluoride (~50 MBq) was recovered from QMA-CO_3 with *n*-BuOH solution (300 µL) of Et_4NOTf (11 µmol), **10b** (X µmol), $Cu(OTf)_2(py)_4$ (30 µmol), 100 °C, 10 min, *n*-BuOH:DMA/3:7 (volume 1 mL).

Precursor concentration [µmol/mL]	RCY [%]

60	73±8
40	78±1
30	70±4
20	63±2
10	44±2

5.2.4.11 $Cu(OTf)_2(py)_4$ concentration

Reaction conditions: [^{18}F]Fluoride (~50 MBq) was recovered from QMA-CO_3 with *n*-BuOH solution (300 µL) of Et_4NOTf (11 µmol), **10b** (30 µmol), $Cu(OTf)_2(py)_4$ (X µmol), 100 °C, 10 min, *n*-BuOH:DMA/3:7 (volume 1 mL).

$Cu(OTf)_2(py)_4$ concentration [µmol/mL]	**RCY [%]**
40	61±9
30	70±4
20	66±5
10	54±2

5.2.5 General procedure for model compounds and [^{18}F]**1c**

[^{18}F]Fluoride (50-100 MBq) was loaded on an anion exchange cartridge from the male side (QMA carbonate, precedenced with 1 mL water and dry with air). The cartridge was rinsed with MeOH (1 mL) and dried with air, then [^{18}F]fluoride was eluted with methanolic solution (500 µL) of Et_4NOTf (2.79 mg, 10 µmol) into V-vial. Methanol was removed under reduced pressure (600 mBar) with a stream of argon at 100 °C within 3 min. After removing methanol the pressure was reduced to 50 mBar and the V-vial was purged with air. To the dry salt $Cu(OTf)_2(py)_4$ (20.34 mg, 30 µmol) and the corresponding precursor (30 µmol) dissolved in DMA (1 mL) was added. The reaction mixture was stirred at 100 °C for 10 min, and then it was cooled to room temperature in an ice bath. The reaction mixture was quenched with water (4 mL) and a sample was taken to determine the RCY.

Compound	RCY [%]	HPLC conditions
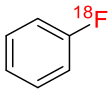	72±4($SnMe_3$) 88±1($SnBu_3$)	SpeedRod, t_R = 4.87 min, gradient: 0–2 min: 5% MeCN, 2–2.5 min: 5–20% MeCN, 2.5–6 min: 20% MeCN, 6–

		7 min: 20–70% MeCN, 7–9 min: 70% MeCN
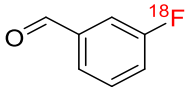	17±1	SpeedRod, t_R = 6.35 min, XX% aq. MeCN, flow rate: 3 mL/min
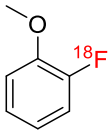	16±1	SpeedRod, t_R = 4.32 min, 25% aq. MeCN, flow rate: 1.5 mL/min
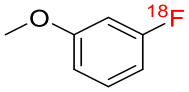	84±2	SpeedRod, t_R = 6.03 min, 25% aq. MeCN, flow rate: 1.5 mL/min
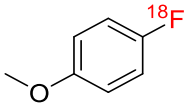	59±3($SnMe_3$) 44±2($SnBu_3$)	SpeedRod, t_R = 5.12 min, 25% aq. MeCN, flow rate: 1.5 mL/min
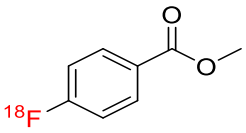	34±3	SpeedRod, t_R = 4.92 min, 25% aq. MeCN, flow rate: 1.5 mL/min
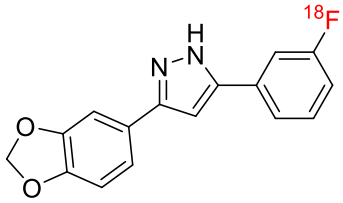	62±8	Gemini 250×4.6 mm, t_R = 7.3 min, 50% aq. MeCN+0.1% TFA, flow rate: 2 mL/min

5.2.6 Optimization of ^{18}F-fluorodestannylation of amino acid derivatives precursors

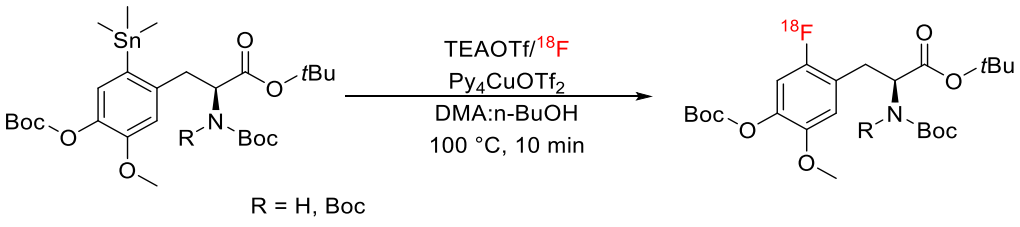

R = H, Boc

5.2.6.1 $Cu(OTf)_2(py)_4$ concentration

Reaction Conditions: [^{18}F]Fluoride (50-100 MBq), Et_4NOTf (11 µmol), OMFD (di-Boc) precursor (30 µmol), $Cu(OTf)_2(py)_4$, 100 °C, 10 min, *n*-BuOH:DMA 3:7 (reaction volume 1 mL).

$Cu(OTf)_2(py)_4$:Precursor [eq.]	RCY [%]
1:1	22

1.5:1	24
2:1	27
3:1	25

5.2.6.2 Solvent optimization

Reaction Conditions: [^{18}F]Fluoride (50-100 MBq), Et_4NOTf (11 µmol), OMFD precursor (30 µmol), $Cu(OTf)_2(py)_4$ (30 µmol), 100 °C, 10 min, solvents (reaction volume 1 mL).

Solvent	RCY [%]	
	OMFD (di-Boc)	OMFD (tri-Boc)
DMA	6	78
n-BuOH:DMA (1:9)	20	74
n-BuOH:DMA (3:7)	22	66

5.2.7 General procedure for radiofluorinated amino acid derivatives synthesis

[^{18}F]Fluoride (200-300 MBq) was loaded on an anion exchange cartridge from the male side (QMA carbonate, precondenced with 1 mL water and dry with air). The cartridge was rinsed with MeOH (1 mL) and dried with air, then [^{18}F]fluoride was eluted with methanolic solution (500 µL) of Et_4NOTf (2.79 mg, 10 µmol) into V-vial. Methanol was removed under reduced pressure (600 mBar) with a stream of air at 100 °C within 5 min. To the dry salt $Cu(OTf)_2(py)_4$ (40.68 mg, 60 µmol) and the corresponding precursor (30 µmol) dissolved in DMA (1 mL) was added. The reaction mixture was stirred at 100 °C for 10 min, and then it was cooled to room temperature in an ice bath. The reaction mixture was quenched with water (2 mL) and loaded in Sep-Pak C18 Plus Light Cartridge. The cartridge was washed with 5 mL water and the product was eluted with 1 mL EtOH. HBr (48%, 1 mL) (or HCl, 38% in the case of OMFD) was added and stirred at 130 °C for 10 min. The mixture was cooled to room temperature and then quenched with water.

Compound	RCY [%]	HPLC conditions

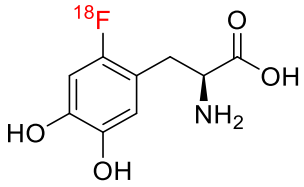	37	ProntoSil, t_R = 4.1 min, phosphate buffer with 4% EtOH (pH 2.5), flow rate: 1 mL/min
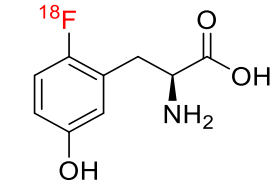	55	ProntoSil, t_R = 5.88 min, phosphate buffer with 4% EtOH (pH 2.5), flow rate: 1 mL/min
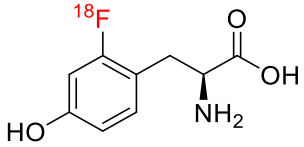	60	ProntoSil, t_R = 5.66 min, phosphate buffer with 4% EtOH (pH 2.5), flow rate: 1 mL/min
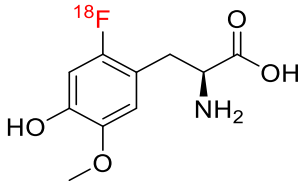	78	ProntoSil, t_R = 7.05 min, phosphate buffer with 4% EtOH (pH 2.5), flow rate: 1 mL/min

5.2.8 Automated synthesis of radiofluorinated amino acid derivatives

[^{18}F]Fluoride (5-10 GBq) was load on QMA-CO_3 cartridge from the female side. After that the cartridge was rinsed with anhydrous MeOH (2 mL) using the same path. In the reverse direction [^{18}F]fluoride was recovered using methanolic solution (700 µL) of Et_4NOTf (5 mg, 18 µmol) to the first reactor. After removing methanol under a stream of dry air (550 mbar) at 100 °C the corresponding precursor (30 µmol) and $Cu(OTf)_2(py)_4$ (40.7 mg, 60 µmol) were added without precooling. After 10 min, the reaction mixture was cooled to 35 °C and quenched with water (1 mL). The mixture in the first reactor was passed through Sep-Pak C18 Plus Long cartridge. The cartridge was rinsed with water (12 mL), and the retained activity was then recovered with DCM (2 mL) into the second reactor. DCM was removed under reduced pressure of helium (600 mbar) at 100 °C within 3 min followed by the addition of HBr (48%, 1 mL) or HCl (38%, 1 mL, in the case of OMFD) then increasing the temperature to 130 °C for further 10 min. After finishing the hydrolysis, the mixture was diluted with NaOH (45% *w/w*, 300 µL) and HPLC mobile phase (3 mL). Finally, the diluted mixture was loaded on the HPLC for purification. Column: Synergi™ 4 µm Hydro-RP 80 Å, flow: 5 ml/min, mobile phase: sodium phosphate buffer (pH 2.45).

Compound	RCY [%]	HPLC conditions
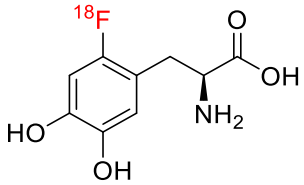	57	ProntoSil, t_R = 4.1 min, phosphate buffer with 4% EtOH (pH 2.5), flow rate: 1 mL/min
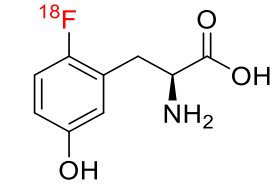	41	ProntoSil, t_R = 5.88 min, phosphate buffer with 4% EtOH (pH 2.5), flow rate: 1 mL/min
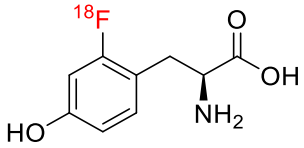	44	ProntoSil, t_R = 5.66 min, phosphate buffer with 4% EtOH (pH 2.5), flow rate: 1 mL/min
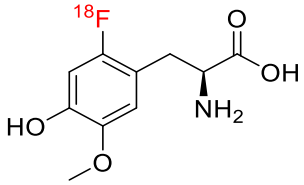	32	ProntoSil, t_R = 7.05 min, phosphate buffer with 4% EtOH (pH 2.5), flow rate: 1 mL/min

5.2.9 Determination of specific activity and tin and copper content

The molar activities (MA) were calculated by one point calibration method determined from the peak area in the UV-HPLC chromatograms (λ= 230 nm).

The contents of tin and copper were determined by Agilent 7900 ICP-MS. The solution of amino acid derivatives obtained after HPLC purification was concentrated under reduced pressure, the residue was then dissolved in water (1 mL). The measured samples were diluted 1:100.

References

(1) Wagner, J.; Ryazanov, S.; Leonov, A.; Levin, J.; Shi, S.; Schmidt, F.; Prix, C.; Pan-Montojo, F.; Bertsch, U.; Mitteregger-Kretzschmar, G.; et al. Anle138b: A Novel Oligomer Modulator for Disease-Modifying Therapy of Neurodegenerative Diseases such as Prion and Parkinson's Disease. *Acta Neuropathol.* **2013**, *125* (6), 795–813.

(2) Mossine, A.; Makaravage, K.; Ichiishi, N.; Brooks, A.; Miller, J.; Sanford, M.; Scott, P. New Strategies for Transition Metal-Mediated Radiofluorination. *J. Nucl. Med.* **2016**, *57* (supplement_2), 2.

(3) Makaravage, K. J.; Brooks, A. F.; Mossine, A. V.; Sanford, M. S.; Scott, P. J. H. Copper-Mediated Radiofluorination of Arylstannanes with [^{18}F]KF. *Org. Lett.* **2016**, *18* (20), 5440–5443.

(4) Preshlock, S.; Calderwood, S.; Verhoog, S.; Tredwell, M.; Huiban, M.; Hienzsch, A.; Gruber, S.; Wilson, T. C.; Taylor, N. J.; Cailly, T.; et al. Enhanced Copper-Mediated ^{18}F-Fluorination of Aryl Boronic Esters Provides Eight Radiotracers for PET Applications. *Chem. Commun.* **2016**, *52* (54), 8361–8364.

(5) *Handbook of Nuclear Chemistry*; Vértes, A., Nagy, S., Klencsár, Z., Lovas, R. G., Rösch, F., Eds.; Springer US: Boston, MA, 2011.

(6) Analoui, M.; Bronzino, J.; Peterson, D. *Medical Imaging*; Analoui, M., Bronzino, J. D. ., Peterson, D. R. ., Eds.; CRC Press, 2012.

(7) Kuhl, D. E.; Edwards, R. Q. Image Separation Radioisotope Scanning. *Radiology* **1963**, *80* (4), 539–726.

(8) Brownell, G.; Sweet, W. Localization of Brain Tumors with Positron Emitters. *Nucleonics* **1953**, *11*, 40–45.

(9) Bauser, M.; Lehmann, L. Positronen-Emissions-Tomographie. *Chemie unserer Zeit* **2012**, *46* (2), 80–99.

(10) Powers, W. J. Positron Emission Tomography (PET). In *Encyclopedia of the Neurological Sciences*; Aminoff, M. J., Daroff, R. B., Eds.; Academic Press: New York, 2003; pp 34–38.

(11) Miller, P. W.; Long, N. J.; Vilar, R.; Gee, A. D. Synthesis of ^{11}C, ^{18}F, ^{15}O, and ^{13}N

Radiolabels for Positron Emission Tomography. *Angew. Chem. Int. Ed. Engl.* **2008**, *47* (47), 8998–9033.

(12) Qaim, S. M.; Coenen, H. H. Produktion Pharmazeutisch Relevanter Radionuklide: An Reaktoren Und Zyklotronen. *Pharm. Unserer Zeit* **2005**, *34* (6), 460–466.

(13) Banerjee, S. R.; Pomper, M. G. Clinical Applications of Gallium-68. *Appl. Radiat. Isot.* **2013**, *76*, 2–13.

(14) Conti, M.; Eriksson, L. Physics of Pure and Non-Pure Positron Emitters for PET: A Review and a Discussion. *EJNMMI Phys.* **2016**, *3* (1), 8.

(15) *Nuclear Technology Review GC(52)/INF/3*; 2008.

(16) Purser, S.; Moore, P. R.; Swallow, S.; Gouverneur, V. Fluorine in Medicinal Chemistry. *Chem. Soc. Rev.* **2008**, *37* (2), 320–330.

(17) Wang, J.; Sánchez-Roselló, M.; Aceña, J. L.; del Pozo, C.; Sorochinsky, A. E.; Fustero, S.; Soloshonok, V. A.; Liu, H. Fluorine in Pharmaceutical Industry: Fluorine-Containing Drugs Introduced to the Market in the Last Decade (2001–2011). *Chem. Rev.* **2014**, *114* (4), 2432–2506.

(18) Cai, L.; Lu, S.; Pike, V. W. Chemistry with [^{18}F]Fluoride Ion. *European J. Org. Chem.* **2008**, *2008* (17), 2853–2873.

(19) Ross, T.; Wester, H. ^{18}F: Labeling Chemistry and Labeled Compounds. In *Handbook of Nuclear Chemistry*; Vértes, A., Nagy, S., Klencsár, Z., Lovas, R. G., Rösch, F., Eds.; Springer US: Boston, MA, 2011; Vol. 4, pp 2051–2056.

(20) Coenen, H. H.; Moerlein, S. M. Regiospecific Aromatic Fluorodemetallation of Group IVb Metalloarenes Using Elemental Fluorine or Acetyl Hypofluorite. *Journal of Fluorine Chemistry*. 1987, pp 63–75.

(21) Visser, G. W. M.; v. Halteren, B. W.; Herscheid, J. D. M.; Brinkman, G. a.; Hoekstra, A. Reaction of Acetyl Hypofluorite with Aromatic Mercury Compounds: A New Selective Fluorination Method. *J. Chem. Soc. Chem. Commun.* **1984**, No. 10, 655.

(22) Visser, G. W. M.; Bakker, C. N. M.; Van Halteren, B. W.; Herscheid, J. D. M.; Brinkman, G. a.; Hoekstra, A. Fluorination and Fluorodemercuration of Aromatic Compounds with Acetyl Hypofluorite. *J. Org. Chem.* **1986**, *51* (10), 1886–1889.

(23) Luxen, A.; Barrio, J. R. Fluorination of Substituted Veratroles via Regioselective Mercuration. *Tetrahedron Lett.* **1988**, *29* (13), 1501–1504.

(24) Adam, M. J.; Pate, B. D.; Ruth, T. J.; Berry, J. M.; Hall, L. D. Cleavage of Aryl–tin Bonds with Elemental Fluorine: Rapid Synthesis of [^{18}F]fluorobenzene. *J. Chem. Soc., Chem. Commun.* **1981**, No. 15, 733–733.

(25) Di Raddo, P.; Diksic, M.; Jolly, D. The 18F Radiofluorination of Arylsilanes. *J. Chem. Soc. Chem. Commun.* **1984**, No. 3, 159.

(26) Speranza, M.; Shiue, C.-Y.; Wolf, A. P.; Wilbur, D. S.; Angelini, G. Electrophilic Radiofluorination of Aryltrimethylsilanes as a General Route to ^{18}F-Labeled Aryl Fluorides. *J. Fluor. Chem.* **1985**, *30* (1), 97–107.

(27) Hess, E.; Sichler, S.; Kluge, A.; Coenen, H. H. Synthesis of 2-[^{18}F]fluoro-L-Tyrosine via Regiospecific Fluoro-de-Stannylation. *Appl. Radiat. Isot.* **2002**, *57* (2), 185–191.

(28) Bergmann, R.; Pietzsch, J.; Fuechtner, F.; Pawelke, B.; Beuthien-Baumann, B.; Johannsen, B.; Kotzerke, J. 3-*O*-Methyl-6-^{18}F-Fluoro-L-Dopa, a New Tumor Imaging Agent: Investigation of Transport Mechanism in Vitro. *J. Nucl. Med.* **2004**, *45* (12), 2116–2122.

(29) VanBrocklin, H. F.; Blagoev, M.; Hoepping, A.; O'Neil, J. P.; Klose, M.; Schubiger, P. A.; Ametamey, S. A New Precursor for the Preparation of 6-[^{18}F]Fluoro-L-*m*-Tyrosine ([^{18}F]FMT): Efficient Synthesis and Comparison of Radiolabeling. *Appl. Radiat. Isot.* **2004**, *61* (6), 1289–1294.

(30) Dolle, F.; Demphel, S.; Hinnen, F.; Fournier, D.; Vaufrey, F.; Crouzel, C. 6-[^{18}F]Fluoro-L-DOPA by Radiofluorodestannylation: A Short and Simple Synthesis of a New Labelling Precursor. *J. Label. Compd. Radiopharm.* **1998**, *41* (2), 105–114.

(31) Coenen, H. H. Biochemistry and Evaluation of Fluoroamino Acids. In *PET Studies on Amino Acid Metabolism and Protein Synthesis*; Springer Netherlands: Dordrecht, 1993; pp 109–131.

(32) *PET Chemistry The Driving Force in Molecular Imaging*; Schubiger, P. A., Lehmann, L., Friebe, M., Eds.; Springer: Heidelberg, 2007.

(33) Richarz, R.; Krapf, P.; Zarrad, F.; Urusova, E. A.; Neumaier, B.; Zlatopolskiy, B. D. Neither Azeotropic Drying, nor Base nor Other Additives: A Minimalist Approach to ^{18}F-Labeling. *Org. Biomol. Chem.* **2014**, *12* (40), 8094–8099.

(34) Schäfer, D.; Weiß, P.; Ermert, J.; Castillo Meleán, J.; Zarrad, F.; Neumaier, B. Preparation of No-Carrier-Added 6-[^{18}F]Fluoro-L-Tryptophan via Cu-Mediated Radiofluorination. *European J. Org. Chem.* **2016**, *2016* (27), 4621–4628.

(35) Zlatopolskiy, B. D.; Zischler, J.; Krapf, P.; Zarrad, F.; Urusova, E. a.; Kordys, E.; Endepols, H.; Neumaier, B. Copper-Mediated Aromatic Radiofluorination Revisited: Efficient Production of PET Tracers on a Preparative Scale. *Chem. - A Eur. J.* **2015**, *21* (15), 5972–5979.

(36) Ermert, J.; Hocke, C.; Ludwig, T.; Gail, R.; Coenen, H. H. Comparison of Pathways to the Versatile Synthon of No-Carrier-Added 1-Bromo-4-[^{18}F]fluorobenzene. *J. Label. Compd. Radiopharm.* **2004**, *47* (7), 429–441.

(37) Lemaire, C.; Libert, L.; Franci, X.; Genon, J.-L.; Kuci, S.; Giacomelli, F.; Luxen, A. Automated Production at the Curie Level of No-Carrier-Added 6-[^{18}F]fluoro-L-DOPA and 2-[^{18}F]fluoro-L-Tyrosine on a FASTlab Synthesizer. *J. Label. Compd. Radiopharm.* **2015**, *58* (7), 281–290.

(38) Richter, S.; Wuest, F. ^{18}F-Labeled Peptides: The Future Is Bright. *Molecules* **2014**, *19* (12), 20536–20556.

(39) Malik, N.; Machulla, H.-J.; Solbach, C.; Winter, G.; Reske, S. N.; Zlatopolskiy, B. Radiosynthesis of a New PSMA Targeting Ligand ([^{18}F]FPy-DUPA-Pep). *Appl. Radiat. Isot.* **2011**, *69* (7), 1014–1018.

(40) Jelinski, M.; Hamacher, K.; Coenen, H. H. C-Terminal ^{18}F-Fluoroethylamidation Exemplified on [Gly-OH9] Oxytocin. *J. Label. Compd. Radiopharm.* **2002**, *45* (3), 217–229.

(41) Höhne, A.; Mu, L.; Honer, M.; Schubiger, P. A.; Ametamey, S. M.; Graham, K.; Stellfeld, T.; Borkowski, S.; Berndorff, D.; Klar, U.; *et al.* Synthesis, ^{18}F-Labeling, and *in vitro* and *in vivo* Studies of Bombesin Peptides Modified with Silicon-Based Building Blocks. *Bioconjug. Chem.* **2008**, *19* (9), 1871–1879.

(42) Lindner, S.; Michler, C.; Leidner, S.; Rensch, C.; Wängler, C.; Schirrmacher, R.; Bartenstein, P.; Wängler, B. Synthesis and in Vitro and in Vivo Evaluation of

SiFA-Tagged Bombesin and RGD Peptides as Tumor Imaging Probes for Positron Emission Tomography. *Bioconjug. Chem.* **2014**, *25* (4), 738–749.

(43) Lee, E.; Hooker, J. M.; Ritter, T. Nickel-Mediated Oxidative Fluorination for PET with Aqueous [^{18}F]Fluoride. *J. Am. Chem. Soc.* **2012**, *134* (42), 17456–17458.

(44) Kamlet, A. S.; Neumann, C. N.; Lee, E.; Carlin, S. M.; Moseley, C. K.; Stephenson, N.; Hooker, J. M.; Ritter, T. Application of Palladium-Mediated ^{18}F-Fluorination to PET Radiotracer Development: Overcoming Hurdles to Translation. *PLoS One* **2013**, *8* (3), e59187.

(45) Tredwell, M.; Preshlock, S. M.; Taylor, N. J.; Gruber, S.; Huiban, M.; Passchier, J.; Mercier, J.; Génicot, C.; Gouverneur, V. A General Copper-Mediated Nucleophilic ^{18}F-Fluorination of Arenes. *Angew. Chemie Int. Ed.* **2014**, *53* (30), 7751–7755.

(46) Ichiishi, N.; Brooks, A. F.; Topczewski, J. J.; Rodnick, M. E.; Sanford, M. S.; Scott, P. J. H. Copper-Catalyzed [^{18}F]Fluorination of (Mesityl)(aryl)iodonium Salts. *Org. Lett.* **2014**, *16* (12), 3224–3227.

(47) Mossine, A. V.; Brooks, A. F.; Makaravage, K. J.; Miller, J. M.; Ichiishi, N.; Sanford, M. S.; Scott, P. J. H. Synthesis of [^{18}F]Arenes via the Copper-Mediated [^{18}F]Fluorination of Boronic Acids. *Org. Lett.* **2015**, *17* (23), 5780–5783.

(48) Hoover, A. J.; Lazari, M.; Ren, H.; Narayanam, M. K.; Murphy, J. M.; van Dam, R. M.; Hooker, J. M.; Ritter, T. A Transmetalation Reaction Enables the Synthesis of [^{18}F]5-Fluorouracil from [^{18}F]Fluoride for Human PET Imaging. *Organometallics* **2016**, *35* (7), 1008–1014.

(49) Lee, E.; Kamlet, A. S.; Powers, D. C.; Neumann, C. N.; Boursalian, G. B.; Furuya, T.; Choi, D. C.; Hooker, J. M.; Ritter, T. A Fluoride-Derived Electrophilic Late-Stage Fluorination Reagent for PET Imaging. *Science* **2011**, *334* (6056), 639–642.

(50) Zlatopolskiy, B. D.; Zischler, J.; Urusova, E. A.; Endepols, H.; Kordys, E.; Frauendorf, H.; Mottaghy, F. M.; Neumaier, B. A Practical One-Pot Synthesis of Positron Emission Tomography (PET) Tracers via Nickel-Mediated Radiofluorination. *ChemistryOpen* **2015**, *4* (4), 457–462.

(51) Kurti, L.; Czako, B. *Strategic Applications of Named Reactions in Organic Synthesis*, 1st ed.; Academic Press, 2005.

(52) Fier, P. S.; Hartwig, J. F. Copper-Mediated Fluorination of Aryl Iodides. *J. Am. Chem. Soc.* **2012**, *134* (26), 10795–10798.

(53) Ye, Y.; Schimler, S. D.; Hanley, P. S.; Sanford, M. S. $Cu(OTf)_2$-Mediated Fluorination of Aryltrifluoroborates with Potassium Fluoride. *J. Am. Chem. Soc.* **2013**, *135* (44), 16292–16295.

(54) Ye, Y.; Sanford, M. S. Mild Copper-Mediated Fluorination of Aryl Stannanes and Aryl Trifluoroborates. *J. Am. Chem. Soc.* **2013**, *135* (12), 4648–4651.

(55) Ichiishi, N.; Canty, A. J.; Yates, B. F.; Sanford, M. S. Cu-Catalyzed Fluorination of Diaryliodonium Salts with KF. *Org. Lett.* **2013**, *15* (19), 5134–5137.

(56) Graskemper, J. W.; Wang, B.; Qin, L.; Neumann, K. D.; DiMagno, S. G. Unprecedented Directing Group Ability of Cyclophanes in Arene Fluorinations with Diaryliodonium Salts. *Org. Lett.* **2011**, *13* (12), 3158–3161.

(57) Wang, B.; Graskemper, J. W.; Qin, L.; DiMagno, S. G. Regiospecific Reductive Elimination from Diaryliodonium Salts. *Angew. Chem. Int. Ed. Engl.* **2010**, *49* (24), 4079–4083.

(58) Ichiishi, N.; Canty, A. J.; Yates, B. F.; Sanford, M. S. Mechanistic Investigations of Cu-Catalyzed Fluorination of Diaryliodonium Salts: Elaborating the Cu^{I}/Cu^{III} Manifold in Copper Catalysis. *Organometallics* **2014**, *33* (19), 5525–5534.

(59) Zischler, J.; Kolks, N.; Modemann, D.; Neumaier, B.; Zlatopolskiy, B. D. Alcohol-Enhanced Cu-Mediated Radiofluorination. *Chem. - A Eur. J.* **2017**.

(60) Barthel, H.; Schroeter, M. L.; Hoffmann, K.-T.; Sabri, O. PET/MR in Dementia and Other Neurodegenerative Diseases. *Semin. Nucl. Med.* **2015**, *45* (3), 224–233.

(61) Kovacs, G. G. Introduction: Classification of Neurodegenerative Diseases. In *Neuropathology of Neurodegenerative Diseases A Practical Guide*; Kovacs, G. G., Ed.; 2014; pp 1–7.

(62) Brooks, D. J.; Tambasco, N. Imaging Synucleinopathies. *Mov. Disord.* **2016**, *31* (6), 814–829.

(63) Furumoto, S.; Okamura, N.; Furukawa, K.; Tashiro, M.; Ishikawa, Y.; Sugi, K.; Tomita, N.; Waragai, M.; Harada, R.; Tago, T.; et al. A ^{18}F-Labeled BF-227 Derivative as a Potential Radioligand for Imaging Dense Amyloid Plaques by

Positron Emission Tomography. *Mol. Imaging Biol.* **2013**, *15* (4), 497–506.

(64) Seibyl, J. P.; Chen, W.; Silverman, D. H. S. 3,4-Dihydroxy-6-[^{18}F]-Fluoro-L-Phenylalanine Positron Emission Tomography in Patients With Central Motor Disorders and in Evaluation of Brain and Other Tumors. *Semin. Nucl. Med.* **2007**, *37* (6), 440–450.

(65) de Vries, E. F. .; Luurtsema, G.; Brüssermann, M.; Elsinga, P. H.; Vaalburg, W. Fully Automated Synthesis Module for the High Yield One-Pot Preparation of 6-[^{18}F]fluoro-L-DOPA. *Appl. Radiat. Isot.* **1999**, *51* (4), 389–394.

(66) Levin, J.; Schmidt, F.; Boehm, C.; Prix, C.; Bötzel, K.; Ryazanov, S.; Leonov, A.; Griesinger, C.; Giese, A. The Oligomer Modulator anle138b Inhibits Disease Progression in a Parkinson Mouse Model Even with Treatment Started after Disease Onset. *Acta Neuropathologica*. 2014, pp 779–780.

(67) Wagner, J.; Krauss, S.; Shi, S.; Ryazanov, S.; Steffen, J.; Miklitz, C.; Leonov, A.; Kleinknecht, A.; Göricke, B.; Weishaupt, J. H.; et al. Reducing Tau Aggregates with anle138b Delays Disease Progression in a Mouse Model of Tauopathies. *Acta Neuropathol.* **2015**, *130* (5), 619–631.

(68) Zarrad, F.; Urusova, E. A.; Zlatopolskiy, B. D.; Mottaghy, F. M.; Neumaier, B. Synthesis of ^{18}F-Labelled Compounds via Metal free Cross-Coupling Reactions of Radiofluorinated Tosylhydrazones. *Nuklearmedizin/NuclearMedicine* **2014**, *53* (1), A25.

(69) Manzetti, S.; Lu, T. The Geometry and Electronic Structure of Aristolochic Acid: Possible Implications for a Frozen Resonance. *J. Phys. Org. Chem.* **2013**, *26* (6), 473–483.

(70) Imakura, Y.; Konishi, T.; Uchida, K.; Sakurai, H.; Kobayashi, S.; Haruno, A.; Tajima, K.; Yamashita, S. Regioselective Cleavage Reaction of the Aromatic Methylenedioxy Ring. V. Synthesis of Phenothiazine Analogues by Using the Cleavage Reaction with Sodium Methoxide-Thiols in Dimethyl Sulfoxide and Evaluation of Their Biological Activities. *Chem. Pharm. Bull. (Tokyo).* **1994**, *42* (3), 500–511.

(71) Kobayashi, S.; Okimoto, K.; Imakura, Y. Cleavage of the Methylenedioxy Ring. III. Cleavage with Sodium Benzyloxide in Dimethyl Sulfoxide. *Chem. Pharm.*

Bull. (Tokyo). **1982**, *30* (5), 1567–1573.

(72) Kobayashi, S.; Imakura, Y.; Horikawa, R. Cleavage of the Methylenedioxy Ring. II. Cleavage with Sodium Phenoxide and Methoxide in Dimethyl Sulfoxide. *Chem. Pharm. Bull. (Tokyo).* **1980**, *28* (4), 1287–1293.

(73) Kobayashi, S.; Kihara, M.; Yamahara, Y. Cleavage of the Methylenedioxy Group with Sodium Methoxide in Dimethyl Sulfoxide. *Chem. Pharm. Bull. (Tokyo).* **1978**, *26* (10), 3113–3116.

(74) Borch, R. F.; Hassid, A. I. New Method for the Methylation of Amines. *J. Org. Chem.* **1972**, *37* (10), 1673–1674.

(75) Yang, J.; Marriner, G. a; Wang, X.; Bowman, P. D.; Kerwin, S. M.; Stavchansky, S. Synthesis of a Series of Caffeic Acid Phenethyl Amide (CAPA) Fluorinated Derivatives: Comparison of Cytoprotective Effects to Caffeic Acid Phenethyl Ester (CAPE). *Bioorg. Med. Chem.* **2010**, *18* (14), 5032–5038.

(76) Moreau, A.; Couture, A.; Deniau, E.; Grandclaudon, P.; Lebrun, S. A New Approach to Isoindoloisoquinolinones. A Simple Synthesis of Nuevamine. *Tetrahedron* **2004**, *60* (29), 6169–6176.

(77) Aggarwal, V. K.; de Vicente, J.; Bonnert, R. V. A Novel One-Pot Method for the Preparation of Pyrazoles by 1,3-Dipolar Cycloadditions of Diazo Compounds Generated in Situ. *J. Org. Chem.* **2003**, *68* (13), 5381–5383.

(78) Pérez-Aguilar, M. C.; Valdés, C. Regioselective One-Step Synthesis of Pyrazoles from Alkynes and *N*-Tosylhydrazones: [3+2] Dipolar cycloaddition/[1,5] Sigmatropic Rearrangement Cascade. *Angew. Chem. Int. Ed. Engl.* **2013**, *52* (28), 7219–7223.

(79) Liu, P.; Xu, Q. Q.; Dong, C.; Lei, X.; Lin, G. Q. A Complementary Approach to 3,5-Substituted Pyrazoles with Tosylhydrazones and Terminal Alkynes Mediated by TfOH. *Synlett* **2012**, *23*, 2087–2092.

(80) Heller, S. T.; Natarajan, S. R. 1,3-Diketones from Acid Chlorides and Ketones: A Rapid and General One-Pot Synthesis of Pyrazoles. *Org. Lett.* **2006**, *8* (13), 2675–2678.

(81) Matveenko, M.; Kokas, O. J.; Banwell, M. G.; Willis, A. C. Chemoenzymatic

Approaches to Lycorine-Type Amaryllidaceae Alkaloids: Total Syntheses of Ent -Lycoricidine, 3- Epi - Ent -Lycoricidine, and 4-Deoxy-3- Epi - Ent -Lycoricidine. *Org. Lett.* **2007**, *9* (18), 3683–3685.

(82) Sadimenko, A. P.; Basson, S. S. Organometallic Complexes of Heterocycles II. Complexes of Pyrazoles. *Coord. Chem. Rev.* **1996**, *147*, 247–297.

(83) Grotjahn, D. B.; Van, S.; Combs, D.; Lev, D. A.; Schneider, C.; Incarvito, C. D.; Lam, K.; Rossi, G.; Rheingold, A. L.; Rideout, M.; et al. Substituent Control of Hydrogen Bonding in Palladium(II)−Pyrazole Complexes. *Inorg. Chem.* **2003**, *42* (10), 3347–3355.

(84) Bailey, W. D.; Luconi, L.; Rossin, A.; Yakhvarov, D.; Flowers, S. E.; Kaminsky, W.; Kemp, R. A.; Giambastiani, G.; Goldberg, K. I. Pyrazole-Based PCN Pincer Complexes of Palladium(II): Mono- and Dinuclear Hydroxide Complexes and Ligand Rollover C–H Activation. *Organometallics* **2015**, *34* (16), 3998–4010.

(85) Chen, B.; Hou, X.-L.; Li, Y.-X.; Wu, Y.-D. Mechanistic Understanding of the Unexpected Meta Selectivity in Copper-Catalyzed Anilide C–H Bond Arylation. *J. Am. Chem. Soc.* **2011**, *133* (20), 7668–7671.

(86) Kim, D. W.; Jeong, H.; Lim, S. T.; Sohn, M.; Katzenellenbogen, J. A.; Chi, D. Y. Facile Nucleophilic Fluorination Reactions Using *tert*-Alcohols as a Reaction Medium: Significantly Enhanced Reactivity of Alkali Metal Fluorides and Improved Selectivity. *J. Org. Chem.* **2008**, *73* (3), 957–962.

(87) Rosenker, C. J.; Wipf, P. Transmetalation Reactions Producing Organocopper Compounds. In *The Chemistry of Organocopper Compounds*; Rappoport, Z., Marek, I., Eds.; John Wiley & Sons, 7 Jan 2010, 2010; pp 496–501.

(88) Knochel, P.; Betzemeier, B. Transmetalation Reactions Producing Organocopper Reagents. In *Modern Organocopper Chemistry*; Wiley-VCH Verlag GmbH: Weinheim, FRG, 2002; pp 45–78.

(89) Kim, D. W.; Jeong, H.; Lim, S. T.; Sohn, M. Tetrabutylammonium Tetra(*tert*-Butyl Alcohol)-Coordinated Fluoride as a Facile Fluoride Source. *Angew. Chem. Int. Ed. Engl.* **2008**, *47* (44), 8404–8406.

(90) Cheng, X.; Jia, J.; Kuang, C. Convenient Synthesis of Terminal Alkynes from Anti-3-Aryl-2,3-Dibromopropanoic Acids Using a K_2CO_3/DMSO System.

Chinese J. Chem. **2011**, *29* (30873153), 2350–2354.

(91) Mahindroo, N.; Ahmed, Z.; Bhagat, A.; Lal Bedi, K.; Kant Khajuria, R.; Kumar Kapoor, V.; Lal Dhar, K. Synthesis and Structure-Activity Relationships of Vasicine Analogues as Bronchodilatory Agents. *Med. Chem. Res.* **2005**, *14* (6), 347–368.

(92) Thiebes, C.; Thiebes, C.; Prakash, G. K. S.; Petasis, N. a.; Olah, G. a. Mild Preparation of Haloarenes by Ipso-Substitution of Arylboronic Acids with N-Halosuccinimides. *Synlett* **1998**, *1998* (February), 141–142.

(93) Fan-Chiang, T.-T.; Wang, H.-K.; Hsieh, J.-C. Synthesis of Phenanthridine Skeletal Amaryllidaceae Alkaloids. *Tetrahedron* **2016**, *72* (36), 5640–5645.

(94) Thomé, I.; Besson, C.; Kleine, T.; Bolm, C. Base-Catalyzed Synthesis of Substituted Indazoles under Mild, Transition-Metal-Free Conditions. *Angew. Chemie - Int. Ed.* **2013**, *52* (29), 7509–7513.

(95) Kabalka, G. W.; Yang, K.; Reddy, N. K.; Narayana, C. Bromination of Alkenes Using a Mixture of Sodium Bromide and Sodium Perborate. *Synthetic Communications*. 1998, pp 925–929.

(96) Haynes, J. S.; Rettig, S. J.; Sams, J. R.; Trotter, J.; Thompson, R. C. Pyrazine and Pyridine Complexes of copper(II) Trifluoromethanesulfonate. Crystal Structure of Tetrakis(pyridine)bis(trifluoromethanesulfonato-O)copper(II) and Magnetic Exchange in (Pyrazine)bis(trifluoromethanesulfonato-O)copper(II). *Inorg. Chem.* **1988**, *27* (7), 1237–1241.

(97) van Klink, G. P. M.; de Boer, H. J. R.; Schat, G.; Akkerman, O. S.; Bickelhaupt, F.; Spek, A. L. Carbanions as Intermediates in the Formation of Grignard Reagents. *Organometallics* **2002**, *21* (10), 2119–2135.

(98) Villemagne, V. L.; Fodero-Tavoletti, M. T.; Masters, C. L.; Rowe, C. C. Tau Imaging: Early Progress and Future Directions. *Lancet Neurol.* **2015**, *14* (1), 114–124.

Appendix I: Chromatograms

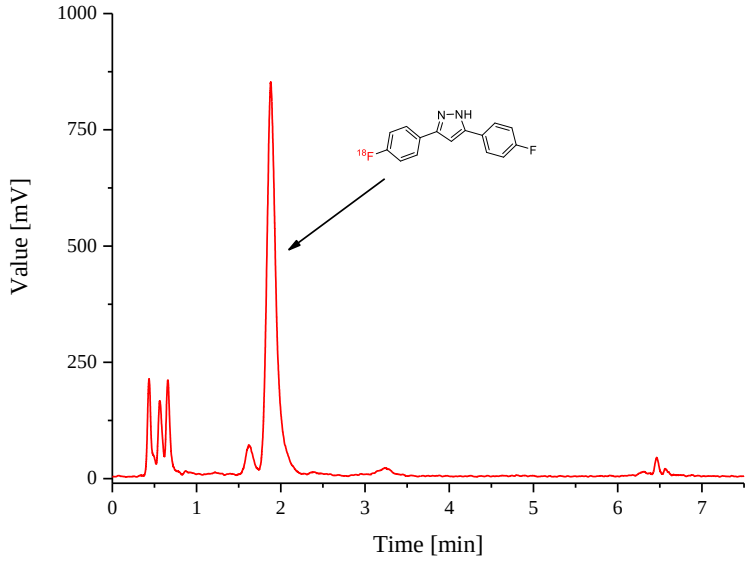

*Chromatogram 1 [^{18}F]**1d**.*

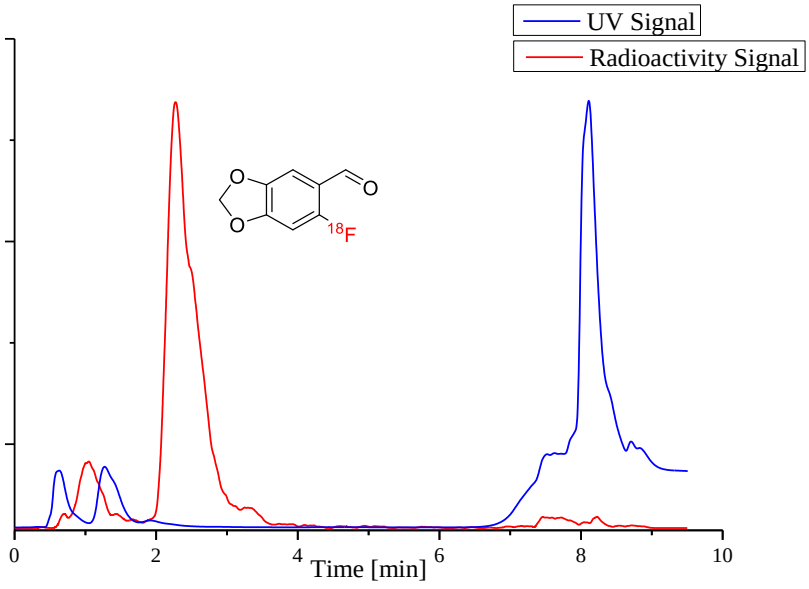

*Chromatogram 2 [^{18}F]**4c** if 6-nitropiperonal was reduced to 6-aminopiperonal.*

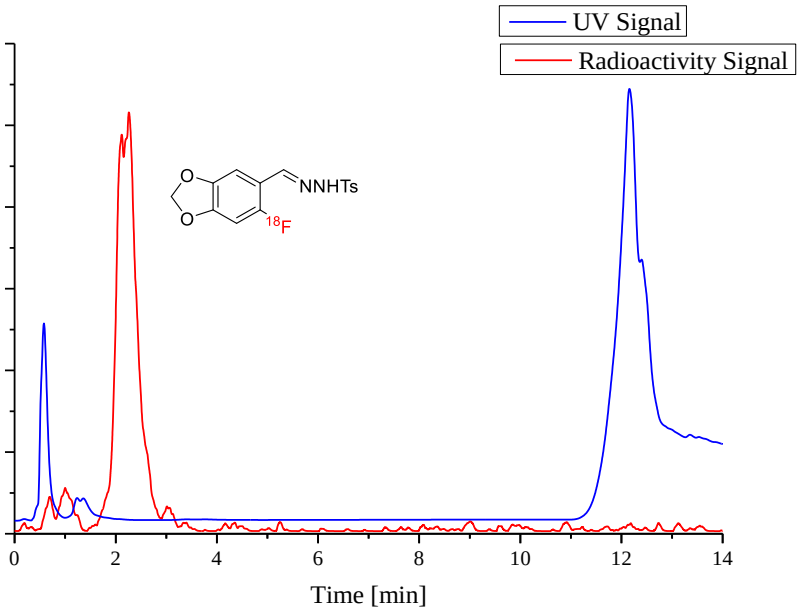

*Chromatogram 3 [^{18}F]**3b**.*

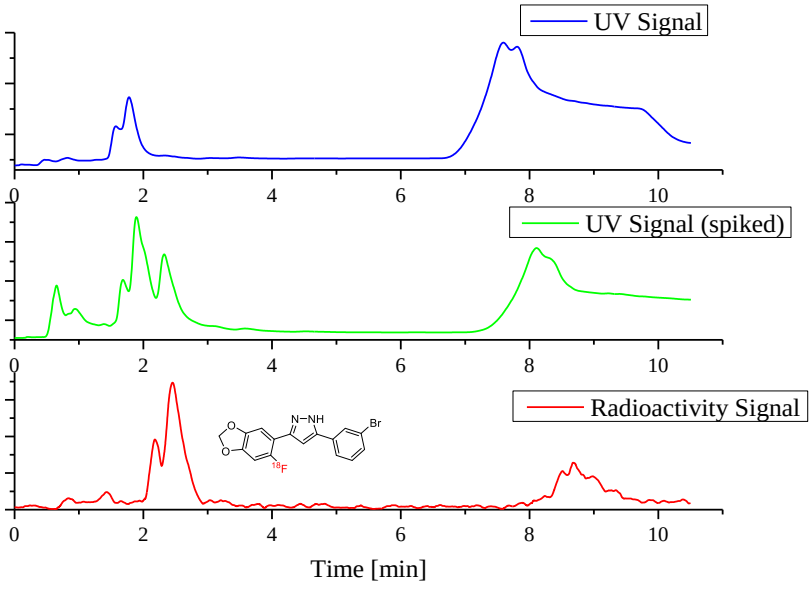

*Chromatogram 4 [^{18}F]**1b** by the three step synthesis if iron was used in the first step.*

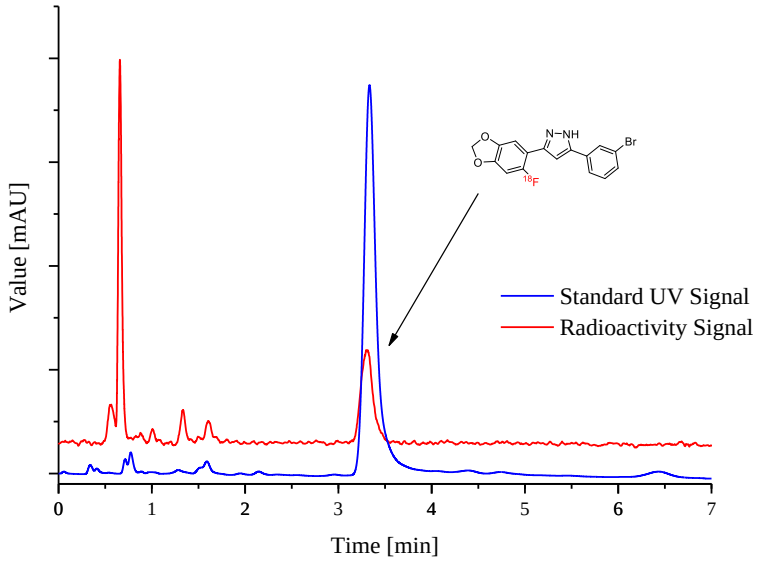

*Chromatogram 5 [^{18}F]**1b** synthesized by three step synthesis.*

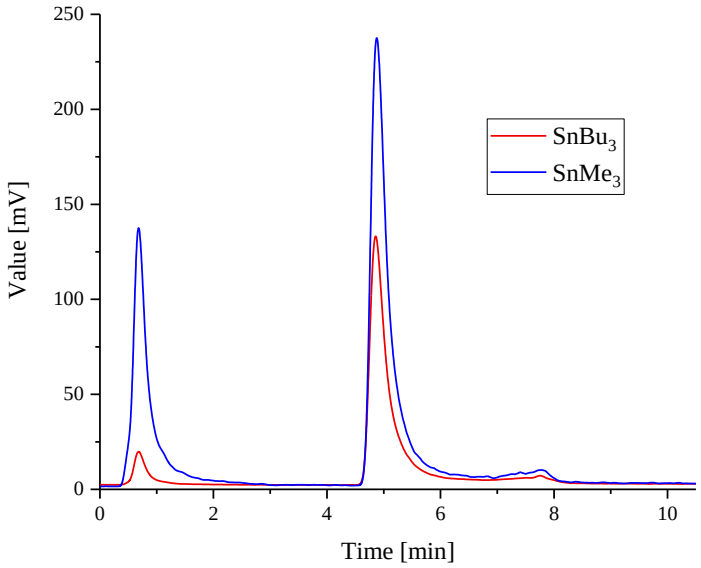

Chromatogram 6 [^{18}F]fluorobenzene.

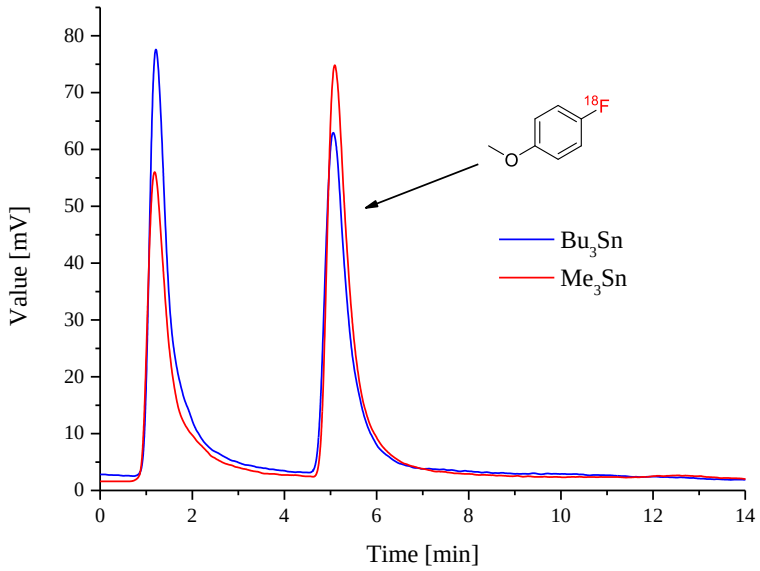

Chromatogram 7 4-[^{18}F]fluoroanisol.

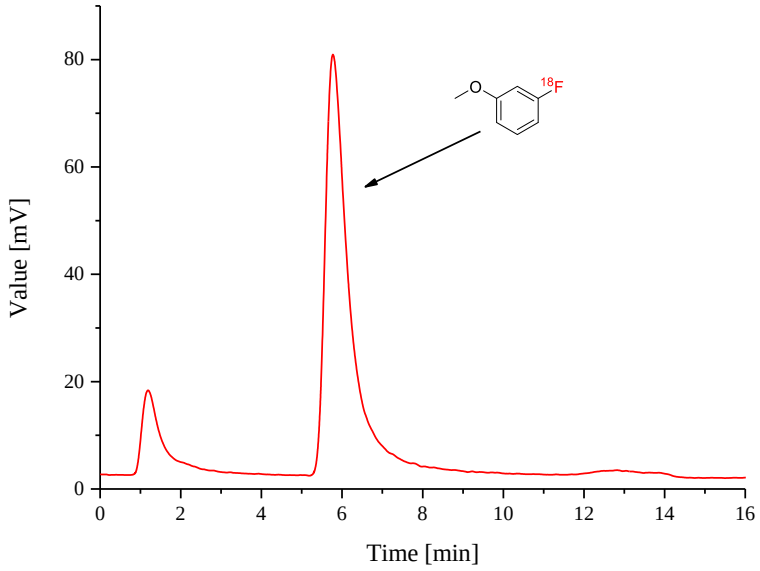

Chromatogram 8 3-[^{18}F]fluoroanisol.

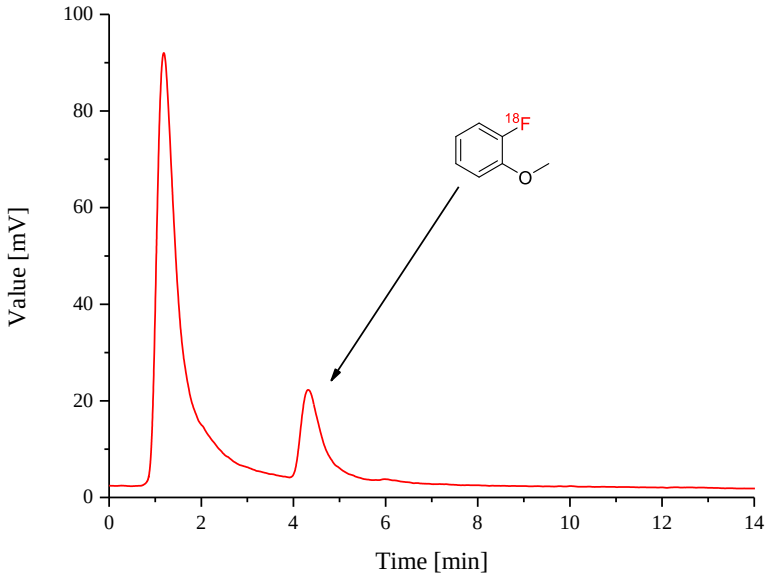

Chromatogram 9 2-[^{18}F]fluoroanisol.

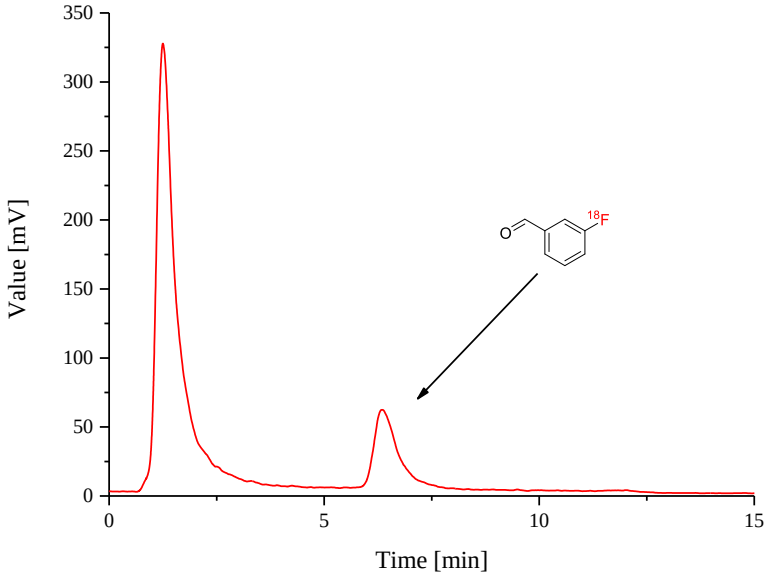

Chromatogram 10 3-[^{18}F]FBA.

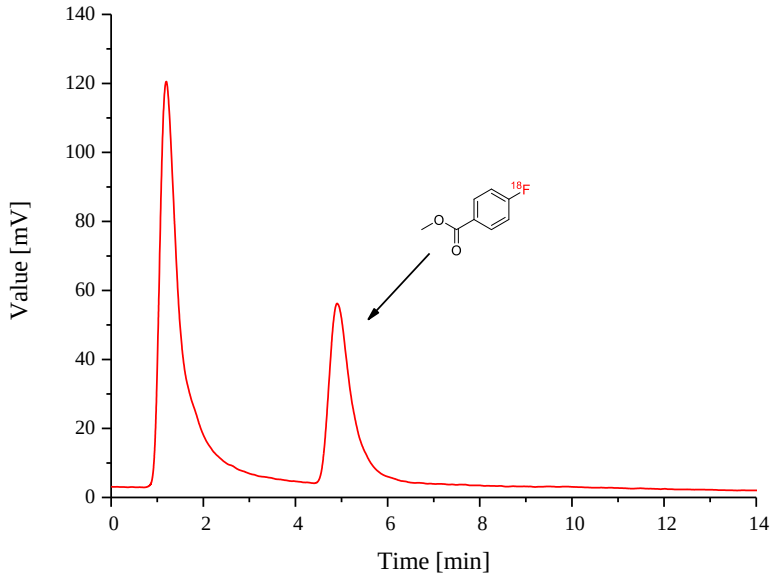

Chromatogram 11 Methyl 4-[^{18}F]fluorobenzoate.

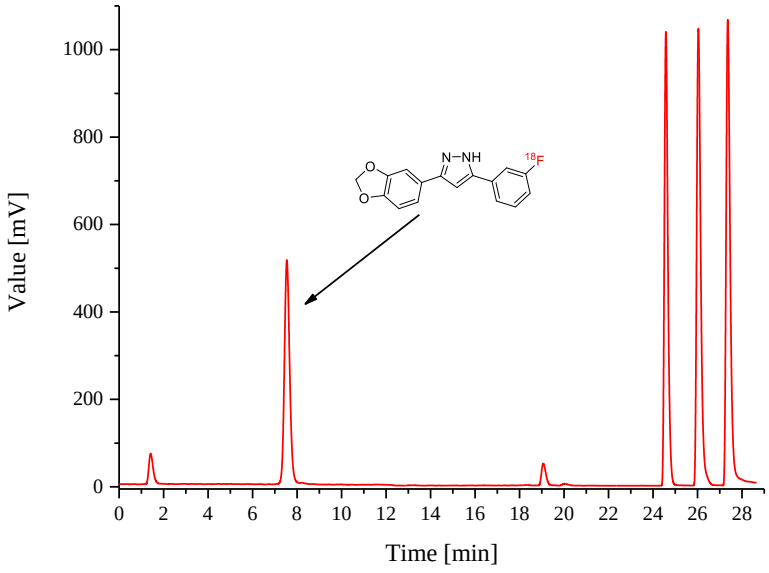

*Chromatogram 12 [^{18}F]**1c** with radioactivity reference peak.*

Automated radiosynthesis of amino acids

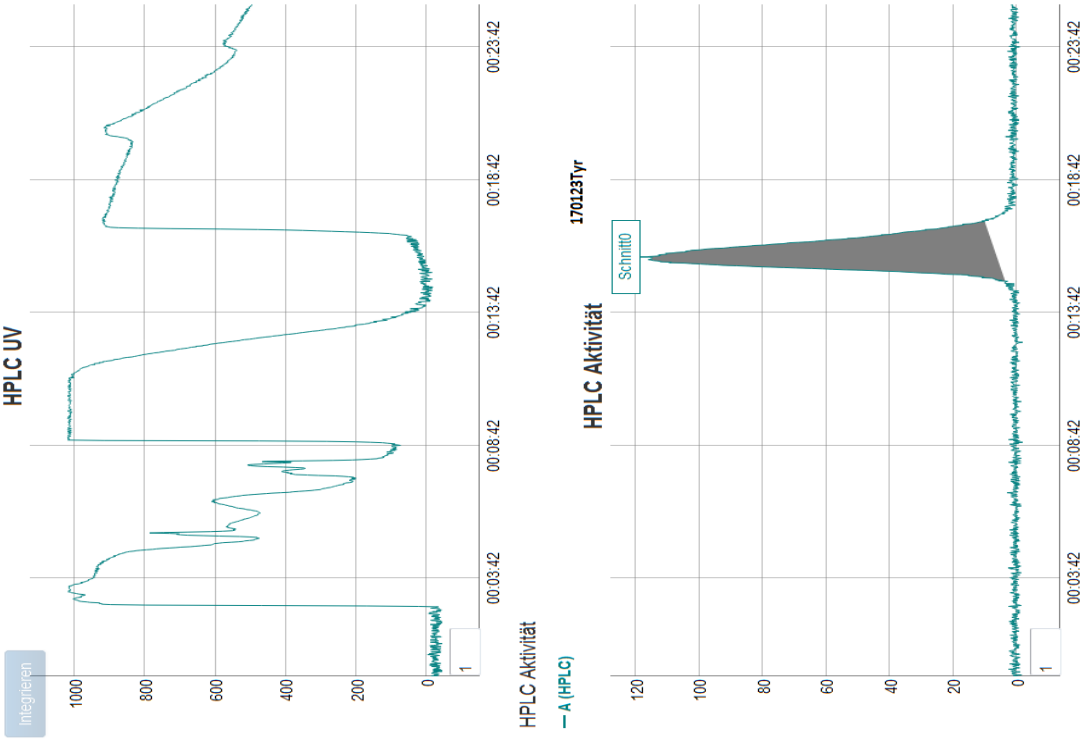

Chromatogram 13 2-[^{18}F]F-Tyr preparative HPLC.

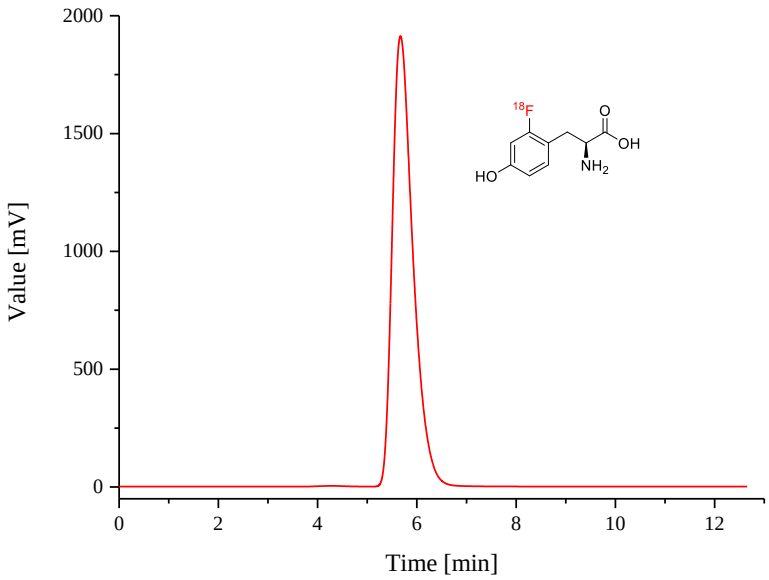

Chromatogram 14 2-[^{18}F]F-Tyr analytical HPLC.

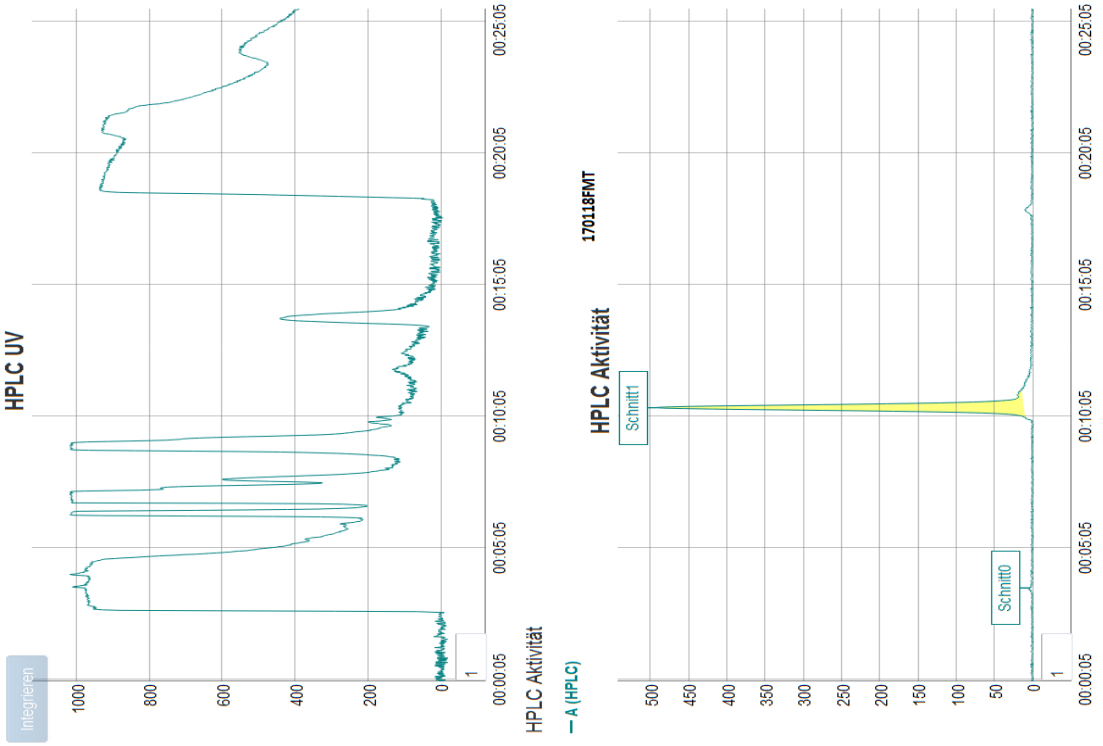

Chromatogram 15 6-[^{18}F]FMT preparative HPLC.

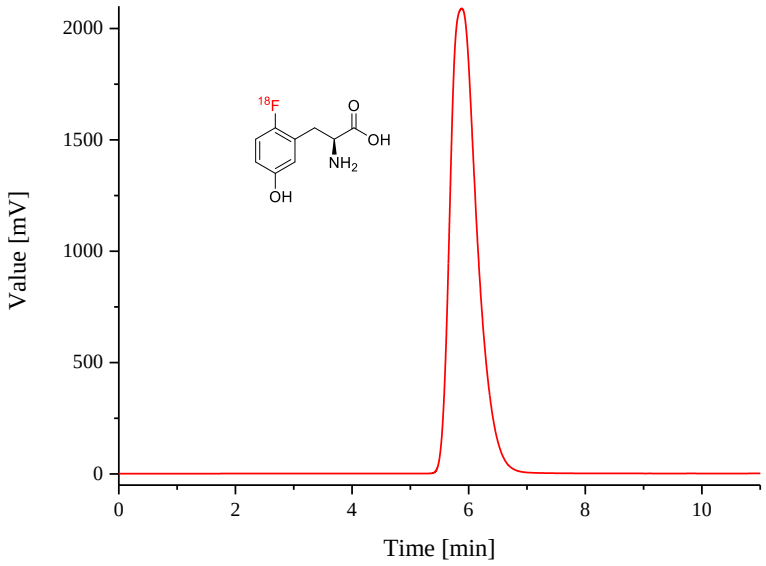

Chromatogram 16 6-[^{18}F]FMT analytical HPLC.

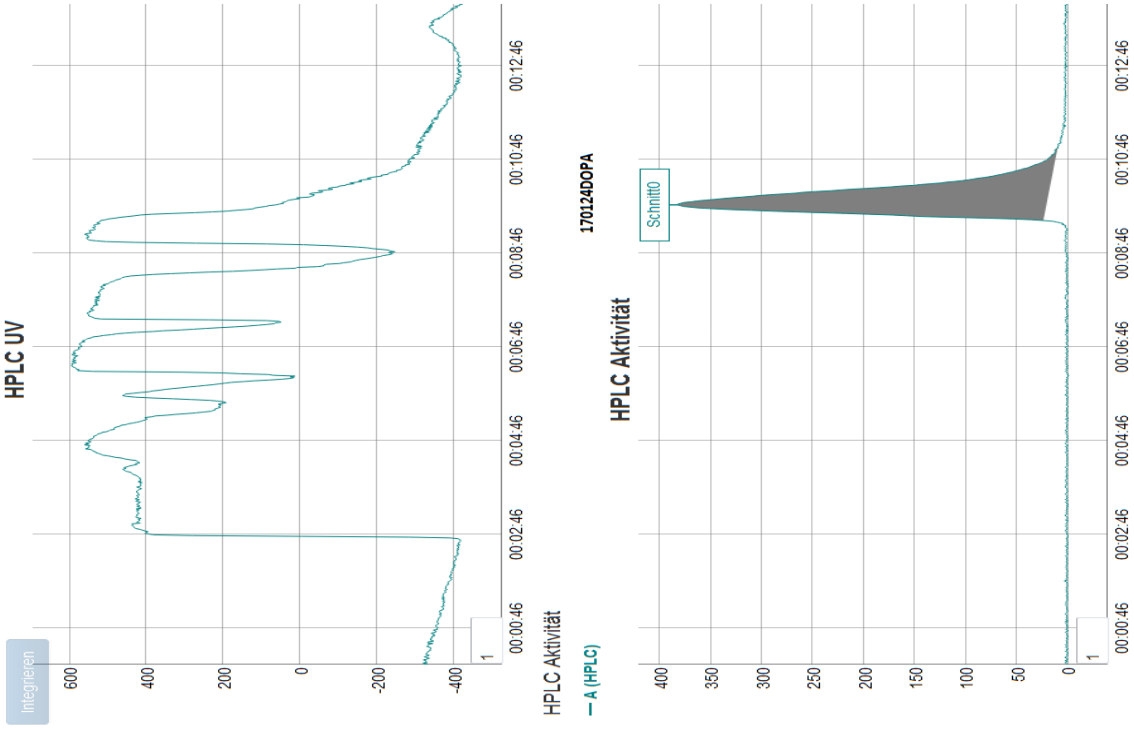

Chromatogram 17 6-[^{18}F]FDOPA preparative HPLC (Synergi™ 4 µm Hydro-RP 80 Å, LC Column 250×10 mm).

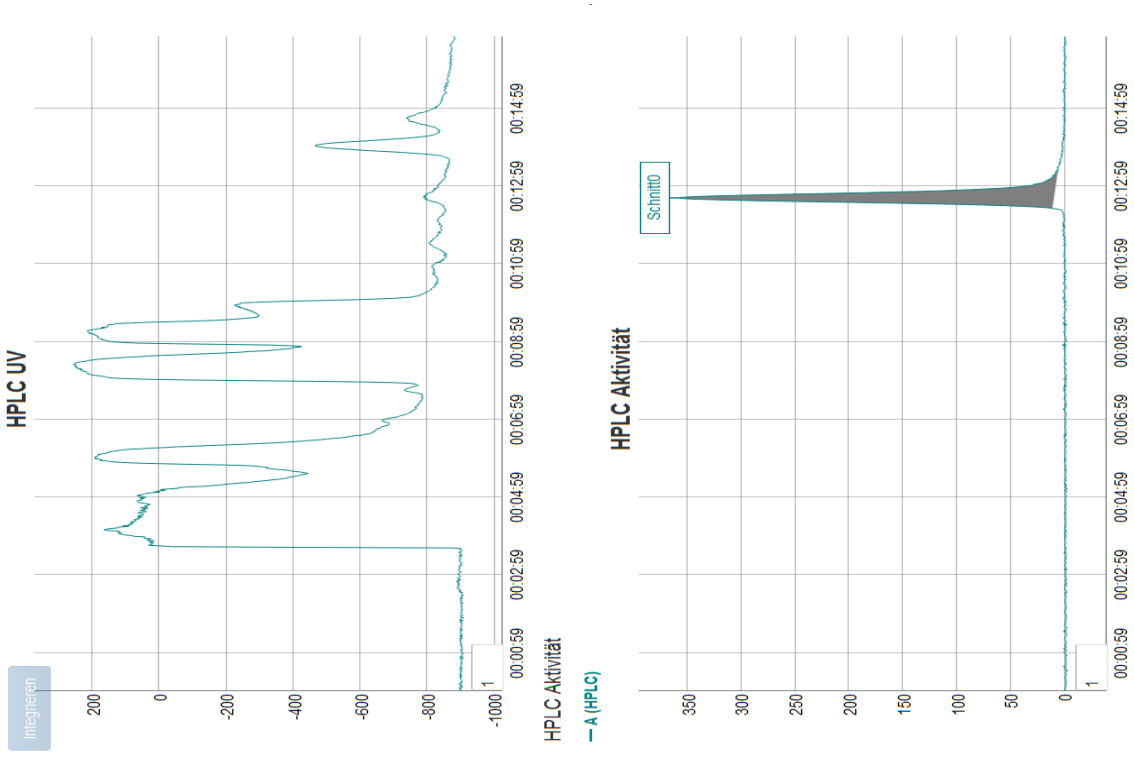

Chromatogram 18 6-[^{18}F]FDOPA preparative HPLC (Synergi™ 4 µm Hydro-RP 80 Å, LC Column 150×21.2 mm).

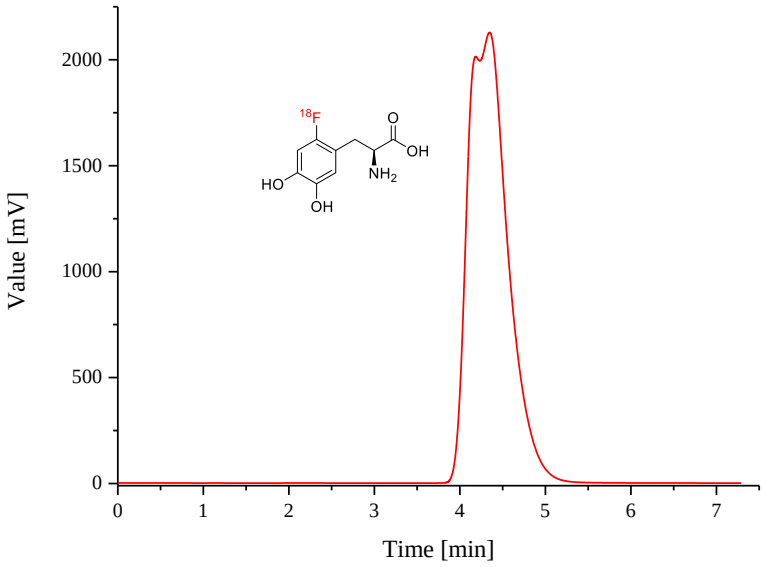

Chromatogram 19 6-[^{18}F]FDOPA analytical HPLC.

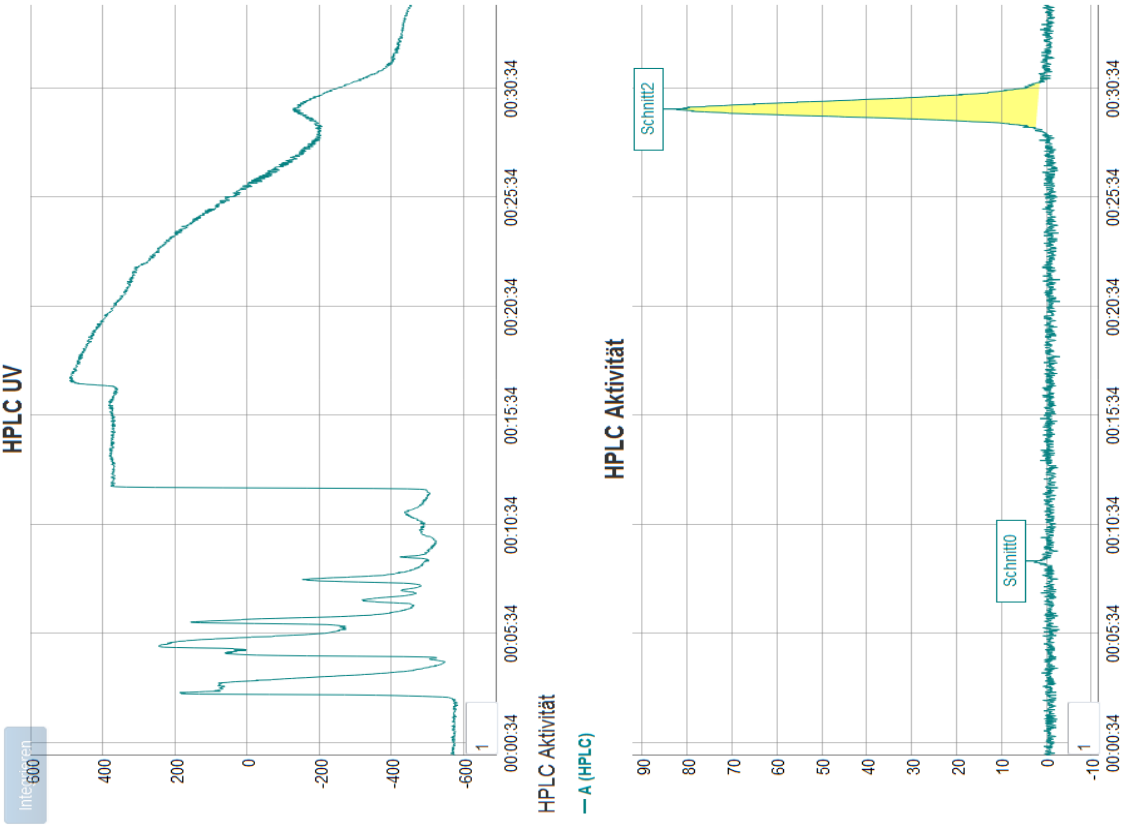

Chromatogram 20 6-[^{18}F]OMFD preparative HPLC.

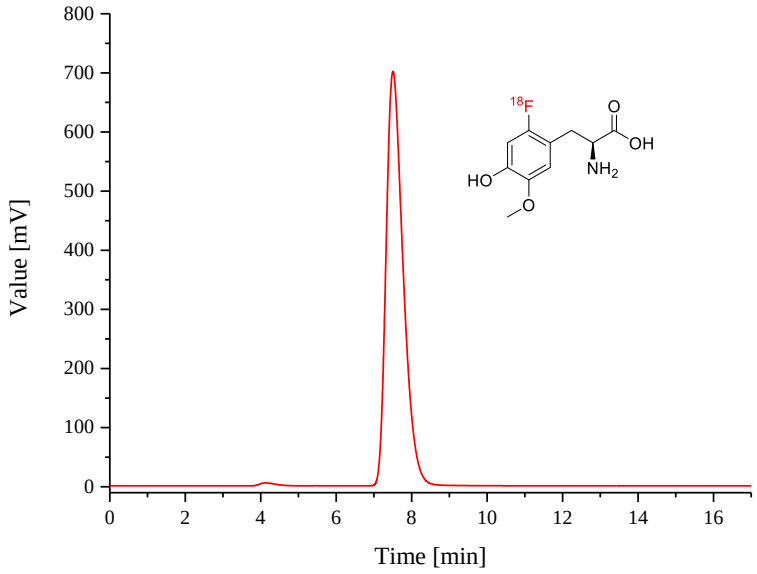

Chromatogram 21 6-[^{18}F]OMFD analytical HPLC.

Appendix II

MS of the crude mixture of **1h**.

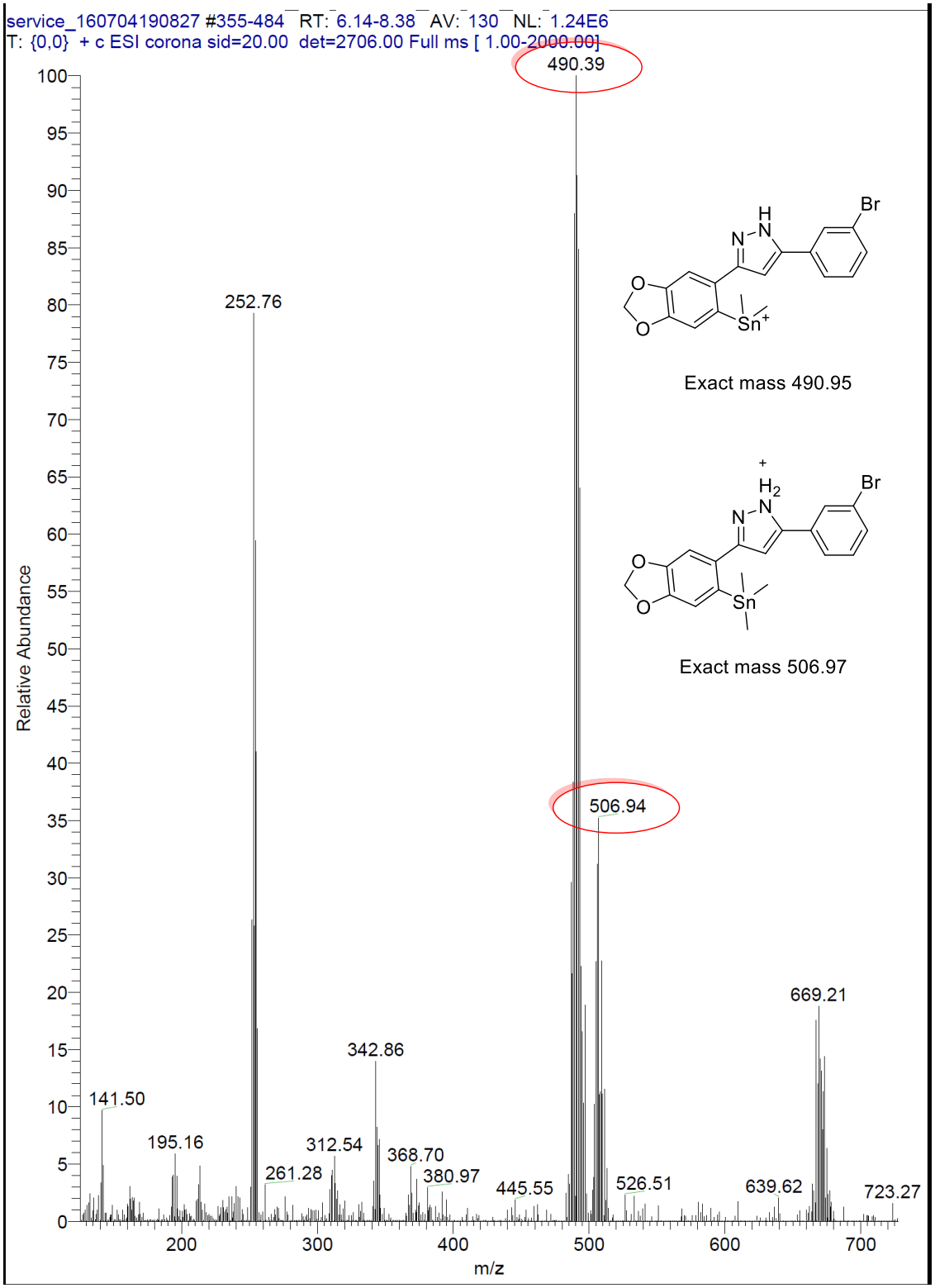

NMR of crude mixture of 6-*N*,*N*,*N*-trimethylbenzo[*d*][1,3]dioxol-5-aminium salt. Mixture (1:3) of 6-*N*,*N*-dimethylaminopiperonal and 6-*N*,*N*,*N*-trimethylbenzo[*d*][1,3]dioxol-5-aminium salt.

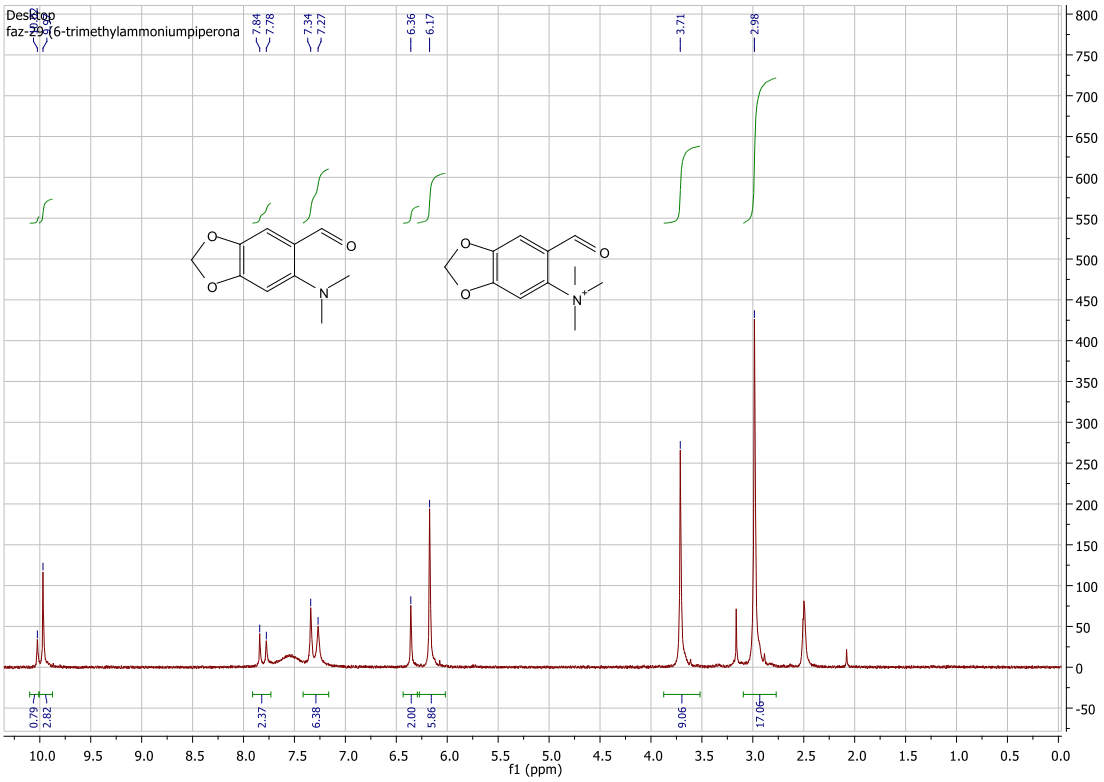

Erklärung zur Dissertation

Ich versichere, dass ich die von mir vorgelegte Dissertation selbstständig angefertigt, die benutzten Quellen und Hilfsmittel vollständig angegeben und die Stellen der Arbeit – einschließlich Tabellen, Karten und Abbildung –, die anderen Werken im Wortlaut oder dem Sinn nach entnommen sind, in jedem Einzelfall als Entlehnung kenntlich gemacht habe; dass diese Dissertation noch keiner anderen Fakultät oder Universität zur Prüfung vorgelegen hat; dass sie – abgesehen von unten angegebenen Teilpublikationen – noch nicht veröffentlicht worden ist sowie, dass ich eine solche Veröffentlichung vor Abschluss des Promotionsverfahrens nicht vornehmen werde.

Nachfolgend genannte Teilpublikationen liegen vor:

Schäfer, D. *et. al. Eur. J. Org. Chem*., **2016**, *27*, 4621.

Zlatopolskiy, B. D. *et. al. Chem. Eur. J*., **2015**, *21*, 5972.

Richarz, R.; *et. al. Org. Biomol. Chem*., **2014**, *12*, 8094.

Zarrad, F. *et. al. J. Label. Compd. Radiopharm.*, **2017**, *60 (S1)*, S425.

Zarrad, F. *et. al. J. Nucl. Med*., **2016**, *57*, 1083.

Zarrad, F. *et. al. Nuklearmedizin/NuclearMedicine*, **2015**, *54 (2)*, A67.

Zarrad, F. *et. al. Eur. J. Nucl. Med. Mol. Imaging*, **2015**, *42 (S1)*, S281.

Zarrad, F. *et. al. J. Label. Compd. Radiopharm.*, **2015**, *58 (S1)*, S242.

Zarrad, F. *et. al. J. Label. Compd. Radiopharm.*, **2015**, *58 (S1)*, S241.

Zarrad, F. *et. al. Nuklearmedizin/NuclearMedicine*, **2014**, *53 (1)*, A25.

Fadi Zarrad